

COLOR CODING FOR A FACSIMILE SYSTEM

by

ROBERT DAVID SOLOMON

B.S.E.E., Polytechnic Institute of Brooklyn
(1967)

S.M., Massachusetts Institute of Technology
(1968)

E.E., Massachusetts Institute of Technology
(1970)

SUBMITTED IN PARTIAL FULFILLMENT OF THE
REQUIREMENTS FOR THE DEGREE OF
DOCTOR OF PHILOSOPHY

at the

MASSACHUSETTS INSTITUTE OF TECHNOLOGY

August 1975

Signature of Author.

Department of Electrical Engineering, August 29, 1975

Certified by

[Signature] Thesis Supervisor

Accepted by.

Chairman, Departmental Committee on Graduate Students



COLOR CODING FOR A FACSIMILE SYSTEM

by

Robert David Solomon

Submitted to the Department of Electrical Engineering and Computer Science on August 29, 1975, in partial fulfillment of the requirements for the Degree of Doctor of Philosophy.

ABSTRACT

A fundamental color coding system suitable for facsimile transmission is initially specified with practical engineering and psychophysical constraints. This system achieves information compression by first accurately transforming the measured red, green, and blue reflectances at each picture element (pel) into a luminance and two CIE UCS chromaticity components which are linear in the sensation domain. The chromaticity components are then spatially filtered, coarse sampled, and coarse quantized. The compressed chromaticity components are then transmitted and linearly interpolated at the receiver and combined with the luminance to yield red, green, and blue signals, which are further processed to correct for the non-linear photographic process.

The processing operations of color scanning, chromaticity quantization, spatial filtering and coarse sampling, and pre-reproduction color correction are examined in detail to optimize their individual and interactive performance characteristics. Four areas of original contribution result from these studies.

Accurate determination of the tristimulus coordinates is achieved by transforming the color head functions in the chromaticity plane. A Hex-Affine-Triangle (HAT) transform is derived which uses a piecewise linear transform approximation to accurately convert the color scanner outputs to chromaticity values.

The gamut of chromaticity values in a three primary color picture is shown to be a function of the luminance level. A luminance scaled chromaticity (LSC) transform is derived which makes the new chromaticity values independent of luminance and also permits a much larger number of reproducible chromaticity values for frequently occurring pastels (such as light flesh tones) for a fixed number of chromaticity quantization levels.

In examining the techniques for spatially compressing the chromaticity components, the operations of filtering and coarse sampling at the transmitter and interpolation at the receiver are shown to yield a number (equal to the spatial compression factor) of different overall filter functions at each pel in the regions between coarse samples. These dissimilar functions can result in significant artifacts, and so the parameters must be carefully chosen to make the filter functions as similar as possible.

Efficient conversion from the CIE transmitted coordinates to red, green, and blue separations for reproduction by a specific subtractive dye process is shown to involve two linear transformations, one in the linear primary domain and the other in the logarithmic density domain. A piecewise-linear matrix transform is developed to approximate the inverse of the dye process which is not representable in closed form.

Color pictures processed by the system are shown to be of excellent quality compared to the original. However, they contain only 1/16 the chromaticity information and 37 percent of the total information of the original. Thus, the encoded picture can be transmitted in one-third the time by multiplexing the chromaticity information in the unused 11 percent scan blanking region of a conventional facsimile signal.

Thesis Supervisor: William F. Schreiber
Title: Professor of Electrical Engineering

Acknowledgments

Due to outside professional commitments, the rate of progress of this thesis has varied considerably over the past four years. During this time Professor Schreiber, my thesis and graduate advisor, has been very understanding and has given me realistic encouragement and support at various critical phases. My choice of readers, Doctors Richards, Tribus, and Troxel, has proven very fortuitous since the readers represented diverse areas of specialization, professional backgrounds, and philosophical outlooks which they enthusiastically applied to provide a broader insight into my multidisciplinary thesis problem. The late Professor Mason was an original reader and I am greatly indebted to him for his personal interest and encouragement in the early stages of my research.

My thesis research utilized the facilities of the Research Laboratory of Electronics and I am grateful for the generous support of many competent staff members. The first four years of my research were supported under a grant to MIT from the Associated Press. In addition, the General Radio Company in part supported the early period of my graduate work.

TABLE OF CONTENTS

	<u>Page</u>
Abstract - - - - -	2
Acknowledgments - - - - -	4
Table of Contents - - - - -	5
List of Figures - - - - -	7
Chapter 1. Introduction - - - - -	10
1.1 - The Basic Problem - - - - -	11
1.2 - Fundamental Constraints on the Color Facsimile System - -	13
1.3 - A Preliminary Model of the Color Facsimile System - - - -	17
1.4 - Summary - - - - -	19
Chapter 2. Color Space and Chrominance Quantization - - - - -	21
2.1 - Colorimetry - - - - -	22
2.2 - Color Space Representations and Transformations - - - - -	26
2.3 - Uniform Sensation Color Space - - - - -	30
2.4 - The Luminance Scaled Chromaticity (LSC) Transform - - - -	35
Chapter 3. The Chrominance Spatial Filtering Process - - - - -	49
3.1 - The Pschophysical Basis For Chrominance Spatial Filtering	50
3.2 - The Overall Filter Function - - - - -	52
3.3 - Luminance Filtering For the LSC Transform - - - - -	67
Chapter 4. Colorimetric Measurement and Photographic Reproduction Approximations - - - - -	70
4.1 - The Color Photographic Process - - - - -	71
4.2 - Quasi-Tristimulus Color Measurement - - - - -	76
4.3 - Colorimetrically Accurate Photographic Reproduction - - -	90

	<u>Page</u>
Chapter 5. Simulation of the Color Facsimile System - - - - -	101
5.1 - Introduction - - - - -	102
5.2 - The Color Scanner - - - - -	104
5.3 - The Computer and Software Systems - - - - -	108
5.4 - Reconstruction of Color Pictures - - - - -	112
Chapter 6. Color Picture Evaluation and Conclusions - - - - -	114
6.1 - Subjective Analysis of Compressed Color Pictures - - - - -	115
6.2 - Topics For Further Research - - - - -	120
6.3 - Conclusions - - - - -	122
Appendix I. Linear Transformation To A New Set of Color Primaries -	123
Appendix II. Inversion of Bilinear Chromaticity Color Space - - - -	125
Appendix III. Derivation of the LSC Transform - - - - -	126
Appendix IV. A Mathematical Analysis of Dye Correction - - - - -	129
Appendix V. Color Transform For New Primaries With Specified Chromaticities - - - - -	134
Appendix VI. Numeric System Parameters and Transforms - - - - -	136
References - - - - -	140
Biographical Note - - - - -	143

LIST OF FIGURES

Figure		Page
1-1	Basic Model of a Color Facsimile System - - - - -	18
2-1	CIE R,G,B Matching Functions - - - - -	23
2-2	Luminous Efficiency Function - - - - -	25
2-3	R,G,B Primary Color Space - - - - -	27
2-4	Linearly Transformed L, C ₁ , C ₂ Color Space - - - - -	29
2-5	UCS Chromaticity Diagram - - - - -	33
2-6	Bilinearly Transformed C ₁ , C ₂ Color Space - - - - -	34
2-7	R,G,B Separations of Group Picture - - - - -	36
2-8	L, C ₁ , C ₂ Components of Group Picture - - - - -	37
2-9	Chromaticity Loci at Constant Luminance - - - - -	38
2-10	L and LSC Transformed C ₁ , C ₂ Components of Group Picture-	42
2-11	R,G,B Separations of Test Picture - - - - -	43
2-12	R,G,B Separations of Compressed Test Picture - - - - -	44
2-13	R,G,B Separations of LSC Transformed Compressed Test Picture - - - - -	47
3-1	The Four Stages of the Overall Filter Function - - - - -	53
3-2	Two Dimension Filter Block Diagram - - - - -	55
3-3	The Symmetric Transmitter Filter Function - - - - -	57
3-4	Two Dimensional Coarse Sampling and Interpolation - - - - -	58
3-5	The Continuous Interpolation Filter Function - - - - -	59
3-6	The Sampled Interpolation Function - - - - -	59
3-7	Triangular Transmitter Filter Function - - - - -	62
3-8	OFF for the Transmitter Filter of Figure 3-7 - - - - -	63
3-9	Modified Transmitter Filter Function - - - - -	64
3-10	OFF for the Modified Filter of Figure 3-9 - - - - -	65
3-11	R,G,B Separations of Test Picture Processed by the OFF of Figure 3-8 - - - - -	66
3-12	LSC Transform Processing - - - - -	68

Figure		Page
4-1	Block Dye Approximation - - - - -	73
4-2	Basic Model of the Color Photographic Process - - - - -	75
4-3	Taking Sensitivity of Ektachrome Reversal Film - - - - -	75
4-4	Dye Transmission Curves for Ektachrome Slides - - - - -	75
4-5	Density - Log Exposure Curves for Ektachrome Film - - - - -	77
4-6	Color Head Sensor Response Functions - - - - -	80
4-7	Color Head Filter Quasi Luminosity Function - - - - -	82
4-8	Dye Gamut for RC Print Paper Dyes - - - - -	83
4-9	Dye Gamut Measured by the Color Head Filters - - - - -	84
4-10	U-V Affine Transform - - - - -	86
4-11	U-V Transform with Second Order u - - - - -	88
4-12	Hex-Affine-Triangular (HAT) Transform - - - - -	89
4-13	Transmitter Encoder with Color Head Correction Transforms - - - - -	91
4-14	Receiver Decoder with Pre-dye Primary and Density Transforms - - - - -	91
4-15	Dye Gamut of Photograph Made Directly from CIE R,G,B Separations - - - - -	93
4-16	CIE R,G,B and R',G',B' Primary Triangles - - - - -	95
4-17	Dye Gamut of Photograph with R',G',B' Coordinates - - - - -	96
4-18	Dye Gamut of Photograph with Hex Dye Correction Transform - - - - -	98
4-19	Overall Chromatic Reproduction Accuracy of the Facsimile System - - - - -	100
5-1	PDP-9 Color Image Processing Computer System - - - - -	103
5-2	Color Facsimile Scanner Optics - - - - -	105
5-3	Schematic Representation of the Color Head Response Functions - - - - -	106
5-4	Monochrome Receiver and Color Transmitter Facsimile Interface - - - - -	107
5-5	COPS System Block Diagram - - - - -	110

Figure		Page
6-1	Group Picture - - - - -	117
	a) Scanned Color Corrected Unprocessed Original	
	b) Scanned Unprocessed Original Without Output Dye Correction	
	c) Fully Processed, Compressed with LSC Transform	
6-2	Cameraman Picture - - - - -	118
	a) Scanned Color Corrected Uncompressed Original	
	b) Compressed Without LSC Transform	
	c) Compressed with LSC Transform	
6-3	Portrait Picture - - - - -	119
	a) Scanned Color Corrected Uncompressed Original	
	b) Compressed Without LSC Transform	
	c) Compressed with LSC Transform	

TABLES

Table		Page
2-1	Frequency of Occurrence of C_1-C_2 Values for the Group Picture - - - - -	41
2-2	Frequency of Occurrence of LSC Transformed C_1-C_2 Values for the Group Picture - - - - -	48
A-1	Quasi-Luminance Function Accuracy - - - - -	137
A-2	Hexagonal Affine Transform for the Color Head Inputs -	138
A-3	Hexagonal Affine Transform for Pre-Dye Correction - - -	139

I. Introduction

1.1: The Basic Problem

1.2: Fundamental Constraints on the Color Facsimile System

1.3: A Preliminary Model of the Color Facsimile System

1.4: Summary

1.1 The Basic Problem

As color pictures become a more common feature in newspapers, increased demands will be made of the wire services to provide fast, high quality color facsimile transmission. In addition, the advent of color office copying equipment suggests the possibility of transmitting color as well as black and white interoffice pictures via telephone lines. Although this dissertation concentrates on the specific problem of color facsimile, a number of general principles are derived, based on the psychophysics of color vision, subtractive dye reproduction theory, and digital signal processing techniques which may be directly applied to a wide range of color picture transmission and storage systems.

Since the infancy of facsimile there have been few innovations in the transmission of color pictures. Today, color facsimile transmissions are still accomplished by scanning a color print with a conventional rotating drum monochrome facsimile transmitter. Three successive scans are required, with first a red, then a green, and finally a blue filter placed in front of the photodetector. The three received monochrome pictures correspond to the cyan, magenta, and yellow printers from which the color printing plates are made. The number of color facsimile transmissions relative to black and white is very small due to the threefold increase in transmission time (over 24 minutes) and the poor color quality which results from the crude color scanning techniques.

This dissertation examines and develops solutions for the two major problems of present day color facsimile:

- 1) How can the information contained in the added dimension of

color (chrominance¹) be compressed and coded to a small fraction of the black and white luminance information so that a color picture may be transmitted in the same time as a monochrome picture (8 minutes) and be subjectively equivalent to the original?

- 2) What techniques are necessary to scan an original color print and make a photographic reproduction from red, green, and blue separations, so that the color rendition and overall subjective quality of the output print is acceptably similar to the input print?

It might be suggested that the second problem has already been solved since methods for high quality color reproduction using an electronic scanner are well known and commonly used.^(1,2) However, in order to solve the first problem, the human eye must be somehow fooled into believing that the compressed picture contains as much information as the original. Colors should be represented in terms of psychophysical coordinates. These coordinates should also be chosen so that information which is visually redundant due to the limited color and spatial acuity of the eye can be easily removed by coarse linear quantization and spatial filtering. Thus techniques can be developed at the transmitter for making valid colorimetric measurements at each picture element (pel) on the scanned print. In addition, due to the discrete nature of digital systems, the chrominance and luminance components should be chosen so that linear quantization will yield equal

¹In parallel with the etymological structure of luminosity and luminance, the author is taking the liberty of defining "chrominance" to be the two dimensional component which when added to the one dimensional luminance yields a three dimensional color space. Chapter Two more fully examines the two dimensional nature of chrominance.

steps in color sensation. At the receiver, a more difficult problem arises in inverse transforming the processed psychophysical variables into color separation reflectances which will yield color photographic prints having the specified colorimetric values (figure 1-1).

This dissertation has two overall contributions. First, it develops practically engineered algorithms (which are compatible with existing facsimile specifications) to significantly compress the chrominance information by coding the psychophysical components. Secondly, efficient transforms are developed for converting back and forth between these components and photographic media with high colorimetric accuracy.

1.2 Fundamental Constraints on the Color Facsimile System

Picture coding operations may be classified according to what portion of the picture is operated on at one time. At one extreme are transform processors (e.g., Fourier and Hadamard) which necessitate storing the entire picture in a random access memory (RAM).⁽³⁾ Digitizing each of the red, green, and blue components of a standard 8 by 10 inch color picture to six bits with a facsimile resolution of 100 pels per inch, results in over ten million bits of storage. Not only are such processors unfeasible from an economic standpoint, but also they incur severe delays between transmission and reception of the picture. A "hot news" picture must first be scanned for eight minutes then processed for at least another eight minutes and finally transmitted, resulting in a three-fold delay in effective transmission time and thereby offsetting the gains of color compression.

The simplest type of processor operates only once on a single pel, which is then immediately transmitted. This limited operation precludes linear filtering and interpolation in two dimensions, which are crucial

for effective color compression. An intermediate solution which effectively permits real time transmission (i.e., the picture is reproduced at the receiver, as it is scanned at the transmitter) is to store and process a small group of lines. The resulting transmission delay of several lines is negligible for a facsimile scan rate of 100 lines per minute. However, the filter and interpolation functions are now restricted to a width of only several sample points and are most easily implemented as superposition functions.

The coding algorithms must be designed to process pels in the 500 μ sec intersample periods of the scanner. Since the entire picture is not stored, the window processor alone cannot use adaptive coding picture processing techniques (e.g., Karhunen-Loeve statistical vector basis) and so the coding algorithms must be designed to reproduce a wide variety of color pictures equally well.

Color television is the only system which makes use of color coding techniques.^(4,5) In the early 1950's the color television researchers were unable to make use of modern solid state digital computer technology. However, the system is very sophisticated for its time and many parallels can be drawn between television and facsimile. Both are electro-optical scanning systems where a one dimensional video signal is transmitted and used to synchronize a similar scanning system at the receiver, provide brightness information at each pel, and set the reference white level. Television requires constant synchronization of the horizontal and vertical sweep since it transmits 60 fields per second or roughly five million pels per second, whereas facsimile only transmits a single, higher resolution frame, of 800,000 pels in eight minutes, and therefore only a single synchronization pulse is needed at the start of the picture. Both the

facsimile transmitter and receiver have inexpensive crystal clocks with an accuracy of one part per ten million which stay in synchronization within 0.1 pel over the duration of a single picture transmission.

Scanning systems all have blanking periods in the direction of scan to enable an electron or laser beam to retrace or to allow a region of the scanning drum to contain a clip for securing the picture. The blanking period in television contains an elaborate synchronization signal, so the chromaticity information has to be frequency multiplexed in a fairly complex way during the active scan region. In facsimile, a regular synchronization signal is not necessary and so the blanking region which is 6 to 12 percent of the scan duration can be used to carry other time multiplexed information. A basic constraint on the color facsimile system developed in this dissertation specifies that the color information which normally necessitates two additional pictures be compressed by a factor of 16:1 and time division multiplexed into an 11 percent scan blanking period. Thus, the three separations can be transmitted in the same time that it takes to send a single monochrome picture. The signal is black and white compatible since the active scan video signal still contains the unaltered full resolution luminance information which is combined with the compressed chrominance to yield the red, green, and blue separations. If received by a monochrome receiver, the chromaticity information in the scan blanking region will be ignored and only the luminance will be reproduced. Thus installation of a color facsimile system will not disrupt, degrade or make obsolete the existing monochrome transmitters and receivers in the network. Chapter Two further discusses psychophysical reasons why the luminance is the best choice for the high resolution color component.

The problem, now, is how to achieve the required compression factor of 16:1 to satisfy the above multiplexing constraint. Fortunately, some research on the spatial acuity for chromaticity^(6,7) has shown that the resolution of each chromaticity component can be reduced to approximately 10 to 30 percent of the luminance resolution before noticeable picture degradation occurs. Color television researchers used this psychophysical property to achieve compression ratios of 8:1 and 8:3 for the Q and I chromaticity signals.^(8,9) At the time of color television development the cost of line storage hardware was prohibitive, and so the chromaticity television signals are only filtered in one dimension by simple analog time domain filters. Much more recent work⁽¹⁰⁾ has shown that the chromaticity signal can in fact be spatially smeared in each direction to at least 1/4 of the full luminance resolution without objectionable degradation in subjective picture quality. Thus the chromaticity components in the facsimile system developed in this dissertation are digitally filtered and coarsely sampled at 1/16 of the full two dimensional resolution, yielding the sought after compression factor of 16:1. The exact details of the filtering operation are examined in Chapter Three.

Another way in which the digitized chrominance information is compressed is by coarsely quantizing it to a small number of discrete levels. Since this thesis deals solely with chrominance compression, various existing luminance compression algorithms are not being implemented. However, techniques have been developed for transmitting high quality luminance with only three to four bits resolution (16 levels).⁽¹¹⁾ Studies indicate that the chromaticity components can also be restricted to four bits each or 256 chromaticity values.⁽¹⁰⁾ Some noticeable quantizing contours will occur at this degree of coarse quantization. With

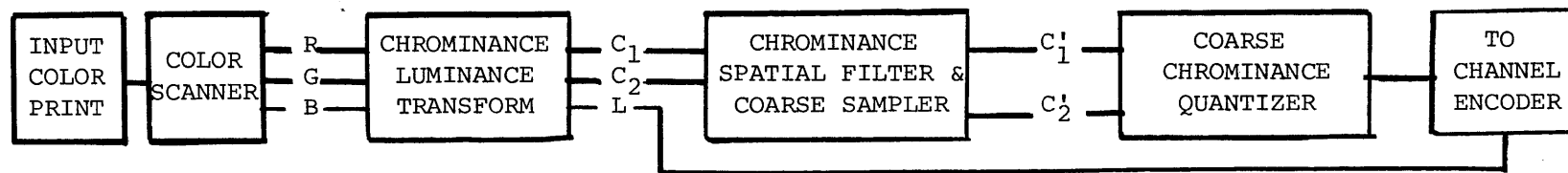
this constraint, sophisticated methods are developed in Chapter Two to effectively utilize the limited number of discrete levels to significantly reduce quantization artifacts.

1.3 A Preliminary Model of the Color Facsimile System

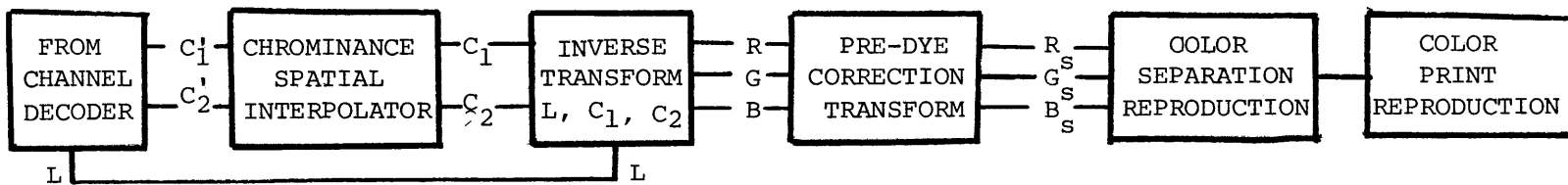
The previous section constrained the system to utilize stream processing, real time algorithms, with several lines of storage for filtering and interpolating the chromaticity components. A compression factor of 16:1 is achieved by coarse sampling the spatially filtered components. The chrominance information is also coarsely quantized to eight bits (four bits for each component) and the coded chrominance signal is time multiplexed into the 11 percent scan blanking period.

A preliminary model of the color facsimile system is shown in figure 1. The transmitter consists of a color scanner with red, green, and blue photodetectors and a chrominance luminance conversion transform, followed by the chrominance spatial filter, coarse sampler, coarse quantizer and encoder. At the receiver, the chromaticity components are interpolated, and then inversely transformed with the luminance to red, green, and blue signals which are pre-corrected for the non-ideal dyes encountered in photographic or printing reproduction processes, and are then simultaneously reproduced as red, green, and blue monochrome separations.

A channel encoder, channel model, and channel decoder should be inserted between the transmitter source encoder and receiver source decoder, but this thesis only examines the source coding problem, and so assumes an ideal channel. In television systems, a relatively poor signal to noise ratio can be tolerated because the eye tends to



COLOR FACSIMILE TRANSMITTER



COLOR FACSIMILE RECEIVER

FIGURE 1-1. BASIC MODEL OF A COLOR FACSIMILE SYSTEM

integrate out the uncorrelated frame to frame noise, yielding a much higher perceived signal to noise ratio. In facsimile, a single frame is transmitted and may be reproduced hundreds of thousands of times in newspapers. Therefore, nearly flawless transmission must be insured by the channel coder since a strategically located error such as a spot on a prominent politician's nose might necessitate retransmission of the entire picture.

The interpel sample period for facsimile is 500μ sec or a few thousand times the corresponding period for television. Therefore, in addition to the operations of sampling, filtering, quantizing, and packing there is sufficient time to perform complex chrominance transforms with a high speed digital processor. Color coders for television systems cannot afford this computational luxury, but color television is an additive primary system and so many of the chrominance transforms required to correct for subtractive dye systems encountered in facsimile are unnecessary in television.

1.4 Summary

There has been much prior "knob-twiddling" by earlier researchers of a limited number of color coding parameters so that several of these (i.e., the chrominance spatial compression factor) can be set to a reasonable value without further experimentation. Having specified these basic parameters, the author is able to enter into new areas of color coding research by developing algorithms which optimize color picture quality given basic system architecture constraints and certain pre-specified key parameter values.

This thesis takes the approach of attempting to work in the mathematically and physically defined colorimetric system in which the psychophysical data of most researchers is usually represented. The next chapter examines various transforms of the chromaticity components in the standard colorimetric color space.

II. Color Space and Chrominance Quantization

2.1: Colorimetry

2.2: Color Space Representations and Transformations

2.3: Uniform Sensation Color Space

2.4: The Luminance Scaled Chromaticity (LSC) Transform

2.1 Colorimetry

The colorimetric design of a system to effectively process color photographs must be based on the psychophysics of color vision and the limitations of color photography. These disciplines must be inter-related in evolving algorithms which efficiently compress and code color pictures.

At the foundation of the psychophysics of color vision is the Young-Helmholtz model of the eye which describes the retina as containing three types of cone receptors, each with independent spectral sensation characteristics. ^(12,13) The three cone responses peak in roughly the red, green, and blue regions of the spectrum. The cone model is the basis of colorimetry where any color sensation due to a stimulus with a particular spectrum can be represented by three numbers, namely the neural response of each cone. This gives rise to the phenomenon of metamerism which occurs when two different spectral distributions equally activate the three cone mechanisms. Thus an infinite number of possible spectra, referred to as metamers, can be mapped by the eye into the same color sensation.

The three dimensional nature of color vision is the basis for the classic matching experiments where the radiances of three additively projected primary light sources with spectral distribution, $p_j(\lambda)$, are adjusted to match an unknown color source. The standard 1931 CIE measurements used three narrowband spectral distributions centered at 700.0 nm, 546.1 nm and 435 nm to match narrowband regions along the visible spectrum. Three color matching functions, $x_j(\lambda)$, result from these measurements and are shown in figure 2-1. Negative values of the

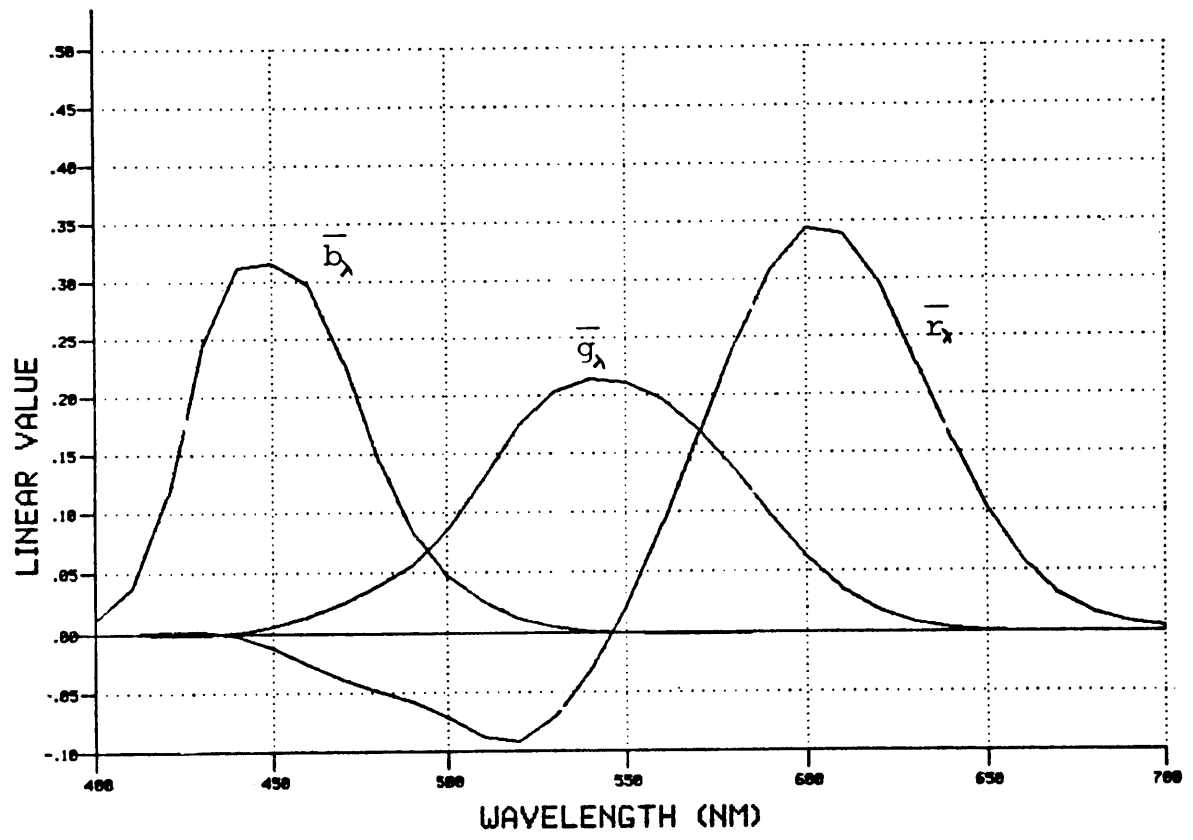


FIGURE 2-1. R, G, B CIE MATCHING FUNCTIONS

matching function indicate that the match required the corresponding primary light source to be added to the light being matched. Further matching experiments show that any color stimulus, $s(\lambda)$, may now be represented by the three chromaticity coordinates, R, G, B, which represent the amount of each primary required to match the stimulus.

$$x_j = \int_{\Lambda_e} x_j(\lambda) s(\lambda) d\lambda \qquad x_j(\lambda) = r(\lambda), g(\lambda), b(\lambda) \qquad (2.1-1)$$
$$x_j = R, G, B$$

where Λ_e is the range of wavelengths of visual response, namely 380 to 770 nanometers (nm).

Many sets of primaries other than the CIE standard primaries may be used as the basis for specifying colors. The conversion to a new primary system is detailed in Appendix I.

The luminance of a color is a measure of the apparent brightness. Its value can be related to the radiant energy of a particular color by the photopic luminosity curve which is a plot of luminous efficiency as a function of wavelength. The luminosity function peaks in the green, falls off in the red and decreases more sharply in the blue (figure 2-2). Luminance is a very important parameter since its value must be transmitted at full spatial resolution as the monochrome signal for black and white system compatibility. Even in a strictly color system, the luminance must be transmitted with maximum spatial resolution since the eye has the greatest acuity for this visual component. (14)

From Grassmann's laws of additive color mixture it follows that the luminance of an additive mixture of colors is a sum of the individual luminances. (15) In particular for a proper set of tristimulus

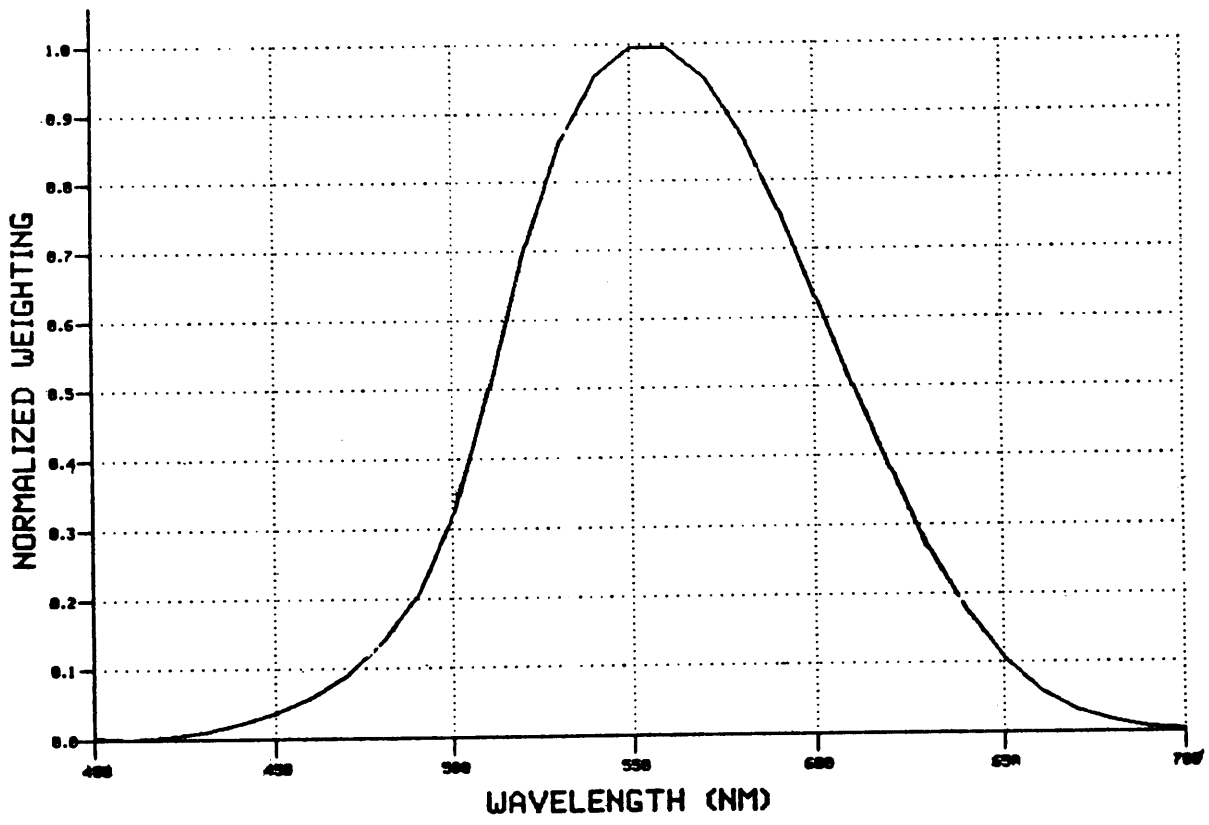


FIGURE 2-2. LUMINOUS EFFICIENCY FUNCTION

primaries, each of the color components contributes to luminance.

$$L = L_r R + L_g G + L_b B \quad (2.1-2)$$

Where each luminosity coefficient, L_i , is the integral of the product of the photopic luminosity curve and the primary distribution $P_i(\lambda)$ over wavelength.

$$L_i = \int L(\lambda) P_i(\lambda) d\lambda \quad (2.1-3)$$

2.2 Color Space Representations and Transformations

Three dimensional color space can be described by a variety of triads of parameters. A color can be specified by its red, green, and blue coordinates in an infinite number of primary bases. In the case of subtractive dyes, a color is completely described by knowing the amount of the cyan, magenta, and yellow dyes, assuming a standard illuminant. A more qualitative description of color results from specifying the brightness, hue (common color name), and saturation (degree of color purity ranging from white through pastel to a fully saturated monochromatic color). The latter representation is noteworthy since now the triad of parameters contains luminance as one term and the hue and saturation pertain solely to the chrominance.

In any physical set of primaries, the range of synthesizable colors can be represented as being contained in a unit cube (figure 2-3) by normalizing maximum values of the primaries (i.e., to maximum white print reflectance under specified illumination)

$$R_{\max} = G_{\max} = B_{\max} = 1 \quad (2.2-1)$$

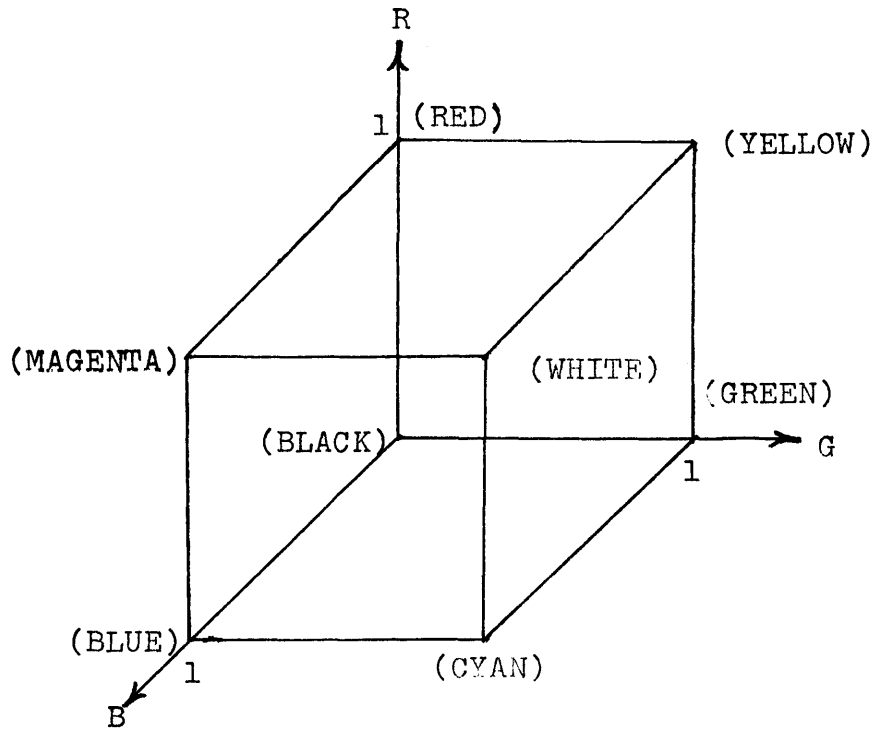


FIGURE 2-3. R, G, B CUBE COLOR SPACE

If the primaries are each quantized to six bits, then over a quarter of a million discrete possible colors lie within the cube. Perpendicular axes, resulting in a cubic region of permissible colors, are used solely as a convenience in drawing, since the exact angular relationships between axes or even the shape of the color space is meaningless unless some spatial distance metric can be defined as a function of the plotted parameters.

It is also convenient to normalize the luminance, so that by 2.1-2 maximum luminance is unity.

$$L_r + L_g + L_b = 1 \quad (2.2-2)$$

The brightest color in a reproduction system is usually the white point and since this occurs when the three primaries are at their maximum unity value, whenever the primaries have the same value, the color specified will be achromatic.

$$\text{at achromatic points: } R = G = B = L \quad (2.2-3)$$

The primaries can be linearly transformed to a new coordinate system, where one of the new components is luminance. The two remaining components are measures of chrominance.

$$\begin{pmatrix} L \\ C_1 \\ C_2 \end{pmatrix} = \underline{\underline{I}} \begin{pmatrix} R \\ G \\ B \end{pmatrix} \quad (2.2-4)$$

This linear transform must be invertible so the C_1 and C_2 must be independent of L and have zero luminance. In figure 2-4 the transformed cubic primary space is shown in the new L, C_1, C_2 space, where the

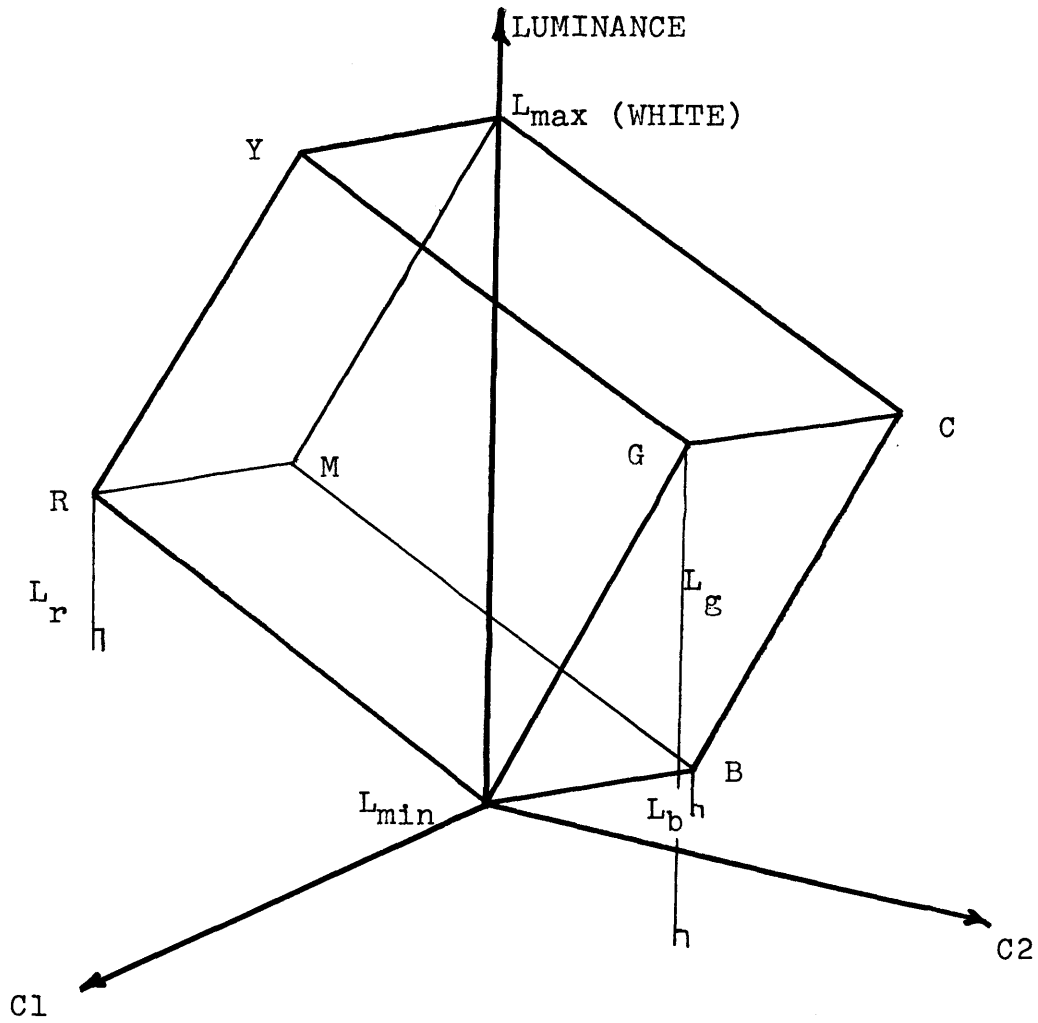


FIGURE 2-4. LINEARLY TRANSFORMED L, C_1, C_2 COLOR SPACE

luminosity of any point in the space is the distance from the point to the plane formed by the C_1 and C_2 axes along a line parallel to the L axis. Thus the exact location of the C_1 - C_2 plane is specified by the L_r, L_g, L_b distances it must be located from the $R_{max}, G_{max},$ and B_{max} vertices of the parallelepiped. The NTSC color television system uses this type of chrominance transformation.

The mapping from R, G, B space to L, C_1, C_2 space is inefficient since the parallelepiped volume spanned by the maximum and minimum L, C_1, C_2 values is larger than the transformed R, G, B parallelepiped volume of real colors. Thus quantization of the L, C_1, C_2 axes yields a volume of color code word boxes where a large number of boxes do not represent a valid color. This is a direct consequence of constraining the space by the R, G, B cube and using luminance as one of the coordinates, thereby placing boundaries on the gamut of realizable chrominance values which vary as a function of luminance.

2.3 Uniform Sensation Color Space

Ignoring statistical weighting, the L, C_1, C_2 coding space will be most efficiently quantized if equal quantum steps along the coordinates produce nearly equal visual sensations. In the case of luminance quantization, much experimentation^(16, 17) has revealed that a modified logarithmic function, \hat{L} , produces the most uniform quantization since it evenly distributes perceived picture noise and contour artifacts over the entire tone scale.

$$\hat{L} = \frac{\text{Log}(1 + aL)}{\text{Log}(1 + a)} \quad (2.3-1)$$

where the *companding* shape factor a has an optimum value found experimentally to lie between .01 and .1 depending on the desired shadow detail in the picture.

As a first step in obtaining a uniform chrominance scale (UCS) sensation plane, researchers determined the just noticeable differences (JND) of chrominance changes for various colors and plotted the loci of these JND points around the particular color point in a bilinear chromaticity plane. (18)

A general bilinearly transformed chromaticity plane can be set up by first linearly transforming the CIE coordinates.

$$\begin{pmatrix} C1 \\ C2 \\ C3 \end{pmatrix} = [T] \begin{pmatrix} R \\ G \\ B \end{pmatrix} \quad (2.3-2)$$

The conical projection of points in the $C1, C2, C3$ space onto the $C1 + C2 + C3 = 1$ plane in that space results in three chromaticity coordinates, $c1, c2, c3$.

$$\begin{aligned} c1 &= \frac{C1}{C1 + C2 + C3} & c2 &= \frac{C2}{C1 + C2 + C3} \\ c3 &= \frac{C3}{C1 + C2 + C3} & c1 + c2 + c3 &= 1 \end{aligned} \quad (2.3-3)$$

The chromaticity coordinates $c1, c2, c3$ are relative values and are therefore independent of the absolute value of the color coordinates $C1, C2, C3$. Since chrominance has only two degrees of freedom, choosing $c1$ and $c2$ as the independent variables projects points on the $C1 + C2 + C3 = 1$ plane onto the $c1, c2$ plane.

The CIE-UCS coordinates u and v may be defined in terms of the R,G,B CIE coordinates:

$$u = \frac{u_r R + u_g G + u_b B}{s_r R + s_g G + s_b B} \quad v = \frac{v_r R + v_g G + v_b B}{s_r R + s_g G + s_b B} \quad (2.3-4)$$

Appendix II shows how 2.3-4 and 2.3-5 may be inverted to yield:

$$\begin{aligned} R &= L(r_u u + r_v v + a)/D(u,v) & \text{where } a, b, c, r_u, r_v, g_u, g_v, b_u, b_v, d_u, d_v, d \\ G &= L(g_u u + g_v v + b)/D(u,v) & \text{are constants.} \\ B &= L(b_u u + b_v v + c)/D(u,v) & D(u,v) = d_u u + d_v v + d \end{aligned} \quad (2.3-5)$$

For most chrominance coordinates (c_1, c_2) the JND loci are ellipses which greatly vary in size, degree of elongation, and angle of rotation. True UCS transformation would map these JND ellipses into equidiameter circles. The 1960 CIE-UCS transform is a particular bilinear transform of the tristimulus coordinates which creates a chrominance plane that is a reasonably close approximation to the ideal UCS chrominance plane.

The widely accepted 1960 CIE-UCS chromaticity plane is illustrated in figure 2-5, with spectrum locus and white point, as well as the triangle whose vertices are the CIE RGB primaries. A color space consisting of the luminance and UCS chromaticity coordinates is sketched in figure 2-6. Compared to the linearly transformed parallelepiped L, C_1, C_2 space, there are much fewer wasted code words at low luminance levels. However, uniform quantization of the C_1 and C_2 coordinates results in very inefficient use of available chrominance code words at moderate luminance levels.

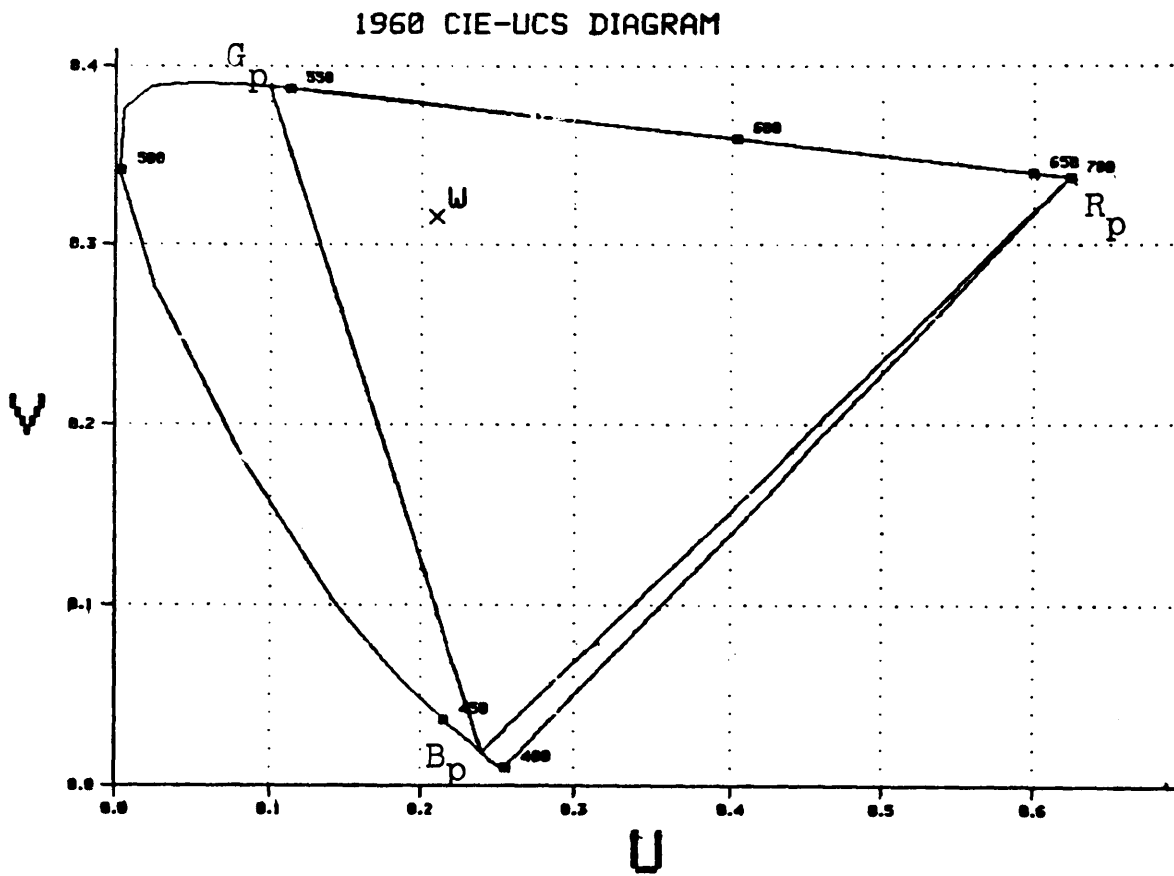


FIGURE 2-5. 1960 CIE UCS CHROMATICITY DIAGRAM

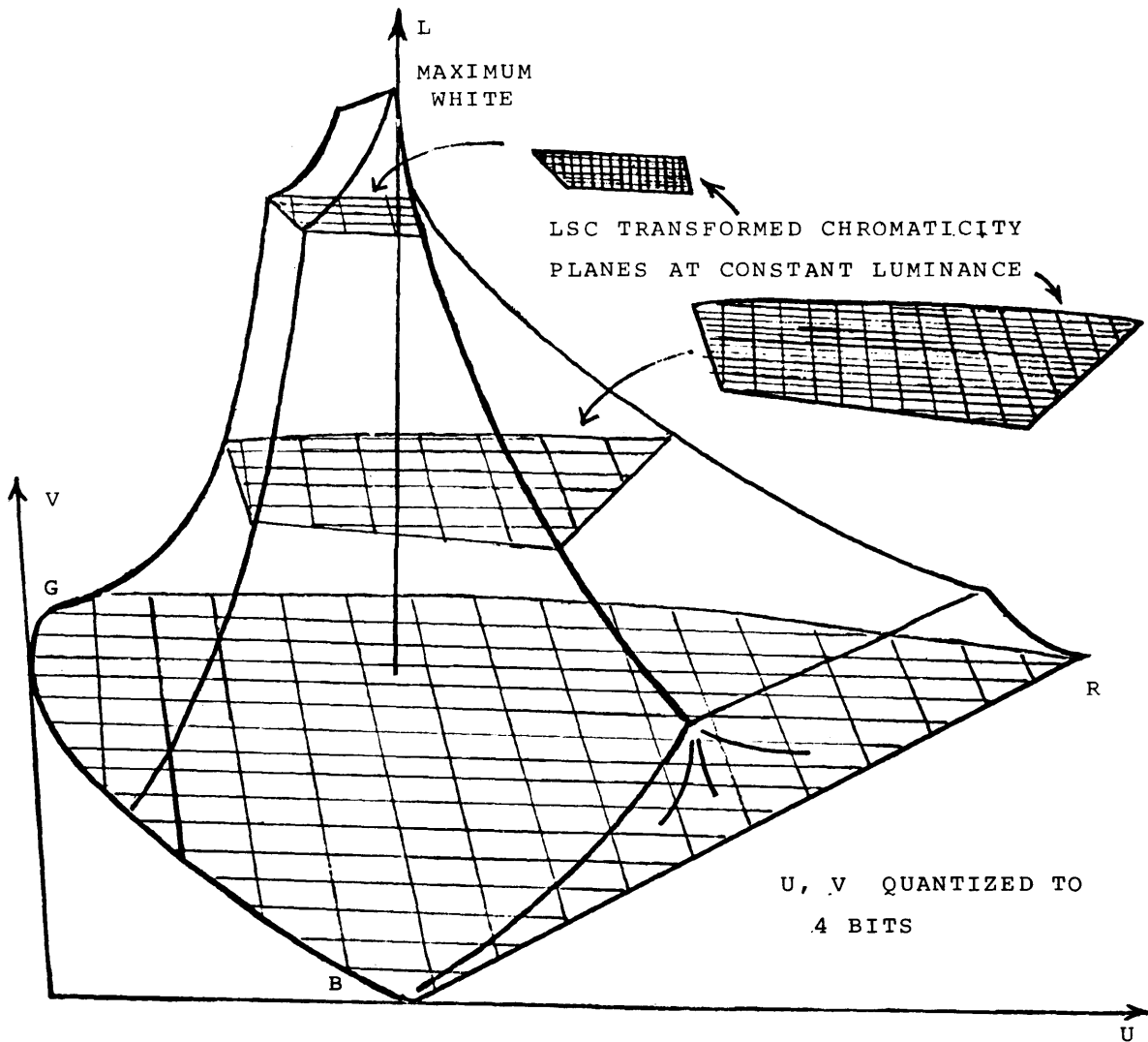


FIGURE 2-6. A SKETCH OF THE GAMUT OF REPRODUCIBLE COLORS FOR THE CIE UCS CHROMATICITY COORDINATES AS A FUNCTION OF LUMINANCE

2.4 The Luminance Scaled Chromaticity (LSC) Transform

In all common color reproduction systems, the gamut of chromaticities is constrained to lie inside a region in the UCS plane. In a typical picture the R, G, B primaries are statistically dependent. Most colors in a typical portrait or natural scene are achromatic or desaturated. Since the primaries must be nearly equal for desaturated colors, it follows that they are highly correlated with each other. This can be intuitively seen by observing the similarity of the red, green, and blue separations of a color picture (figure 2-7).

Transformation of the primary coordinates to a luminance and two independent UCS chrominance components results in a significant reduction of the inter-component correlations (figure 2-8).

When luminance is used as one of the three components, it has been shown that it restricts the values of the chrominance components, u and v (figure 2-6). For very low luminance levels, the R, G, B primaries may take on any ratio of values and u and v may assume any value within the chrominance plane primary triangle. When the luminance is increased above L_b the value of the blue primary luminosity coefficient, u and v are then restricted from taking on values in the saturated blue region of the chrominance plane. As the luminance is further increased, the area of permissible u and v values decreases until the maximum luminance is reached where the only possible chromaticity value is the achromatic point.

A series of constant luminance loci is plotted in figure 2-9. The loci contain the gamut of reproducible colors with the constraints of equations 2.1-3, 2.2-1, 2.2-2, and 2.3-4. Starting at the maximally saturated red value for a particular fixed luminance, the blue component



RED



BLUE



GREEN

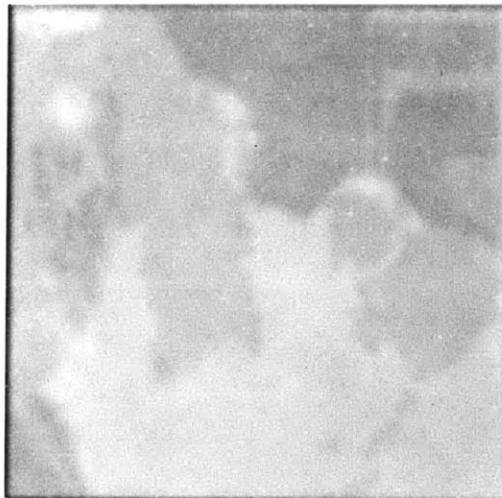
FIGURE 2-7. R, G, B SEPARATIONS OF GROUP PICTURE.



L



C1



C2

FIGURE 2-8. L, C1, C2 COMPONENTS OF GROUP PICTURE

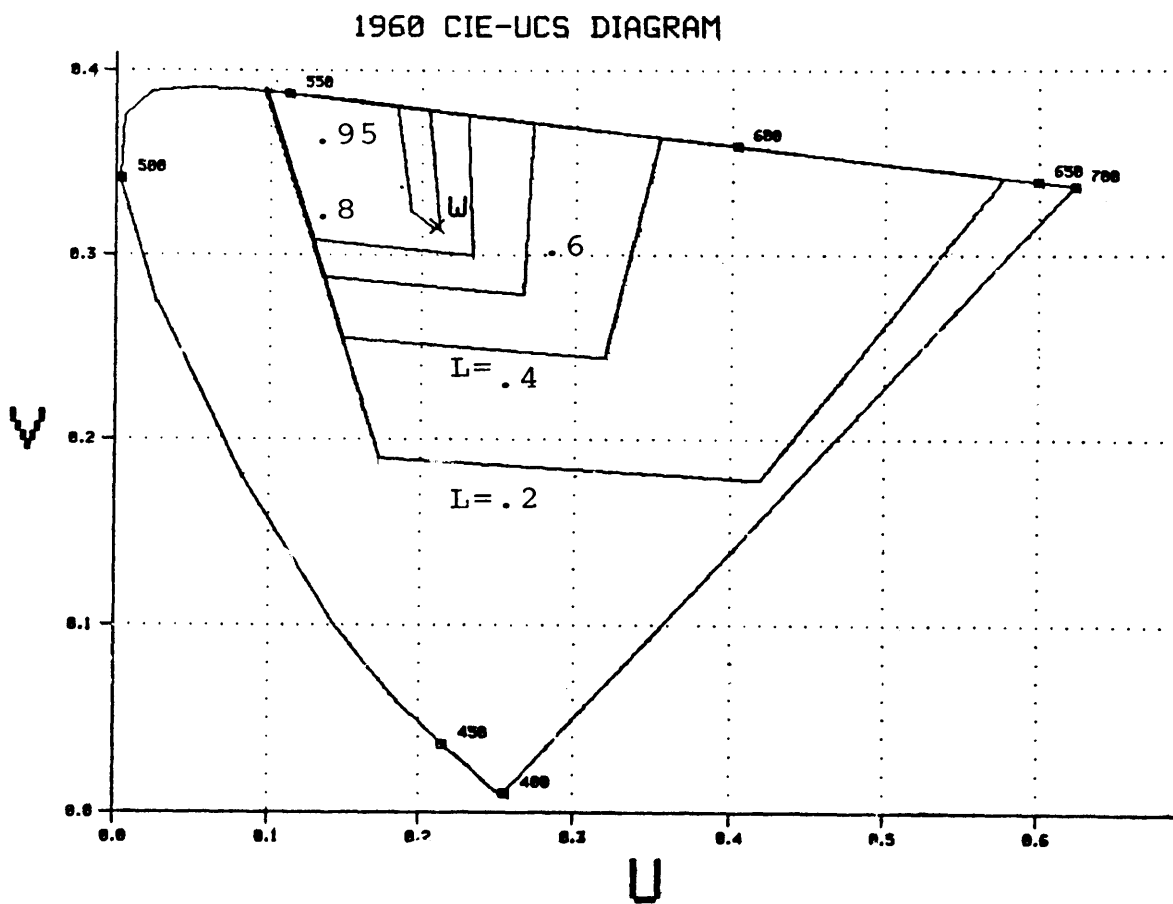


FIGURE 2-9. LOCI OF CONSTANT LUMINANCE ON UCS
CHROMATICITY DIAGRAM

is increased and the red decreased until the most saturated blue-magenta is reached. Then the green is increased and the red further decreased, moving the loci to maximally saturated blue-cyan. By increasing the green and decreasing the blue, the maximally saturated green point is reached. Finally, the green is decreased as the red increases back to its maximum possible value. These constant luminance planes are sketched as volume in color space in figure 2-6.

$$H_{\max} = \frac{L/L_H}{1} \quad \frac{L L_H}{L L_H} \quad \text{for } H = R, G, B \quad (2.4-1)$$

Another way of viewing the restriction of u and v values as a function of luminance is to realize that in a three primary color space (such as a subtractive photographic dye process, additive phosphor television system, or even the eye), the luminance component contains much chromaticity information and has been shown to be correlated with chrominance.⁽¹⁹⁾ Luminance is not highly correlated to low luminosity components such as blue, but is very highly negatively correlated with the relative blue component.

If the u and v coordinates are quantized, then even at very low luminance levels, chromaticity quantization is not too efficient since the right triangle base of figure 2-9 results in an area where only half of the possible number of codewords is utilized. The real colors lie in a horseshoe-shaped spectrum locus contained inside the triangular base and the gamut of reproducible colors lies inside the horseshoe. Thus even at the lowest luminance levels, simple quantization of u and v is less than 50 percent efficient. As the luminance increases the number

of valid chrominance code words is drastically reduced. Similar effects have been noted in the Munsell color system as value is increased.⁽²⁰⁾

To facilitate the development of the color coding algorithms, it is useful to monitor the effects of quantization and filtering on the red, green, and blue separations. The test pattern separations of figure 2-11 generate the full gamut of colors in the system by reproducing over 100,000 different triads of red, green, and blue values in the 256 pel by 256 line test pictures. The quantization contour artifacts resulting from coarse quantization of each chrominance component to four bits are shown in figure 2-12. These artifacts are most severe at high luminance levels. If u and v are each uniformly quantized to 16 levels, then at luminance levels above L_r , only 50 color boxes would be available to represent realizable colors.

In a typical natural scene, most of the chrominance values are clustered near the white point with a few more saturated colors lying along certain dominant hue lines which are different for each particular picture. The frequency of occurrence of C_1 and C_2 values which have been coarsely quantized to four bits (16 levels) each are listed in Table 2-1 for the group picture of figure 6-1A. Even for this rather colorful picture the C_1 and C_2 values are significant only near the white point.

Thus the desaturated colors, many of which often occur at high luminance levels as pastels, constitute the majority of colors in many pictures. Accurate reproduction of pale skin tones is crucial for achieving acceptable subjective color picture quality. As previously discussed, however, the number of available chrominance boxes is very small for these important pastel colors, resulting in objectionable quantization contours due to roundoff errors.

TABLE 2-1. FREQUENCY OF OCCURRENCE OF C1-C2 VALUES FOR THE GROUP PICTURE

<u>C1</u>																	
15 - 0	0	0	0	29	58	9	0	0	0	0	0	0	0	0	0	0	0
14 - 0	0	0	39	201	483	117	458	279	60	5	25	2	0	0	0	0	
13 - 0	0	0	18	442	^w 1106	286	135	442	421	23	49	10	0	0	0	0	
12 - 0	0	0	826	1169	318	40	6	9	2	0	0	0	0	0	0	0	
11 - 0	0	0	211	83	11	0	0	0	0	0	0	0	0	0	0	0	
10 - 0	0	0	69	63	0	0	0	0	0	0	0	0	0	0	0	0	
9 - 0	0	0	402	95	0	0	0	0	0	0	0	0	0	0	0	0	
8 - 0	127	0	0	0	0	0	0	0	0	0	0	0	0	0	0	0	
7 - 0	63	0	0	0	0	0	0	0	0	0	0	0	0	0	0	0	
6 - 0	0	0	0	0	0	0	0	0	0	0	0	0	0	0	0	0	
5 - 0	0	0	0	0	0	0	0	0	0	0	0	0	0	0	0	0	
4 - 1	0	0	0	0	0	0	0	0	0	0	0	0	0	0	0	0	
3 - 0	0	0	0	0	0	0	0	0	0	0	0	0	0	0	0	0	
2 - 0	0	0	0	0	0	0	0	0	0	0	0	0	0	0	0	0	
1 - 0	0	0	0	0	0	0	0	0	0	0	0	0	0	0	0	0	
0 - 0	0	0	0	0	0	0	0	0	0	0	0	0	0	0	0	0	
	0	1	2	3	4	5	6	7	8	9	10	11	12	13	14	15	

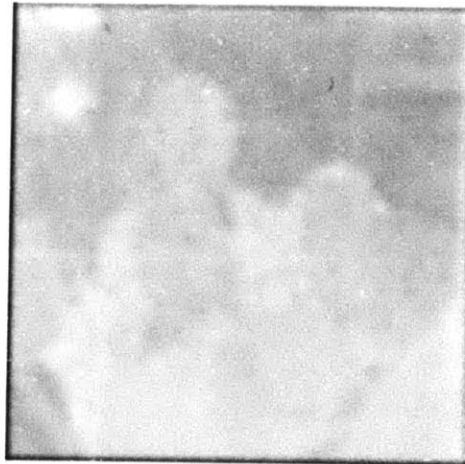
C2



L

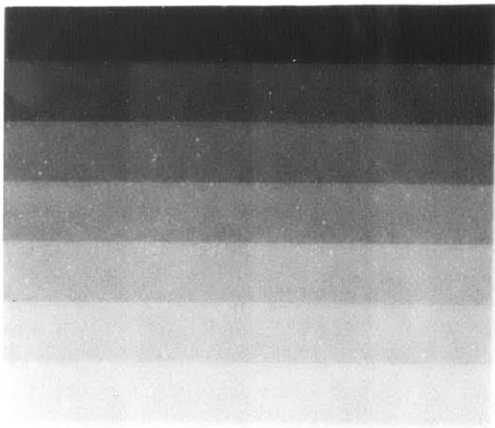


LSC C1

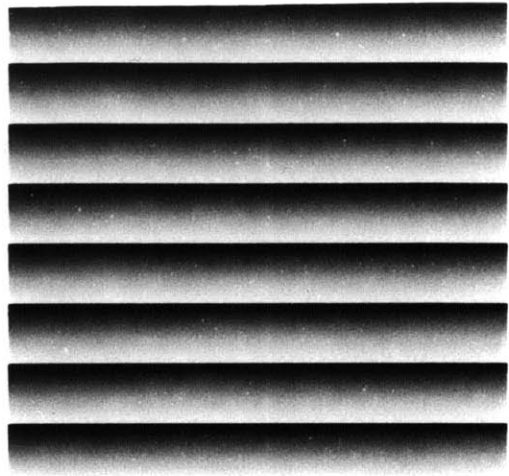


LSC C2

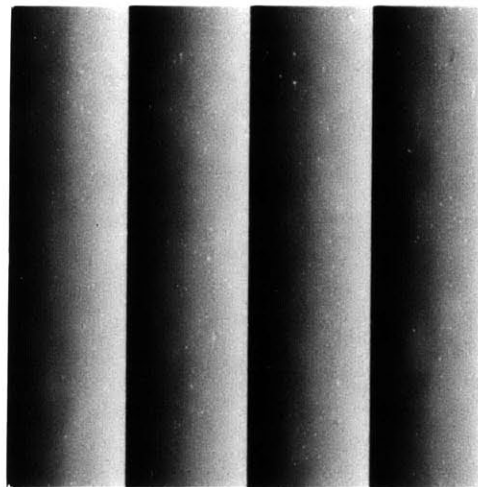
FIGURE 2-10. L AND LSC TRANSFORMED C1, C2 OF GROUP PICTURE



RED

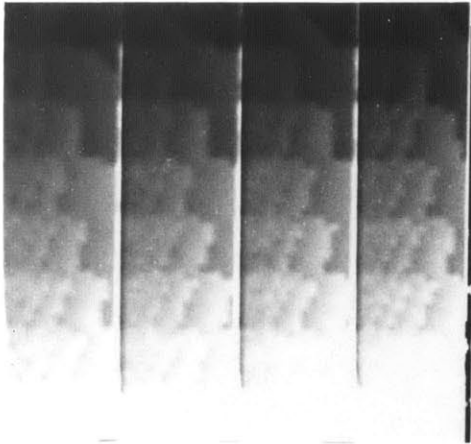


BLUE

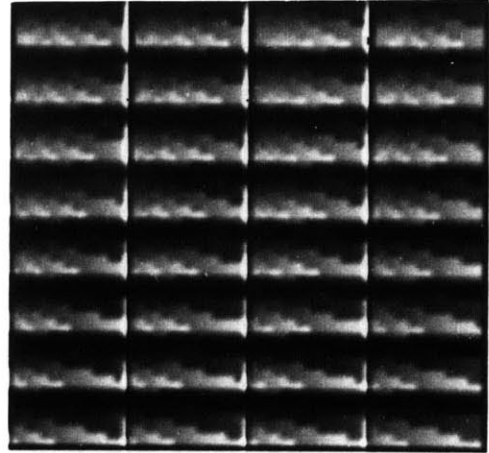


GREEN

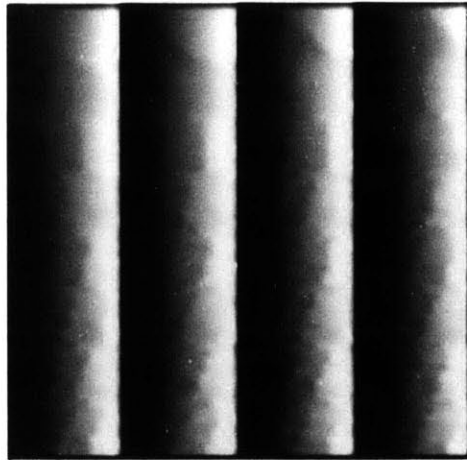
FIGURE 2-11. R, G, B SEPARATIONS OF TEST PICTURE



RED



BLUE



GREEN

FIGURE 2-12. R, G, B SEPARATIONS OF PROCESSED TEST PICTURE

To effectively quantize and code color pictures it is necessary to consider the psychophysical data of UCS space and the restrictions of the reproducible color gamut. The luminance scaled chrominance (LSC) space proposed and derived in this paper seeks to successfully combine the advantages of the UCS space with the luminance restrictions by scaling the UCS coordinates as a function of luminance so that the number of legitimate chrominance boxes at all luminance levels (even high luminance pastels) is nearly as large as for the lower luminance levels.

From figure 2-6 it is seen that the LSC transform cannot be continuous since the shape of the chrominance cross section planes varies at a rate which abruptly changes at the points where the luminance equals the primary luminosity coefficients L_r , L_g , L_b , and their combined sums $L_r + L_g$, $L_g + L_b$, $L_r + L_b$. The LSC transform is derived from the UCS transform by level shifting and scaling the UCS chrominance components as a function of the maximum and minimum values of u or v which are a function of luminance.

$$C_1(L) = N \left[\frac{u - u_{\min}(L)}{u_{\max}(L) - u_{\min}(L)} \right] \quad C_2(L) = N \left[\frac{v - v_{\min}(L)}{v_{\max}(L) - v_{\min}(L)} \right] \quad (2.4-2)$$

where N is the number of chrominance levels.

To preserve the UCS space, $C_1(L)$ and $C_2(L)$ should be equally scaled. However, optimum utilization of available codewords necessitates unequal scaling. The resulting departure from a true UCS space at high luminance levels yields a much finer quantization of the chrominance plane.

The LSC transform (equation 2.4-2) can now be calculated by determining the magnitude range of L by boundary tests. The proper $u_{\min}(L)$

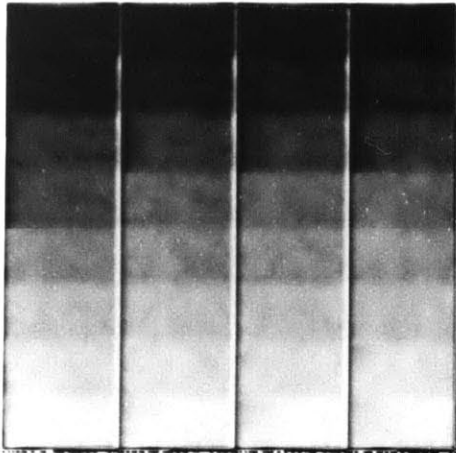
and $u_{\max}(L)$ functions are first evaluated and then $C_1(L)$ and $C_2(L)$ can be derived. The minimum and maximum u and v are shown (in Appendix III) to be of the form:

$$\begin{array}{l} \min \\ \text{or} \\ \max \end{array} \begin{bmatrix} u \\ \text{or} \\ v \end{bmatrix} = [a + bL]/[c + L] \quad (2.4-3)$$

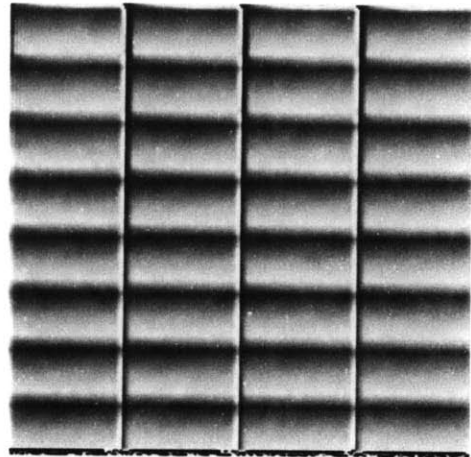
so only six constants (at most) need be stored for each range of L values. The inverse LSC transform is of the same form and uses the same coefficients.

The LSC transform can be simplified by fixing the transform scaling and shifting parameters to their values at L_g for luminance levels greater than L_g . With this limitation, the pastel colors will still have much greater chrominance resolution than with just the UCS transform, and limiting the scaling avoids the problem of scaling up a vanishingly small area of valid chrominance values by very large factors at large luminance values. Figure 2-6 illustrates the substantial increase in reproducible chrominance codeword boxes in the LSC transformed coordinates at high luminance levels.

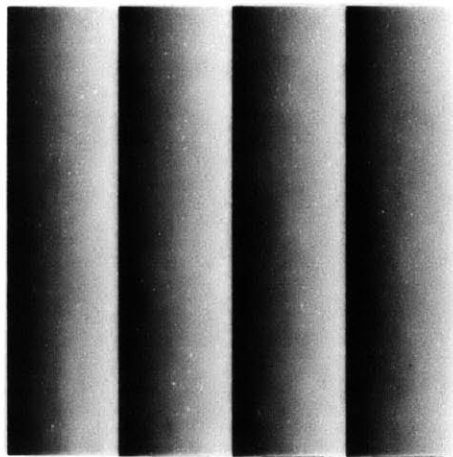
Comparing the processed separation test pattern of figure 2-12 with that of figure 2-13 dramatically illustrates the effectiveness of the LSC transform. In figure 2-10 it can be seen that the LSC transform further reduces the spatial correlations between the luminance and the two chrominance components as compared with figure 2-9. When the two chromaticity components are LSC transformed before four bit quantization, the C_1 and C_2 values are much more uniformly distributed as shown in Table 2-2. After LSC transformation, no one particular set of values of C_1 and C_2 corresponds to the white point.



RED



BLUE



GREEN

FIGURE 2-13. R, G, B SEPARATIONS OF PROCESSED TEST PICTURE
WITH LSC TRANSFORM

TABLE 2-2. FREQUENCY OF OCCURRENCE OF LSC TRANSFORMED C1-C2 VALUES FOR THE GROUP PICTURE

<u>C1</u>																		
15 -	0	0	0	0	0	0	0	0	0	0	0	0	0	0	0	0	0	0
14 -	0	0	11	18	7	1	0	0	0	0	0	0	0	0	0	0	0	0
13 -	0	23	39	318	68	13	12	0	1	0	0	0	0	0	0	0	0	0
12 -	1	11	219	483	35	43	49	129	14	8	12	20	0	0	0	0	0	0
11 -	25	318	496	75	46	53	448	306	20	26	61	35	82	43	14	0		
10 -	0	132	165	134	60	27	21	45	19	11	11	15	13	74	206	111		
9 -	0	273	261	45	14	8	36	45	59	33	24	8	4	7	85	47		
8 -	92	120	17	26	24	13	22	64	60	36	17	4	3	0	0	0		
7 -	0	213	79	19	37	23	30	19	24	35	60	41	19	1	0	0		
6 -	0	334	7	60	28	20	42	17	3	4	22	18	25	1	0	0		
5 -	0	0	0	7	158	244	8	85	1	0	3	9	11	2	1	156		
4 -	0	0	0	0	2	45	14	35	10	2	1	6	1	3	1	2		
3 -	0	0	0	0	1	1	3	27	17	4	0	1	2	7	1	32		
2 -	1	0	0	0	0	0	1	9	1	0	1	2	2	0	0	0		
1 -	0	0	0	0	0	0	0	01	0	4	2	5	3	2	0	0		
0 -	0	0	0	0	0	0	0	0	0	0	0	0	0	0	0	0		
	0	1	2	3	4	5	6	7	8	9	10	11	12	13	14	15	<u>C2</u>	

III. The Chrominance Spatial Filtering Process

3.1: The Psychophysical Basis for Chrominance Spatial Filtering

3.2: The Overall Filter Function

3.3: Luminance Filtering for the LSC Transform

3.1 The Psychophysical Basis for Chrominance Spatial Filtering

The ability to compress the color components of a picture is primarily due to the eye's lower spatial acuity for chrominance detail relative to the luminance acuity. Phrased another way, the lower spatial bandwidth of chrominance in the eye implies a higher degree of spatial correlation in the eye for the chrominance components. In addition, early work in the area⁽²¹⁻²⁴⁾ suggests that the trichromatic visual system becomes dichromatic as the size of a color patch is decreased. For small patches the eye appears to behave as if it were tritanopic (i.e., exhibits blue color blindness). The axis in the chromaticity diagram for the highest resolution was determined to be along the orange-red cyan axis.⁽²⁵⁾

From measurements of the chromatic modulation transfer function of the eye, it has been found that for color spatial variation the high frequency response falls off faster than in the case of luminance.⁽²⁶⁾ This suggests that the effective color receptor area is larger than the luminance receptor area. In addition, no Mach Band effect is noted at heterochromatic, equi-luminance transitions implying that the retinal color mechanism is not spatially organized as Kuffler units as is the luminance system.⁽²⁷⁾ Supporting these observations are chromatic modulation transfer function data which indicate that, unlike the luminance case, there is no low spatial frequency fall-off or peaking noted in tests with colored sinewave gratings.⁽²⁸⁾

The first subjective experiments on chrominance filtering were performed by the NTSC.⁽²⁵⁾ An initial experiment describes testing various subjects with many color pictures, in which the luminance had full resolution, but the R, G and B horizontal resolution could be decreased by a factor of four, before any substantial picture degradation

was noted.⁽²⁹⁾ An experiment by Baldwin⁽³⁰⁾ was the first to demonstrate two dimensional color filtering by defocusing separately the blue, red and green separations with an additive projector until subjective degradation was noticed. This acuity for defocus was found to be almost the same for green as for luminance (white). The red image could be defocused much more than the green without noticeable degradation. Furthermore, the blue could be completely defocused within the limits of the projector with no perceived effects. These measurements, however, are not a result of strict chrominance filtering, and the blue defocusing for high luminance color pictures can be explained by the chromatic aberration in the eye. The first series of experiments which spatially filtered and coarse sampled the chrominance in two dimensions was done by Gronemann, who obtained good quality pictures by spatially sampling the chrominance at 1/20 the resolution of the luminance.⁽¹⁰⁾

Color television makes use of the higher resolution of the chromaticity components in the orange-cyan direction by choosing one chrominance component (the I signal) in this direction to have three times the bandwidth of the other perpendicular chrominance component (Q signal). Most commercial receivers do not have the expensive circuitry to detect the full bandwidth I signal and so for all practical purposes I and Q signals have similar spatial resolution. In the facsimile system, the compression ratio is not appreciably improved if the two chromaticity components are unequally filtered. In addition, Chapter Four discusses linear transforms performed on the coarsely sampled, filtered chromaticity components, requiring that they be identically coarse sampled.

3.2 The Overall Filter Function

There are actually four distinct digital processing operations which give rise to the overall filter function (figure 3-1). First, at the transmitter, the value of the chrominance components at each pel (with horizontal and vertical position indices m,n), $x(m,n)$, is given a weight, $h(m,n)$, and summed, yielding a filtered output point, $w(m,n)$. This superposition method of filtering is the easiest to implement and is feasible if the filter requirements are not too stringent.

$$w(m,n) = \sum_{j=1}^N \sum_{k=1}^N x(m + j, n + k) h(j,k) \quad (3.2-1)$$

For isotropic systems, hexagonal sampling with circularly symmetric filter functions is preferred. However, a rectangular sample structure permits the use of easily implemented filters which are separable in the vertical and horizontal directions.

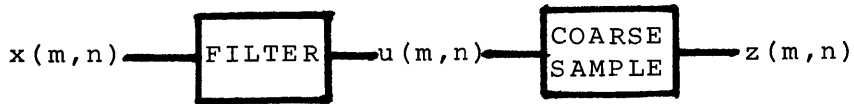
$$h(j,k) = h_1(j) h_2(k) \quad (3.2-2)$$

For a separable filter function, 3.2-1 becomes:

$$w(m,n) = \sum_{k=1}^N h_2(k) \sum_{j=1}^N h_1(j) x(m + j, n + k) \quad (3.2-3)$$

The vertical and horizontal resolutions of the facsimile system are nearly equal and since the eye is basically spatially isotropic, the filters should be the same in both the horizontal and vertical directions.

$$h_1(j) = h_2(j) = h(j) \quad (3.2-4)$$



a) Transmitter Signal Processing



b) Receiver Signal Processing

FIGURE 3-1. THE FOUR STAGES OF THE OVERALL FILTER FUNCTION

The next processing operation at the transmitter operation is coarse sampling which can easily be implemented with superposition filters by performing the filter operation once every N pels and N lines rather than at each pel.

$$z(m,n) = \sum_{k=1}^N h(k) \left[\sum_{j=1}^N x(Nm+j, Nn+k) h(j) \right] \quad (3.2-5)$$

The operation inside the brackets of equation 3.2-5 represents the superposition filter function in the scan direction. Thus, filtering of the chromaticity components can be accomplished by first stream process filtering and coarse sampling in the scan direction and then storing the filtered coarse samples in a line buffer. The stored lines can be weighted, and summed every N lines. The compression factor, therefore, is N^2 (e.g., 16:1 for $N = 4$).

As shown in figure 3-2, the line storage required to implement the two dimensional filter is insignificant, requiring only $1/N$ times the total number of pels per line words of storage for each chromaticity component. The main limitation is the luminance delay buffer which must store at least N lines at full resolution. The luminance delay buffer compensates for the delay in the chrominance filtering and coarse sampling operations. The delay buffering may be done at the transmitter or receiver but since a facsimile network usually has far more receivers than transmitters, it is economical to design the additional line memory into the transmitter. Based on the design requirements, N is chosen to be four, resulting in a 16:1 compression ratio. Fortunately, this is compatible with the psychophysical experimental results referred to in section 3.1. By choosing the filter functions to be symmetric, two

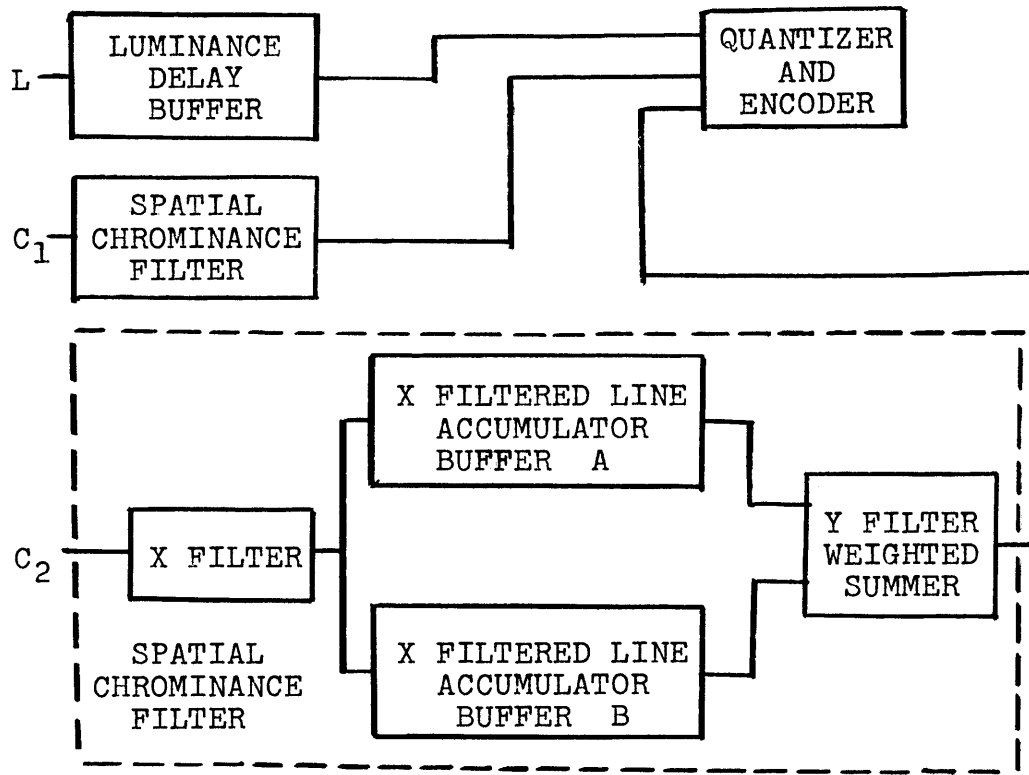


FIGURE 3-2. TWO DIMENSION FILTER BLOCK DIAGRAM

filtered line accumulators may be used to weight the four pels and four lines twice, corresponding to the first and second halves of the filter function shown in figure 3-3. Thus the maximum size of the transmitter filter function is eight pels by eight lines. Figure 3-4 illustrates the two dimensional nature of the sampling and filtering.

Most researchers who have analyzed the problem of filtering and interpolation^(31,32) treat these two operations separately. At the receiver the coarsely sampled and filtered chromaticity components are interpolated between four equally spaced intersample points (figure 3-4) which is equivalent to a continuous interpolation filter (figure 3-5) followed by fine sampling at four points (figure 3-6). The overall filter function (OFF) is really the net result of all four processing operations and it is this filter function, not the transmitter filter function alone which must be chosen to meet psychophysical and system constraints.

In two dimensions, the interpolation function has the form:

$$\begin{aligned}
 y(m,n) = & z(\text{INT}[m/N], \text{INT}[n/N]) a_{(n)_N} + \\
 & z(\text{INT}[m/N]+1, \text{INT}[n/N]) b_{(n)_N} + \\
 & z(\text{INT}[m/N], \text{INT}[n/N]+1) c_{(n)_N} + \\
 & z(\text{INT}[m/N]+1, \text{INT}[n/N]+1) d_{(n)_N}
 \end{aligned}
 \tag{3.2-6}$$

where if $k = \text{INT}[n/N]$, then k is the largest integer such that $k \leq n/N$. $(n)_N$ is "n modulo N" so if $j = (n)_N$ then $j = (n - kN)$, where k is the largest integer such that $n \geq kN$.

There are therefore N different sets of a,b,c,d interpolation coefficients.

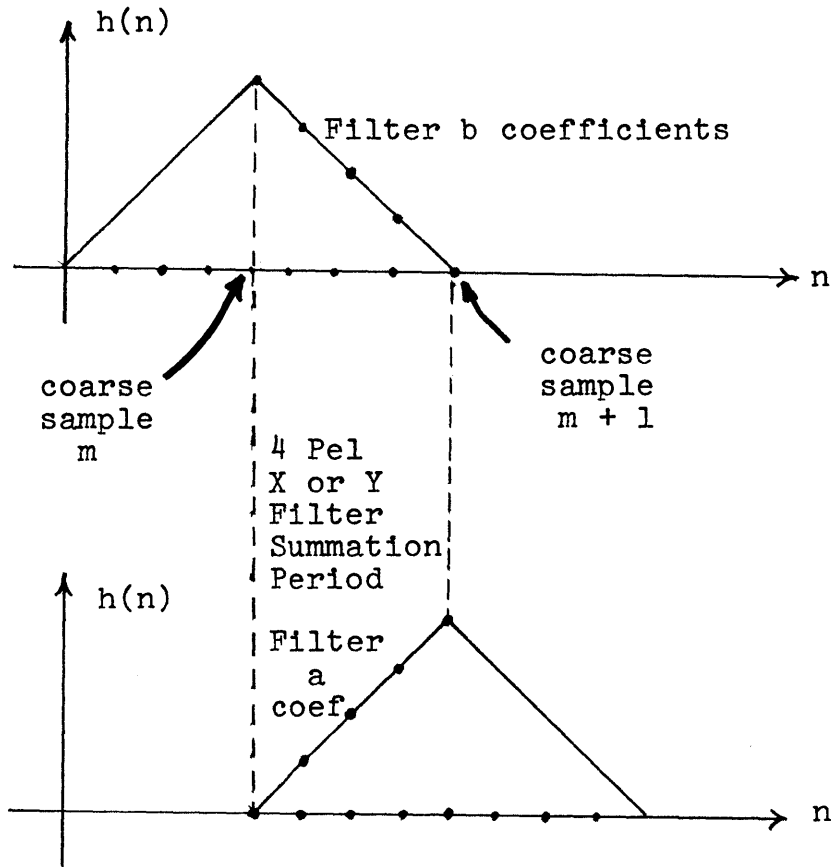


FIGURE 3-3. THE SYMMETRIC FILTER FUNCTION

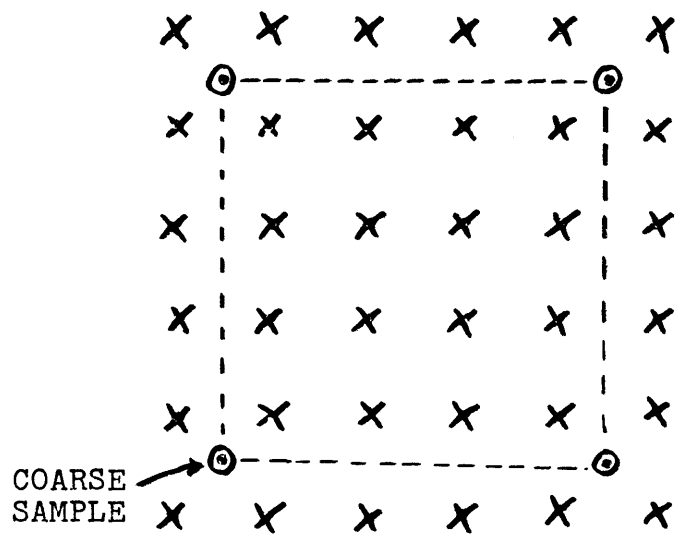


FIGURE 3-4. TWO DIMENSIONAL COARSE SAMPLING AND INTERPOLATION

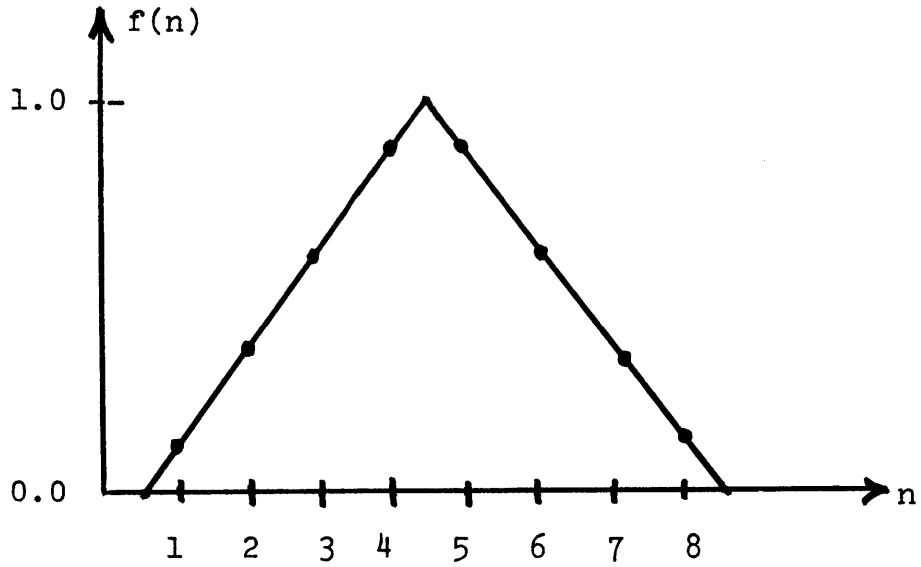


FIGURE 3-5. CONTINUOUS INTERPOLATION FUNCTION

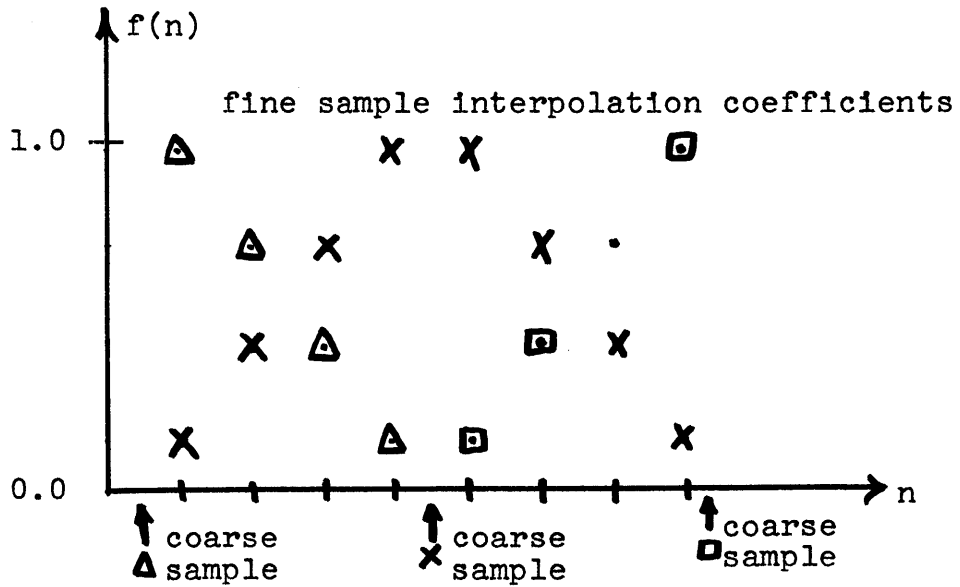


FIGURE 3-6. THE SAMPLED INTERPOLATION FUNCTION

To enable stream processing of the color pels, the interpolation function must be separable. Furthermore, the interpolation coefficients are chosen to be equal in the vertical and horizontal directions as in the case of the transmitter chrominance filter.

$$y(m,n) = \left[\begin{array}{l} a'_{(n)_N} z(\text{INT}[m/N], \text{INT}[n/N]) + \\ b'_{(n)_N} z(\text{INT}[m/N] + 1, \text{INT}[n/N]) \end{array} \right] a'_{(n)_N} + \left[\begin{array}{l} a'_{(n)_N} z(\text{INT}[m/N], \text{INT}[n/N] + 1) + \\ b'_{(n)_N} z(\text{INT}[m/N] + 1, \text{INT}[n/N] + 1) \end{array} \right] b'_{(n)_N} \quad (3.2-7)$$

where the terms in square brackets represent interpolation along a line.

If the two coarse samples (in one dimension) are equal, then the interpolated samples should be equal to this value. This implies that:

$$a_{(n)_N} + b_{(n)_N} = 1 \quad (3.2-8)$$

Thus an equi-valued region which is coarse sampled and then interpolated by a linear or raised cosine function yields equivalued points. However, any interpolator which does not obey equation 3.2-8 (e.g. Gaussian) introduces a non-uniformity into the interpolated values. This would be perceived in a picture as a characteristic ripple over a flat region of chromaticity values.

For symmetrical interpolation about the center point between samples:

$$a_{(n)_N} = b_{(N-(n))_N} \quad (3.2-9)$$

or:
$$b_{(n)_N} = 1 - a_{(N-(n))_N} \quad (3.2-10)$$

A most important result is best illustrated by examining the overall filter function in one dimension. From equations 3.2-5 and 3.2-7 :

$$y(n) = \sum_{k=1}^N h(k) [x(\text{INT}[n/4]+k) a_{(n)_4} + x(\text{INT}[n/4]+1+k) a_{(4-(n)_4)}] \quad (3.2-11)$$

The above equation shows that since the new effective filter coefficients vary with the index 'n' , four different sets of coefficients will yield four different overall filter functions! These four functions are repeated every four pels and every four lines, but they sequentially alternate at adjacent pels between coarse samples. This mathematical form of a function is referred to by the author as "modulo-periodic" . For the two dimensional filter function there will be 16 distinct filter functions. The filter functions are plotted in figure 3-8 for the transmitter filter of figure 3-7. The peaks of the functions are different and the shapes are very asymmetrical and unsymmetric with each other, although the sums of the filter coefficients are the same for each function. By differently weighting the neighboring pels on a modulo periodic basis, artifacts are introduced over monotonically increasing areas as shown in figure 3-11(a) where the chromaticity components of the color picture have been processed by the overall filter function of figure 3-8.

To improve the filter shapes of figure 3-8, the coefficients of the transmitter triangular filter function may be rechosen as in figure 3-9. This results in a more symmetrical group of modulo filter functions (figure 3-10). All of the processed test pictures except figure 3-11 use the overall filter function of figure 3-10. The artifacts introduced by highly asymmetric overall filter functions are worse for less well-behaved functions than the monotonic test separations.

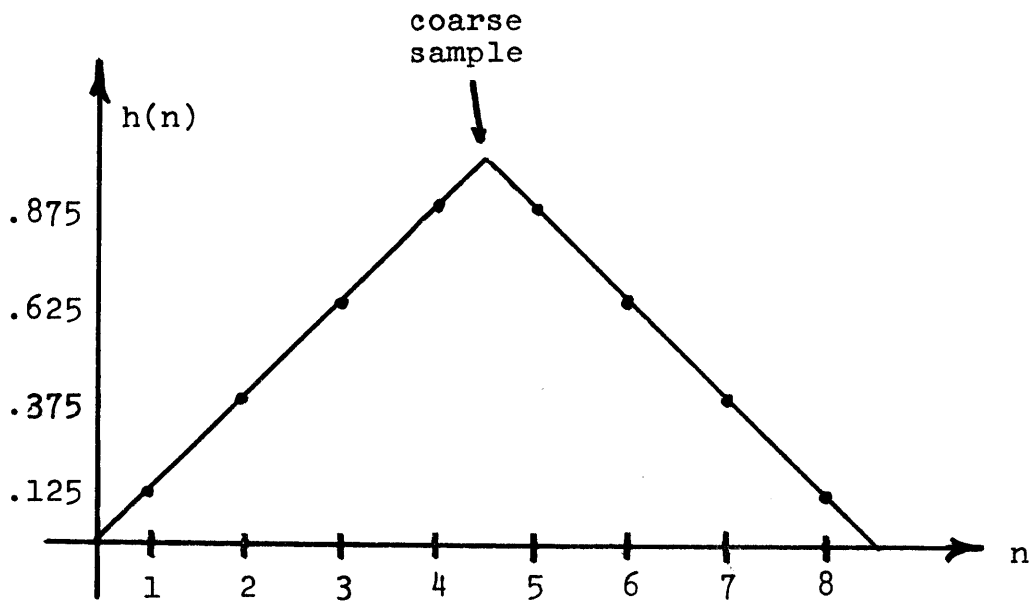


FIGURE 3-7. TRIANGULAR TRANSMITTER FUNCTION

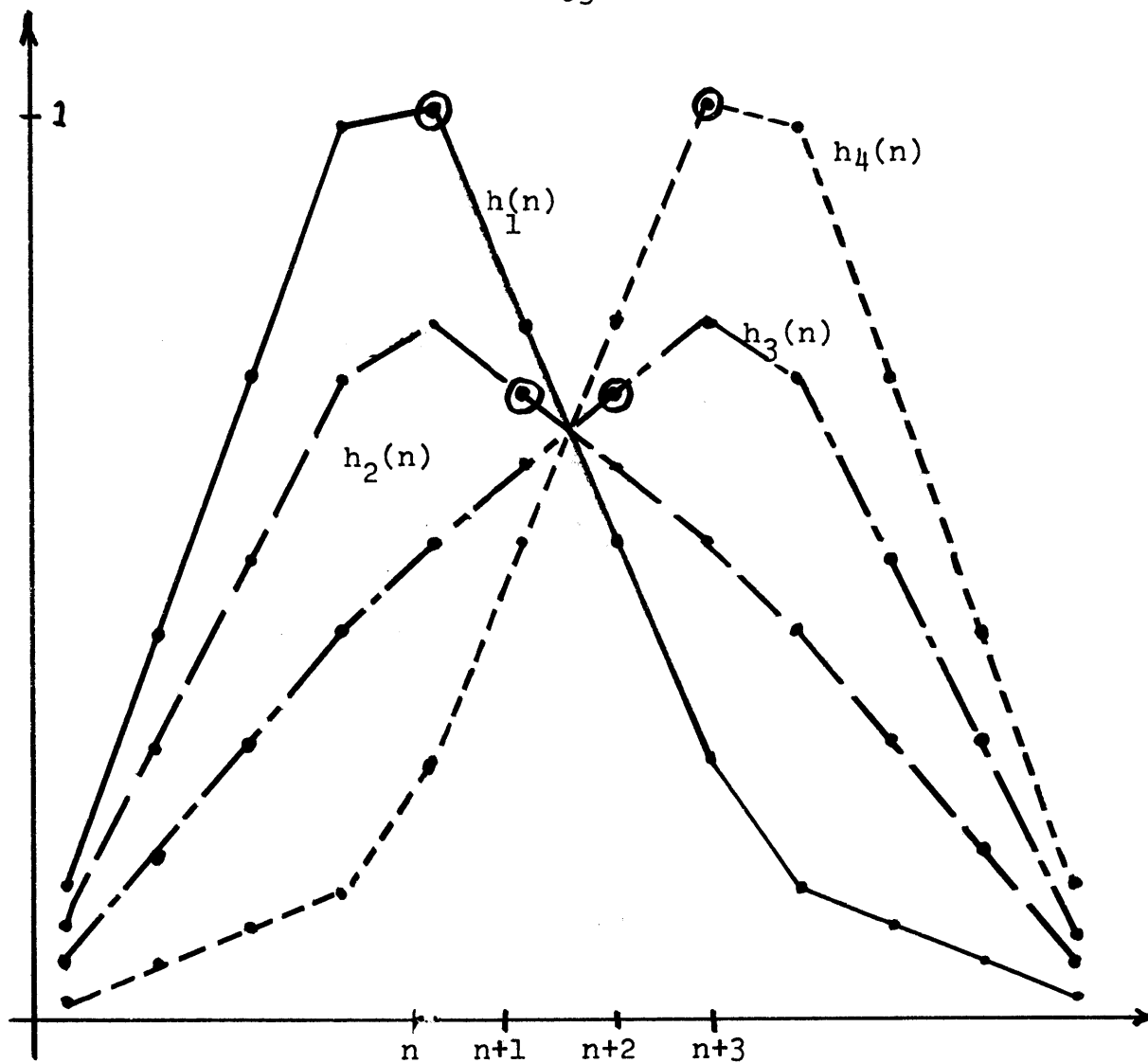


FIGURE 3-8. O.F.F. FOR THE TRANSMITTER FILTER FUNCTION OF FIGURE 3-7

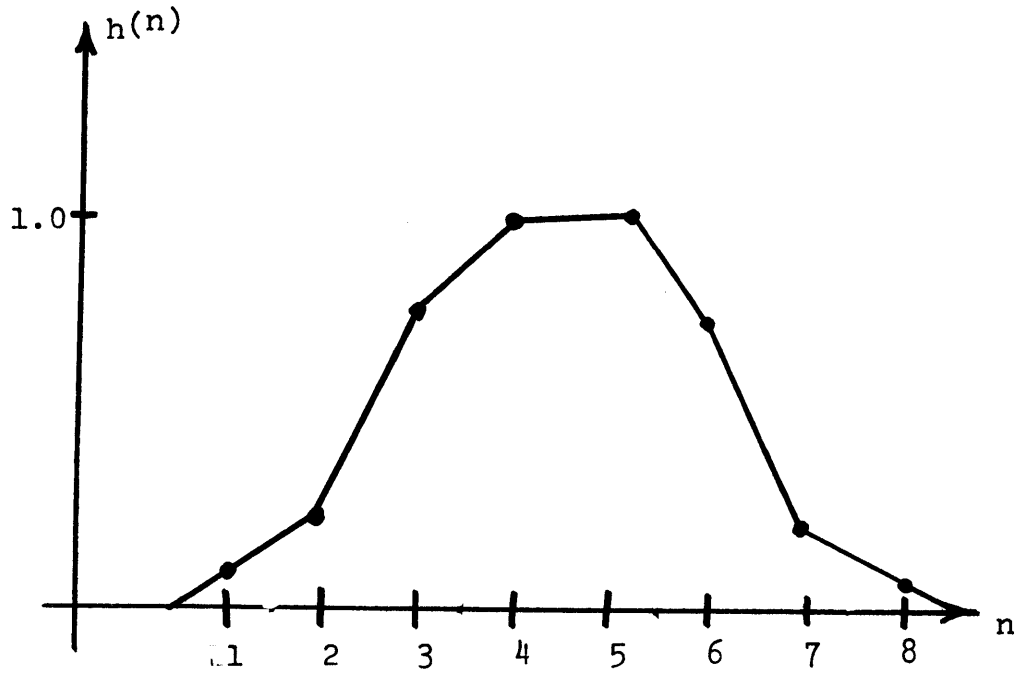


FIGURE 3-9. MODIFIED FILTER FUNCTION

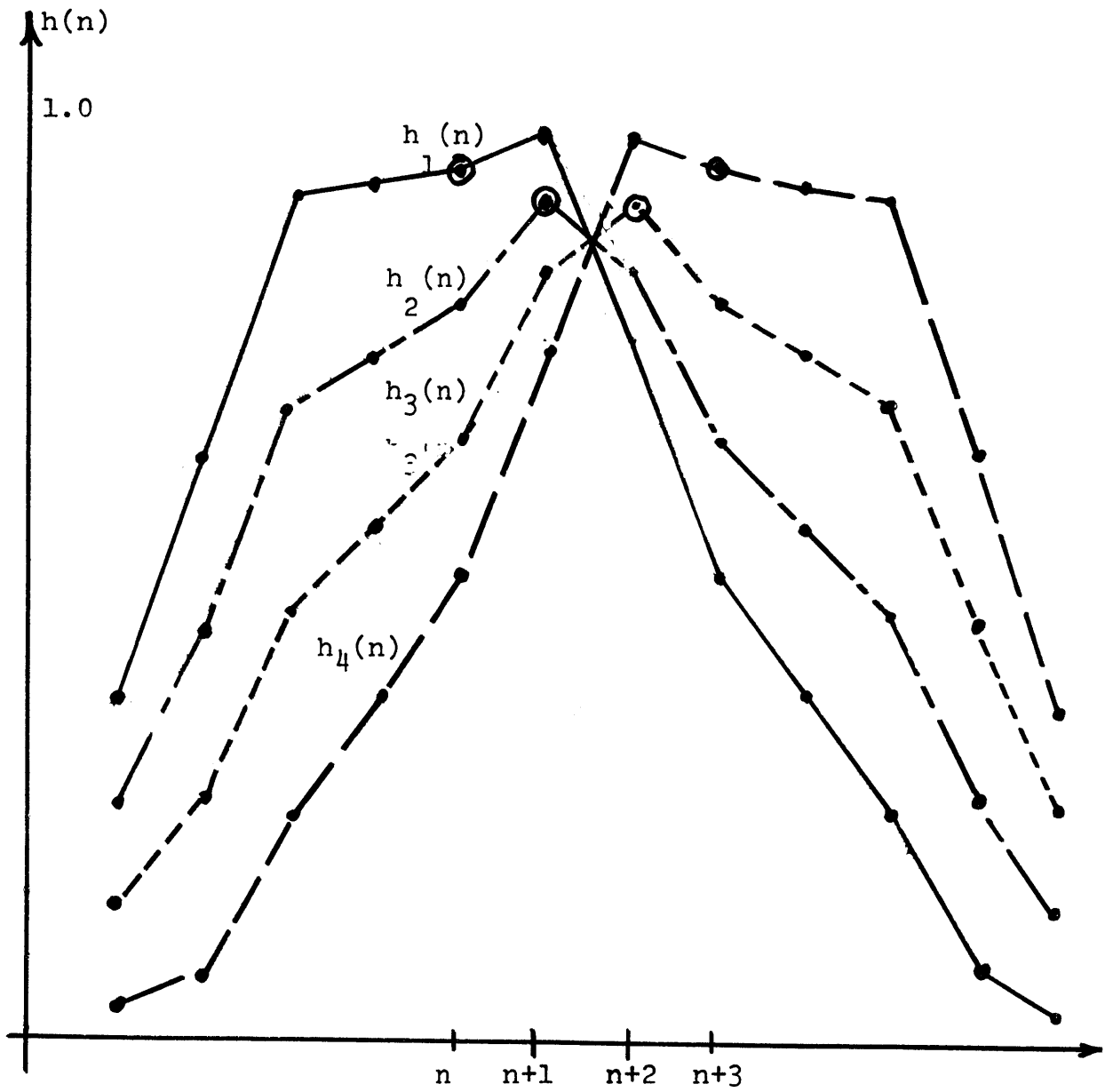
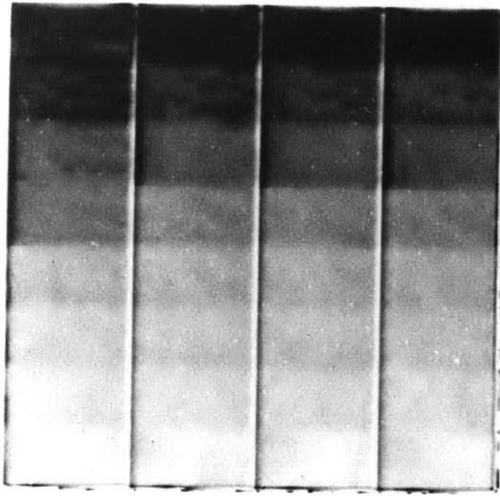
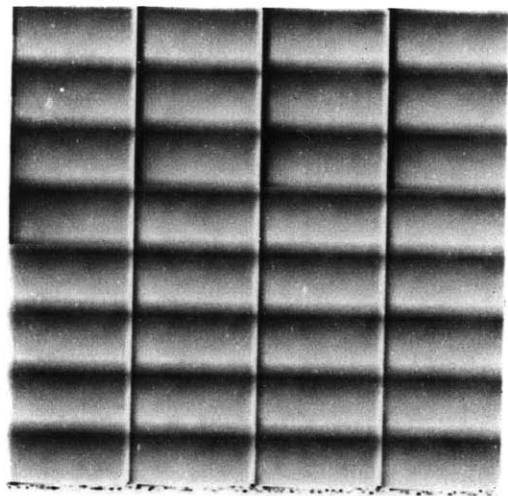


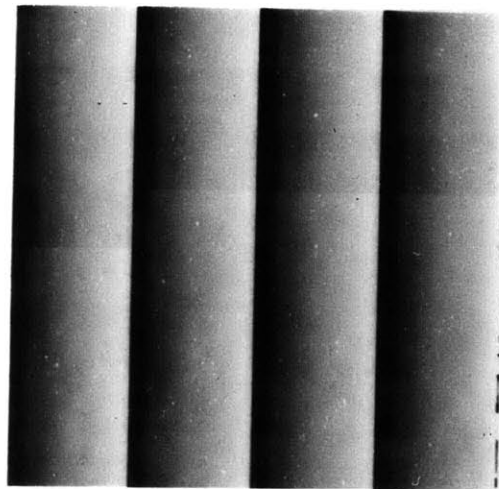
FIGURE 3-10. O.F.F. FOR THE TRANSMITTER FILTER FUNCTION OF FIGURE 3-9



RED



BLUE



GREEN

FIGURE 3-11. R, G, B SEPARATIONS OF TEST PICTURE
PROCESSED BY THE OFF OF FIGURE 3-8.

When C_1 and C_2 are processed by the overall filter function and then inverse transformed with the full resolution luminance to yield the output red, green, and blue CIE color coordinates, at some particular luminance level, the weighted overall filter averages of C_1 and C_2 may yield an illegal triad of R,G,B values necessitating clipping of the R, G, or B at zero or unity. These illegal codeword artifacts will be more pronounced with an overall filter function which is highly asymmetric. Such artifacts are obvious in the processed test picture (figures 2-12 and 2-13) where the green component suddenly changes from its maximum to minimum values.

3.3 Luminance Filtering for the LSC Transform

An important issue arises in deciding what value of L should be used in the LSC transform of Section 2-4, which follows the filter and is the last operation on the chromaticity components before transmission. To avoid decoding illegal values of C_1 and C_2 , L should strictly be chosen as the minimum L among all of the pels contributing to the overall filter function. This, however, would not permit the full power of the LSC transform to be realized. Instead, the luminance should be filtered and coarsely sampled in an identical manner as the chrominance. However, there is no need to perform the additional operations of interpolation resulting in a wider overall filter function, since the LSC transform and its inverse are performed on the chromaticity components before interpolation (figure 3-12)

A more conservative bound on the the filtered luminance results from filtering its logarithmic function. The filtered logarithmic function will of course have to be exponentiated before LSC transforming. Filtering

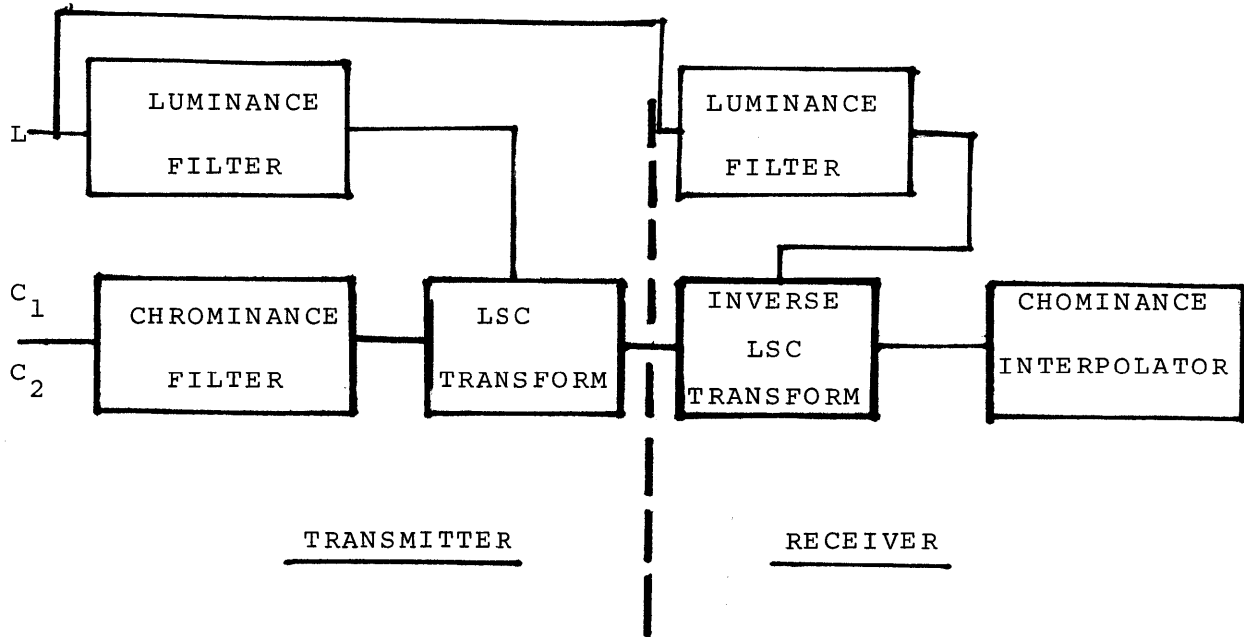


FIGURE 3-12. LSC TRANSFORM DISTRIBUTED BETWEEN TRANSMITTER AND RECEIVER.

in the log domain results in a geometric mean of the luminance values rather than the arithmetic mean obtained in the linear domain. For integer values the geometric mean will always be less than the arithmetic mean.

$$\frac{1}{M} \sum_{i=1}^M L_i \geq \text{Exp} \left[\frac{1}{M} \sum_{i=1}^M \text{Log } L_i \right] = \left(\prod_{i=1}^M L_i \right)^{1/M} \quad (3.3-1)$$

IV. Colorimetric Measurement and Photographic Reproduction Approximations

4.1: The Color Photographic Process

4.2: Quasi-Tristimulus Color Measurement

4.3: Colorimetrically Accurate Photographic Reproduction

4.1 The Color Photographic Process

In the previous two chapters, various color coding techniques have been developed to process psychophysical variables. Therefore, it is assumed that the color measurements at each pel of the scanned input picture constitute a proper tristimulus set. Thus for practical color head filters, transforms must be developed to approximate the tristimulus functions. This chapter also examines the problem of reproducing the processed psychophysical parameters of the original print at each pel. Due to spatial filtering and interpolation of the processed picture, there may not be a strict colorimetric equivalence between the input and output picture at each pel, but over fine detail regions the average color values over an area of several pels should closely match. The photographic subtractive dye process is the major limitation to obtaining perfect color reproduction.

In most commercial applications of color facsimile, the red, green, and blue separations are used to make cyan, magenta, and yellow press plates for reproduction by printing inks. To avoid the expense and delay of obtaining color press proofs, it was decided to reproduce the various test picture separations by photographic techniques. The photographic continuous tone process is somewhat simpler to analyze than the printing process⁽³³⁾ since no half tone screen is required, and the dyes are restricted to overlapping dye layers as contrasted with individually printed colored inks. However, both processes are similar in that they use subtractive dyes to synthesize colors. The entire body of colorimetry, however, has been developed in terms of additive color reproduction and so the analysis of a subtractive dye system is rather complex.^(34,35)

The cyan, magenta, and yellow subtractive dyes reproduce colors by respectively modulating the transmission of the red, green, and blue components of the light through the layered dyes. In a reflectance print, the illuminating light passes through the dyes twice since it is reflected from the white substrate. Thus, the effective dye density for reflectance prints is twice the actual density of the dye. An ideal set of dyes would only absorb light in block bands. For an equi-energy white illuminant, the reflected light spectrum can be expressed as a function of the dye spectral density.

$$\rho(\lambda) = 10^{-D(\lambda)} \quad (4.1-1)$$

In general, the color coordinate X_j of a dye is related to the density by a much more complex relation than a simple exponential function.

$$X_j = \int x_j(\lambda) \rho(\lambda) d\lambda = \int x_j(\lambda) 10^{-D(\lambda)} d\lambda \quad (4.1-2)$$

In a block dye approximation (i.e., as in figure 4-1 the cyan dye absorption is assumed constant over the red band), the spectrally integrated value of the red component is a simple function of the cyan density:

$$D_c(\lambda) = c \quad R = \int \bar{r}_\lambda 10^{-c} d\lambda = c_r 10^{-c} \quad (4.1-3)$$

In fact, the cyan dye has unwanted absorptions in the green and blue range of wavelengths, resulting in a darkening and desaturation of the

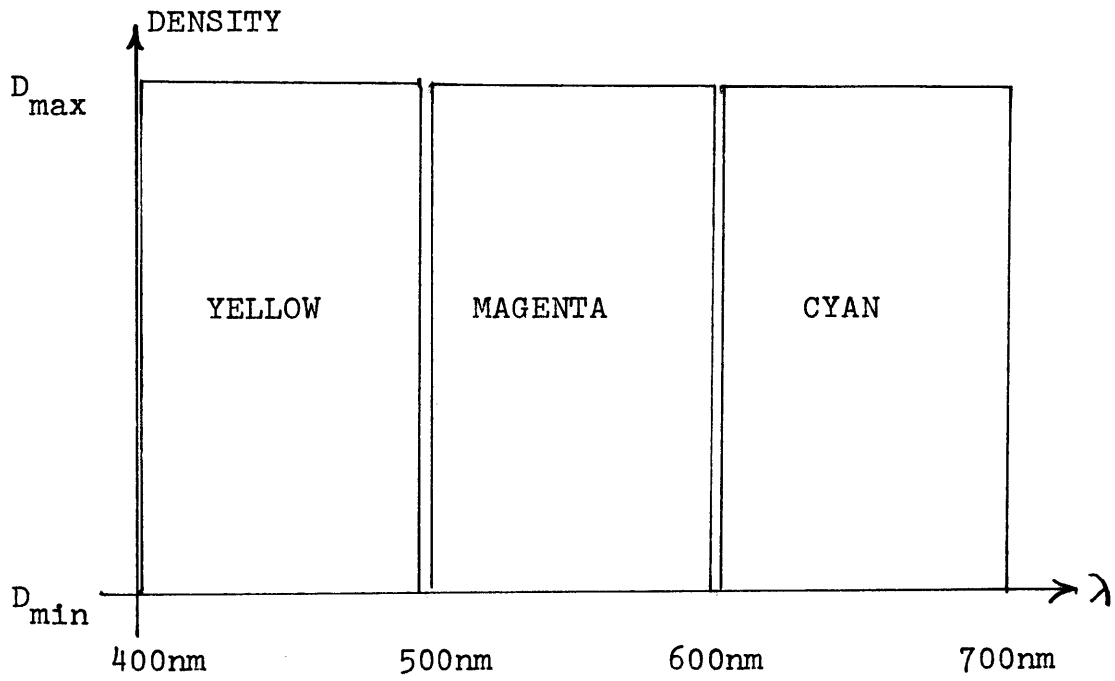


FIGURE 4-1. BLOCK DYE APPROXIMATION

dye. The magenta dye is the least perfect dye, having substantial absorptions in the red and blue regions of the spectrum. The yellow dye is the most ideal (figure 4-4).

The photographic process may be simply modeled with three stages (figure 4-2). There are three layers of film emulsion which are sensitive to red, green, and blue light. Over a restricted range of activation light flux, the taking sensitivities have a specified spectral sensitivity (figure 4-3).⁽³⁶⁾ The taking sensitivities in general are not a linear combination of the eye's pigment curves and thus are not a valid set of tristimulus functions. In fact, since the blue and green sensitive emulsions often do not respond beyond 620 nm, the entire gamut of reds beyond this wavelength will be reproduced with the same chromaticity values. The densities of the cyan, magenta, and yellow dyes are modulated through chemical processes according to the level of sensitization of the red, green, and blue emulsion layers.

The chemical process determines the proportionality between the developed dye density and the logarithm of the total activation flux. For example,

$$C = -\gamma_c \text{Log } R_a \quad (4.1-4)$$

where C is the density of the cyan dye, γ_c is the constant of proportionality for cyan, R_a is the red activation flux, commonly referred to as the red exposure,

$$R_a = \int S(\lambda) T_r(\lambda) d\lambda \quad (4.1-5)$$

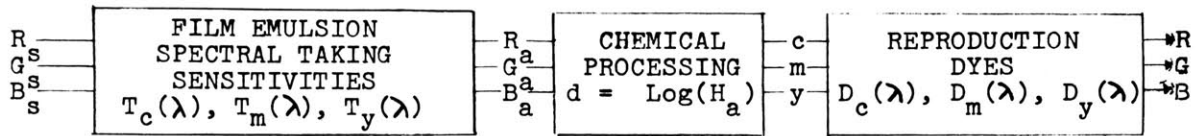


FIGURE 4-2. BASIC MODEL OF THE COLOR PHOTOGRAPHIC PROCESS

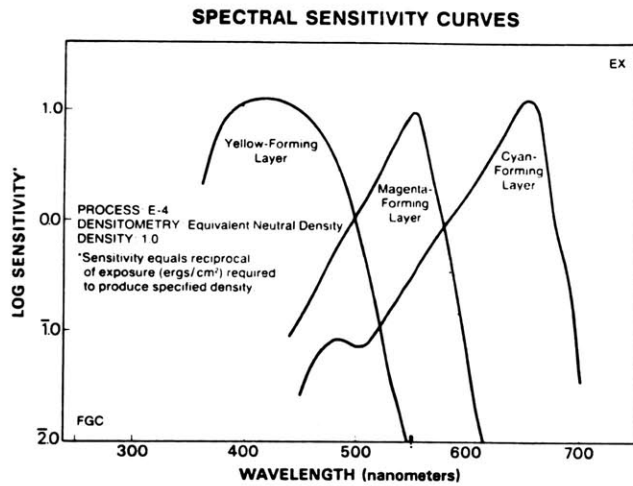


FIGURE 4-3. TAKING SENSITIVITY OF EKTACHROME REVERSAL FILM

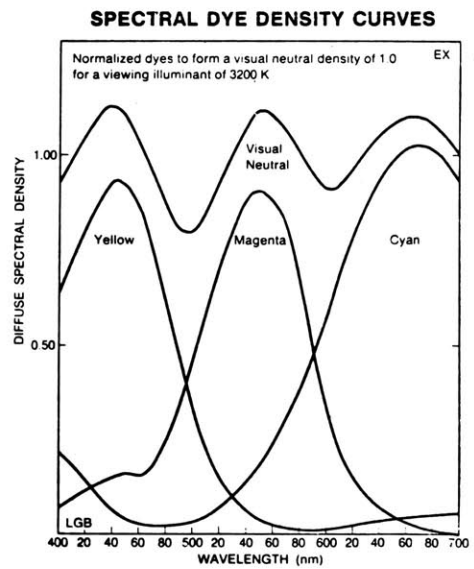


FIGURE 4-4. DYE TRANSMISSION CURVES FOR EKTACHROME SLIDES

where $S(\lambda)$ is the subject spectrum and $T_r(\lambda)$ is the red sensitive emulsion spectral taking sensitivity function.

The net spectral reflectance of the print can be calculated from the three dye layer spectral densities. From 4.1-1 and 4.1-4:

$$\rho(\lambda) = 10^{-(\gamma_c D_c(\lambda) \text{Log} R_a + \gamma_m D_m(\lambda) \text{Log} G_a + \gamma_y D_y(\lambda) \text{Log} B_a)} \quad (4.1-6)$$

A convenient way of defining a single density parameter for a color dye is in terms of the equivalent neutral density (END).⁽³⁷⁾ For a given dye density, certain amounts of the other two dyes may be added to yield a neutral color. The END of a color dye is set equal to the well-defined density of the neutral color obtained by adding sufficient amounts of the other two dyes to the first dye. The dye distributions $D_c(\lambda)$, $D_m(\lambda)$, $D_y(\lambda)$ are usually normalized to produce a neutral reflectance for a particular illuminant. Thus, to reproduce a grey scale with accurate neutral balance, the gammas, γ_c' , γ_m' , γ_y' must be equal over the reproduction range of densities (figure 4-5).

4.2 Quasi Tristimulus Color Measurement

Commercial color scanners generate separations by electronically color masking the unwanted absorptions.^(38,39) This is done by measuring the print reflectance through narrowband red, green, and blue filters and converting these quantities to the logarithmic density domain. Appendix IV details the methods by which the actual cyan, magenta, and yellow dye concentrations can be calculated. The spectral characteristics of the original scene may be approximated, knowing the dye concentrations and film characteristics. Since the

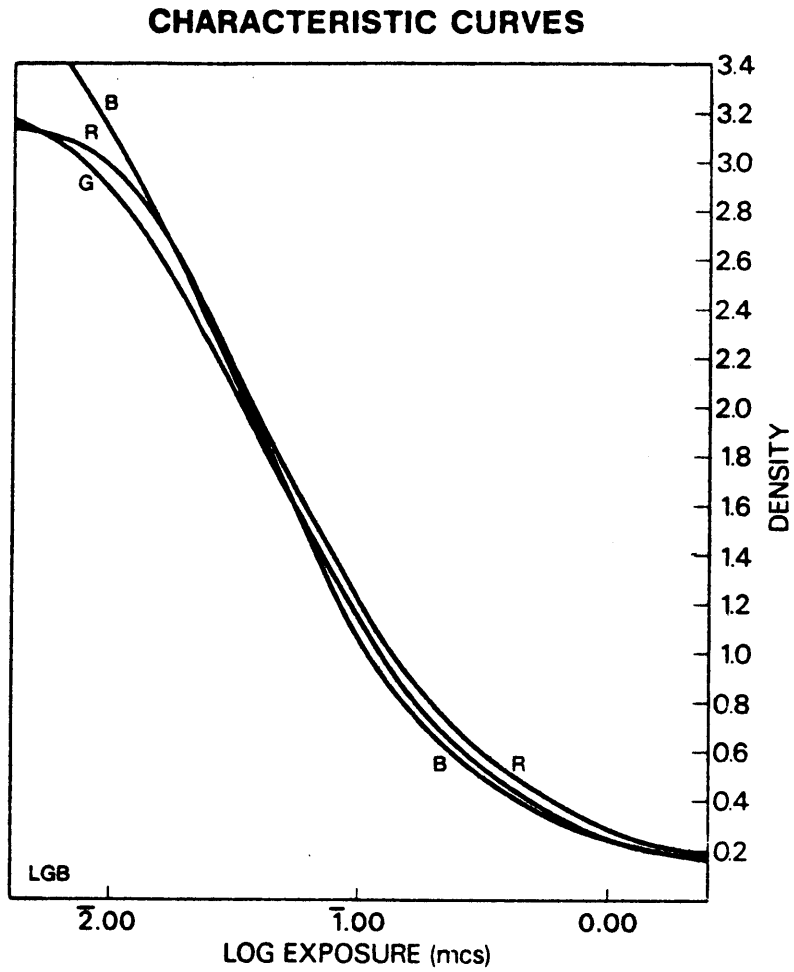


FIGURE 4-5. DENSITY-LOG EXPOSURE CURVES FOR
EKTACHROME FILM

taking sensitivities are not a proper set of tristimulus curves, the metamerism of two colors in an original scene may be destroyed. Also, since the spectral dye density functions are not constant over three color bands (e.g., 400-500 nm, 500-600 nm, 600-700 nm), the shape of the reflectance function will not be constant as the density varies.

In color facsimile, the exact colors in the original scene are usually of little importance. The photograph to be transmitted is assumed to be of good quality as judged by a photo editor or other qualified specialist. It is this original photograph which must be regarded as the subject to be accurately reproduced. A typical subjective evaluation of the effectiveness of the color coder is to compare the original and processed pictures side by side. Thus the reflectance measurement of the original scanned print must "see" the print as an observer's eye would (i.e., the R,G,B measurement functions should be a proper set of tristimulus functions).

As an aside, it should be noted that the aforementioned color masking technique can be used to exactly determine the color coordinates at each pel. Once the dye concentrations are known, the reflectance spectral function may be calculated from equation 4.1-6. The color coordinates may then be found by multiplying this reflectance by the tristimulus color matching functions and integrating over wavelength. Such a calculation, however, is far too lengthy to perform at each pel.

A simple method for making valid color measurements at each pel is to use a proper tristimulus set of detector spectral response functions. Since these functions are everywhere positive, one or more of them must have two peaks (from figure 2-1). Filters which closely approximate a tristimulus set are rather costly. Chapter Five describes

a very economical color head in which the filter functions are primarily determined by Wratten filters (figure 4-6). A comparison of figures 4-6 and 2-1 shows that the color head response functions least accurately approximate the tristimulus functions where the red and green responses overlap. The problem of approximating the CIE R,G,B coordinates from the color head R_H , G_H , B_H measurements is the topic of this section. One solution is to linearly transform the color head coordinates.

$$\begin{pmatrix} R \\ G \\ B \end{pmatrix} = \underline{T} \begin{pmatrix} R_H \\ G_H \\ B_H \end{pmatrix} \quad (4.2-1)$$

For a one-to-one mapping of the luminance axis, the $R_H = G_H = B_H = 1$ point must map into the $R = G = B = 1$ point. Thus, only six independent coefficients are available for exactly determining the CIE color coordinates for two color points.

Another approach is to separately determine linear transforms of the color head response functions which approximate the luminance and chromaticity coordinates. Such a quasi-luminance function will be correct at all achromatic points if the luminosity coefficients sum to unity. This follows since R_H , G_H , and B_H are set equal to one for maximum white, and equation 2.2-3 is therefore valid.

Thus the luminance for the frequently occurring desaturated colors will be closely approximated by the quasi-luminance function. The coefficients may be derived to fit the 1931 luminous efficiency function $y(\lambda)$ (with the 1951 Judd correction) of figure 2-2, with minimum mean square error.

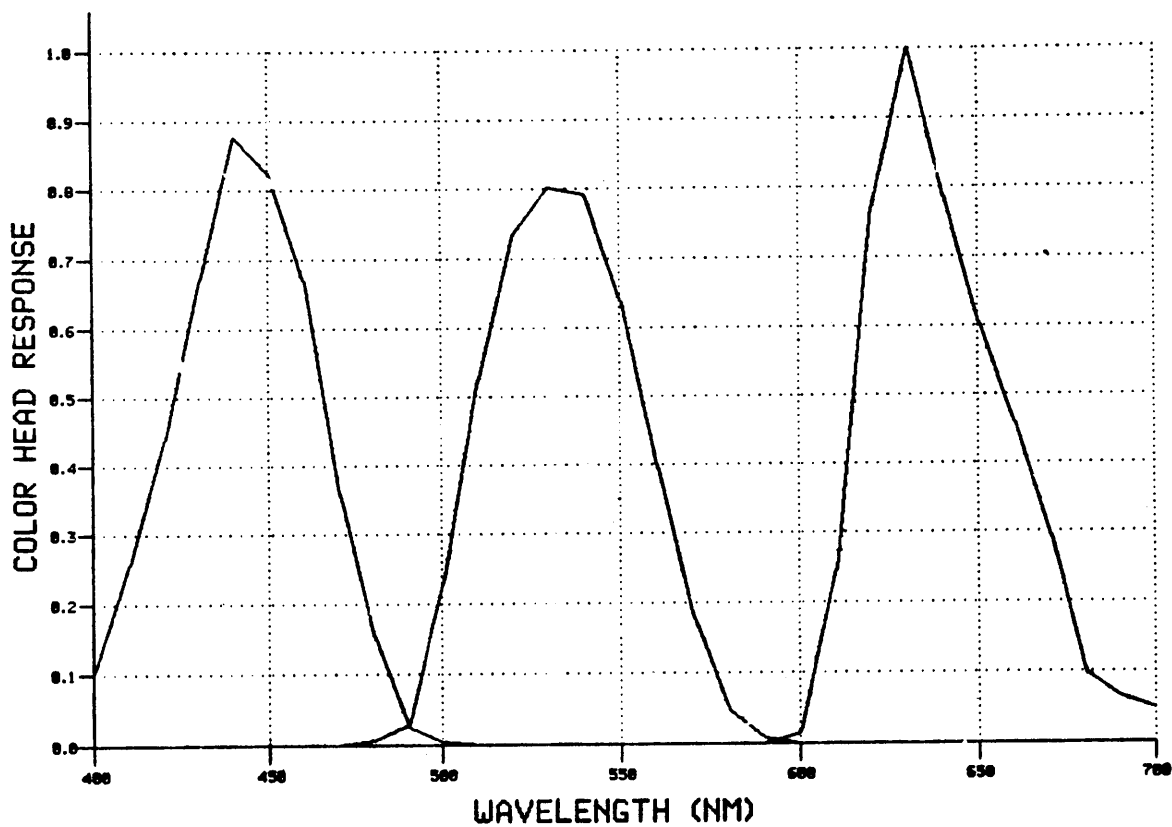


FIGURE 4-6. COLOR HEAD SENSOR RESPONSE FUNCTIONS

The approximation error, ϵ , may be defined in terms of the color head functions $F_j(\lambda)$.

$$\epsilon = \int (Y(\lambda) - \sum_i L_i F_i(\lambda))^2 d\lambda \quad (4.2-2)$$

then

$$\frac{\partial \epsilon}{\partial F_n} = 2 \int (Y(\lambda) - \sum_i L_i F_i(\lambda)) \cdot F_n(\lambda) d\lambda = 0 \quad (4.2-3)$$

$$\int Y(\lambda) F_n(\lambda) d\lambda = \sum_i L_i \int F_i(\lambda) F_n(\lambda) d\lambda \quad (4.2-4)$$

with the constraint: $\sum_i L_i = 1 \quad (4.2-5)$

The coefficients, L_i , may be found from Cramer's rule. Figure 4-7 shows the quasi-luminance function for the L_i coefficients. From Table A-1 it can be noted that even for the worst case (saturated colors) the quasi-luminance function is an excellent approximation.

The problem of approximating the chromaticity coordinates is a more complex two dimensional problem. Varying the dye densities individually and together in pairs from zero to a maximum of 2.0 with one dye at density zero generates the dye gamut plot of chromaticities in figure 4-8.

The inner locus is generated by varying one dye density from zero to 1.0 while holding the second dye density at 1.0 and the third at zero. Markers are generated at 0.4 density unit increments. Figure 4-9 in addition shows the dye gamut locus as seen by the color

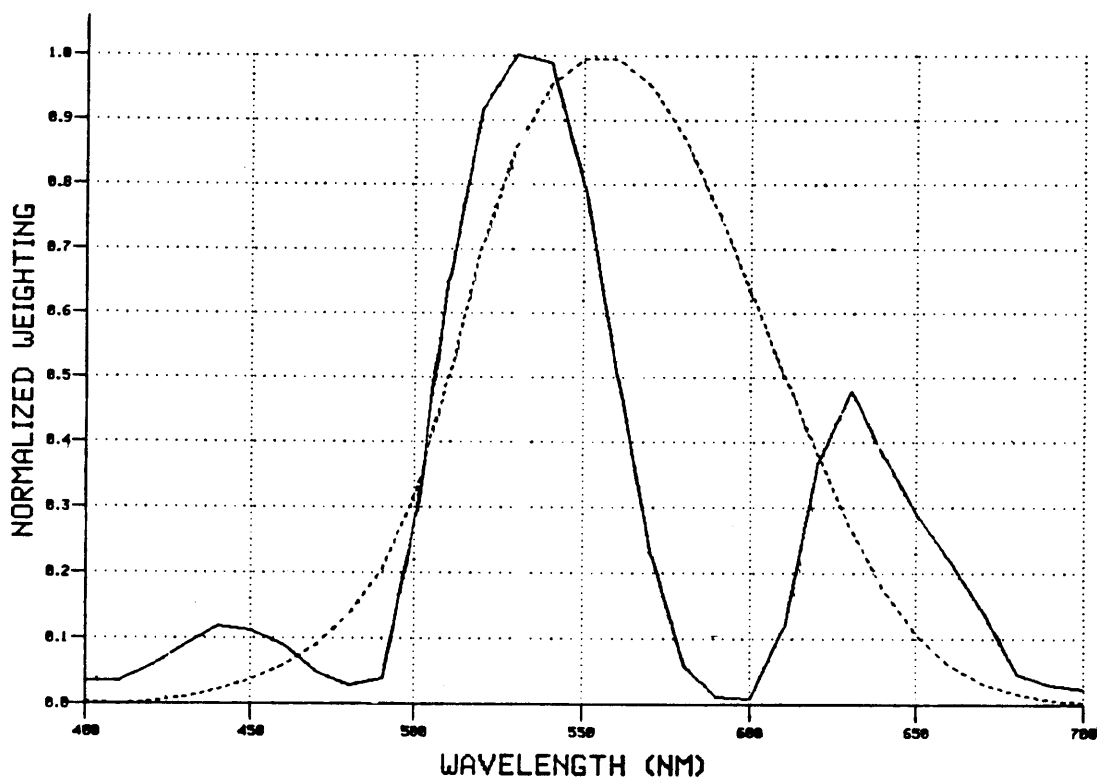


FIGURE 4-7. COLOR HEAD FILTERS QUASI-LUMINOSITY FUNCTION (solid line) AND LUMINOUS EFFICIENCY FUNCTION (dotted line)

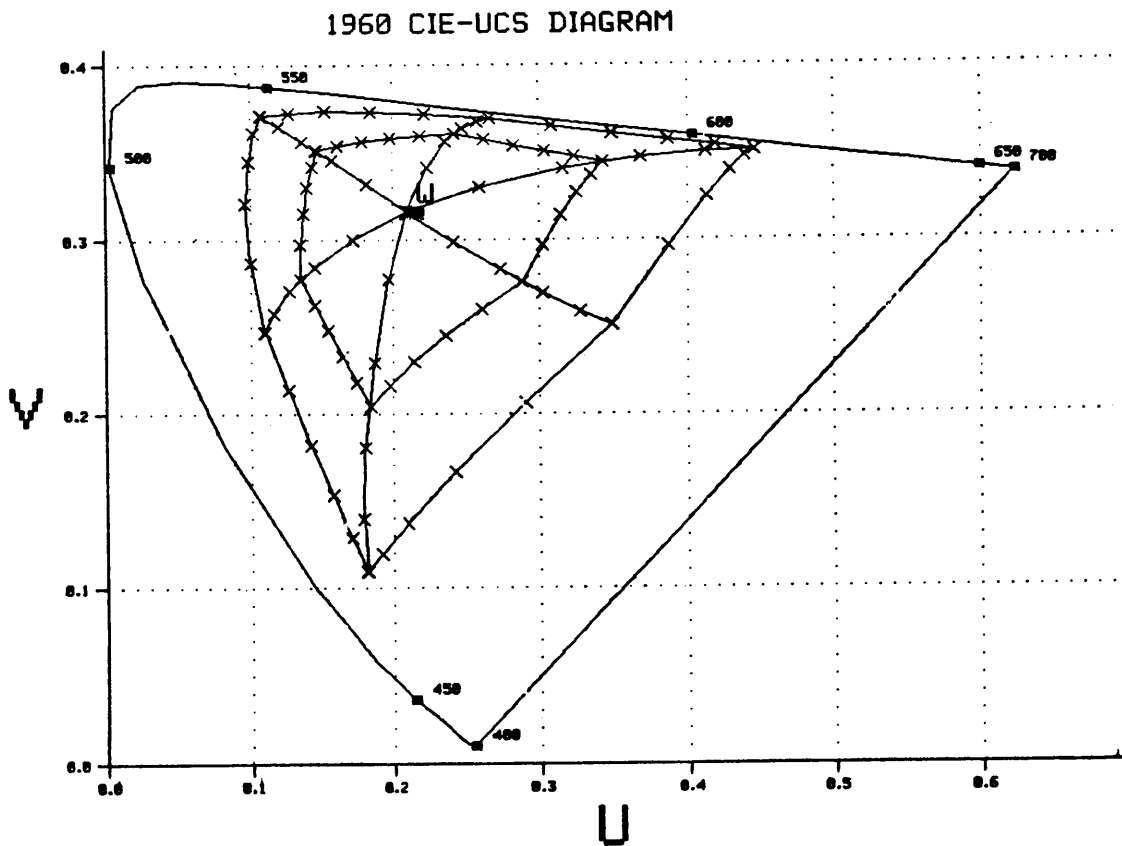


FIGURE 4-8. DYE GAMUT FOR EQUIVALENT NEUTRAL DENSITY
OF THE DYES FOR RC PRINT PAPER
(ILLUMINANT C)

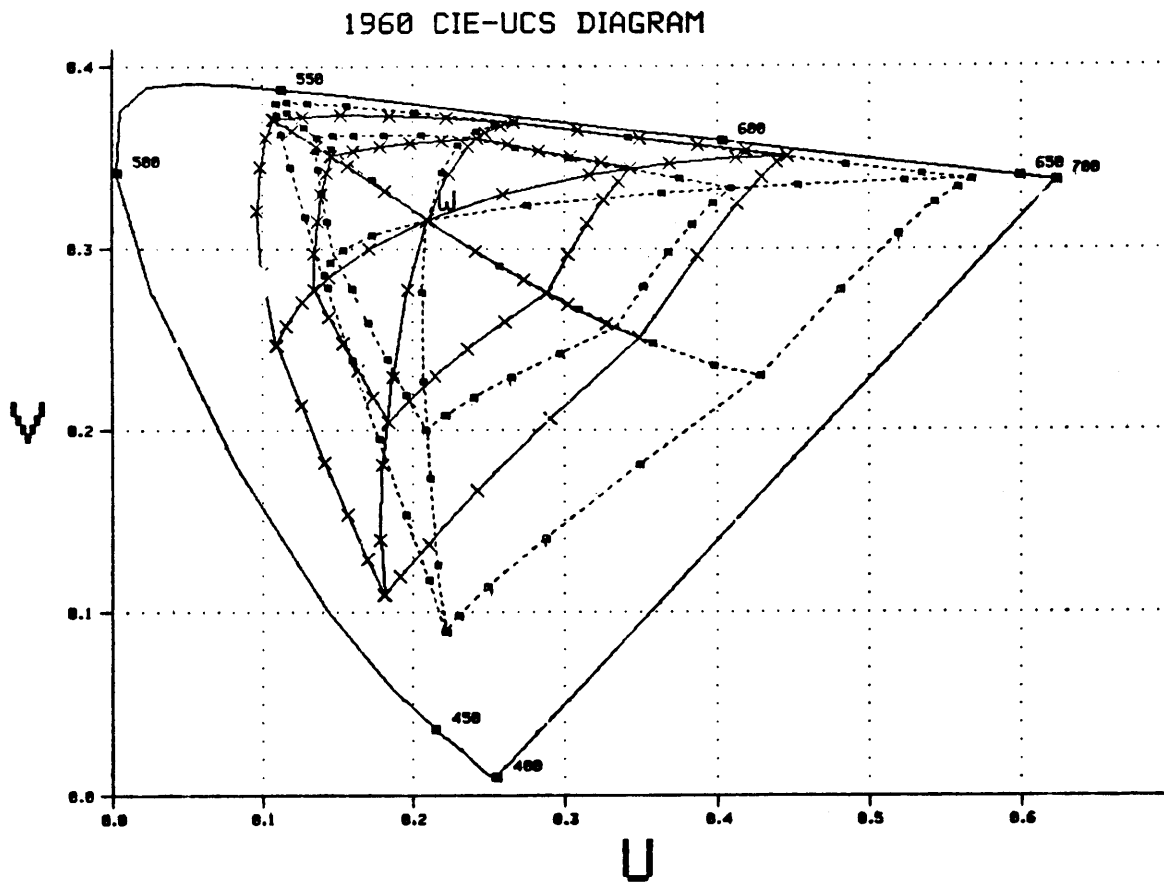


FIGURE 4-9. DYE GAMUT FOR RC PAPER (solid line)
AND FOR THE COLOR HEAD FILTERS ASSUMED TO BE R,G,B
CIE FUNCTIONS

head where it is falsely assumed that the R_H, G_H, B_H sensor functions are the R,G,B CIE functions. Since the two loci are somewhat similar it seems reasonable that an approximation to the CIE locus can be obtained by scaling and rotating the color head loci about the white point.

A linear affine transformation has two degrees of freedom and so two points on one loci may be exactly mapped onto the other loci.

$$\begin{pmatrix} u \\ v \end{pmatrix} = \begin{pmatrix} u_0 \\ v_0 \end{pmatrix} + \frac{T_1}{1} \begin{pmatrix} u' \\ v' \end{pmatrix} \quad (4.2-6)$$

To always correctly map the white points

$$\begin{pmatrix} u - u_w \\ v - v_w \end{pmatrix} = \frac{T_2}{1} \begin{pmatrix} u' - u_w \\ v' - v_w \end{pmatrix} \quad (4.2-7)$$

The four coefficients of T_2 are chosen to perfectly map the chromaticity coordinates of the red and blue points at density 2.0 (figure 4-10). Significant errors, however, are encountered for greens and cyans.

Another approximation generalizes the form of equation 4.2-7, realizing that the equation is the first term of a vector Taylor series expansion about the white point. An expansion which includes higher order terms will allow additional color head points to be exactly mapped onto the CIE dye loci. Since the major errors are in the u direction, a second order u term may be added to equation 4.2-7 to yield:

$$\begin{pmatrix} u - u_w \\ v - v_w \end{pmatrix} = \frac{T_3}{1} \begin{pmatrix} u - u_w \\ v - v_w \\ (u - u_w)^2 \end{pmatrix} \quad (4.2-8)$$

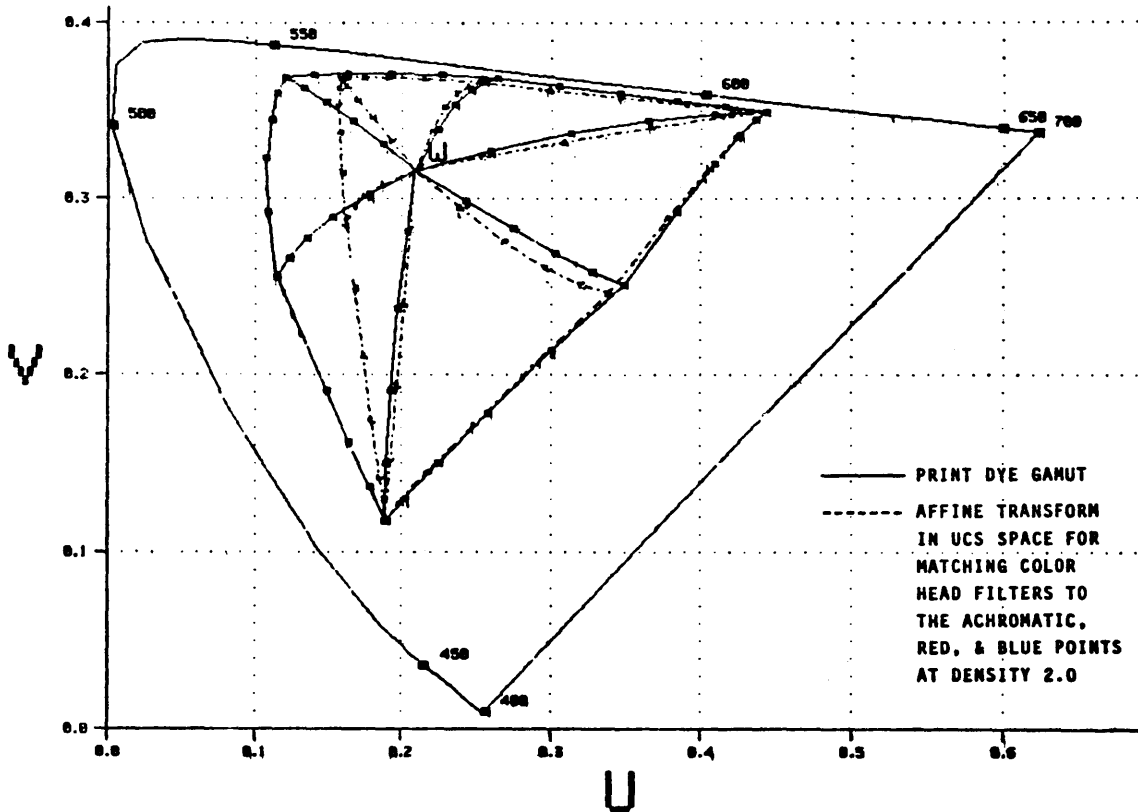


FIGURE 4-10. U-V AFFINE TRANSFORM FOR RED AND BLUE POINTS AT DENSITY 2.0 MAPPING

The above transform is shown in figure 4-11 where the nine T_2 coefficients have been chosen to exactly map the chromaticities of the red, green, and blue dye points at density 2.0. Due to the second order u term, severe nonlinearities are found for density values between 0.4 and 1.6 on loci with large span in the u direction.

A much more accurate mapping can be accomplished if the simple computer operation of branching is used to choose one of several piecewise continuous mapping functions. Transforms of the form of equation 4.2-7 can be used to specify an exact mapping of two points. If the inaccurate color head locus of figure 4-9 is divided into six small adjacent triangular regions, then six transformations for each region may be specified. To determine the region, the quadrant and slope, S, of the chromaticity values with respect to the white point are calculated.

$$S = \frac{v - v_w}{u - u_w} \quad (4.2-9)$$

Table A-2 lists the quadrants, slopes and transform coefficients for the triangular regions formed by the white points and two of the red, magenta, blue, cyan, green, and yellow points at density 2.0, which are used as the other two vertices. The result of this hex-affine-triangle (HAT) transform is a very good approximation of chromaticity values by a relatively poor set of color head functions (figure 4-12) In summary, the six independent coefficients of 4.2-1 are now optimally utilized by choosing two of them to least mean square approximate the luminosity function and by using the remaining four to independently best fit the dye gamut chromaticity locus.

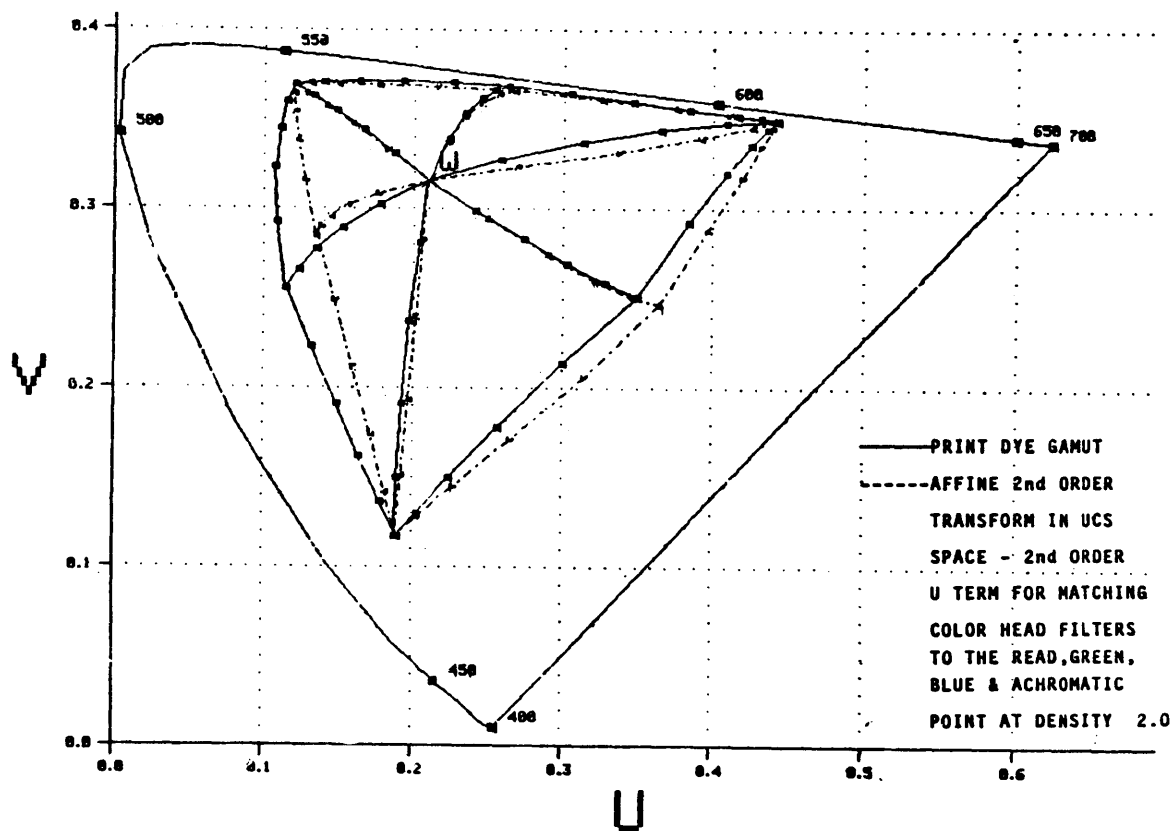


FIGURE 4-11. U-V TRANSFORM WITH SECOND ORDER U TERM FOR EXACT MAPPING OF THE RED, GREEN, AND BLUE POINTS AT DENSITY 2.0

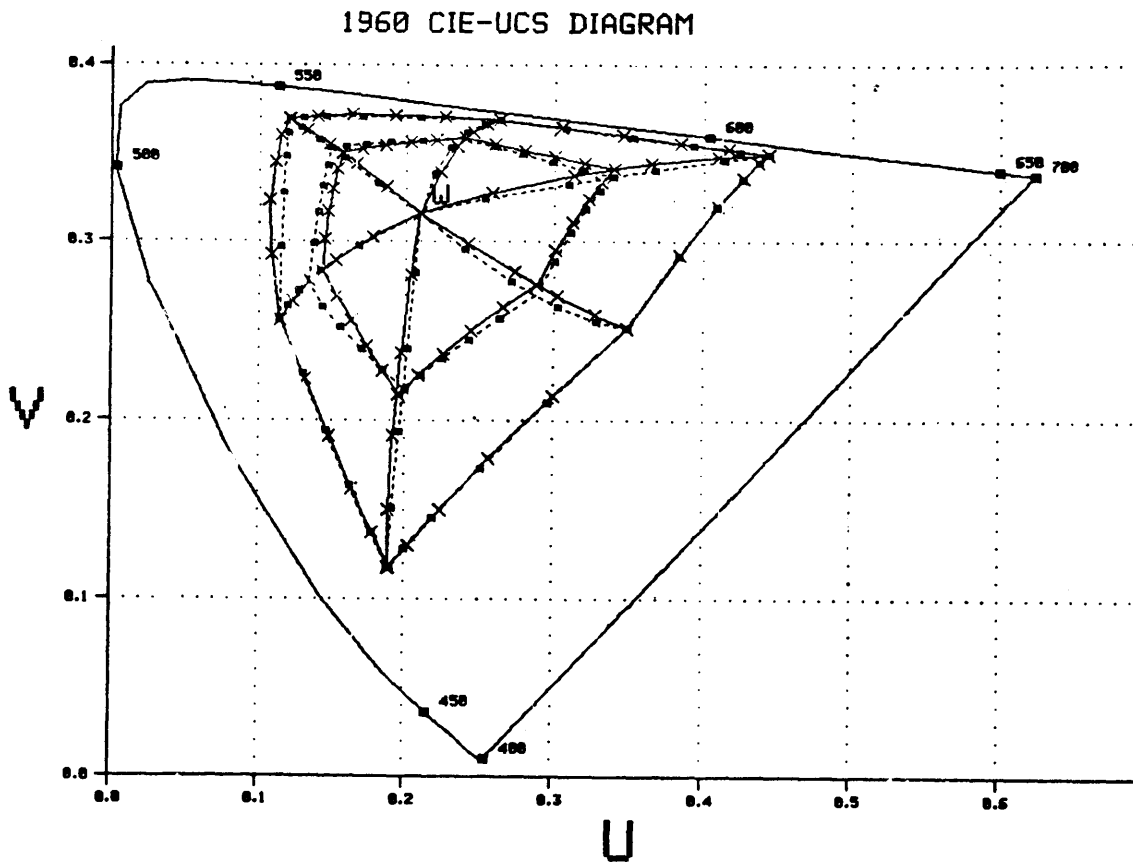


FIGURE 4-12. HEX-AFFINE-TRIANGLE TRANSFORM FOR EXACT MAPPING OF THE RED, MAGENTA, BLUE, CYAN, GREEN, AND YELLOW POINTS AT DENSITY 2.0

To substantially reduce computation time at the transmitter, the HAT transform can be performed after the chrominance spatial filter and before the LSC coarse quantizer at 1/16 the total number of pels. Filtering the pseudo UCS chromaticity coordinates derived directly from the color head color coordinates, instead of from the proper CIE UCS coordinates, should not result in any perceivable distortion (figure 4-13).

4.3 Colorimetrically Accurate Photographic Reproduction

The problem of reproducing a specified set of CIE color coordinate x_j values with a photographic subtractive dye process is an exceedingly difficult problem. The film transform to be inverted is from 4.1-6:

$$x_j = \int x_j(\lambda) 10^{-[\text{Log } \bar{H}_a] \cdot \bar{D}(\lambda)} d\lambda \quad (4.3-1)$$

where $D(\lambda)$ is the dye spectral distribution vector

$$D(\lambda) = \begin{pmatrix} c & D_c(\lambda) \\ m & D_m(\lambda) \\ y & D_y(\lambda) \end{pmatrix} \quad (4.3-2)$$

The H_a are the red, green, and blue film sensitizations

$$\text{Log } \bar{H}_a = \begin{bmatrix} \text{Log } R \\ \text{Log } G_a \\ \text{Log } B_a \end{bmatrix} \quad (4.3-3)$$

The inverse cannot be expressed in closed form, and so approximation techniques must be developed.

Since the gamut of dye colors (figure 4-8) does not lie within the 1931 CIE primary triangle (figure 2-5), certain dye colors will have

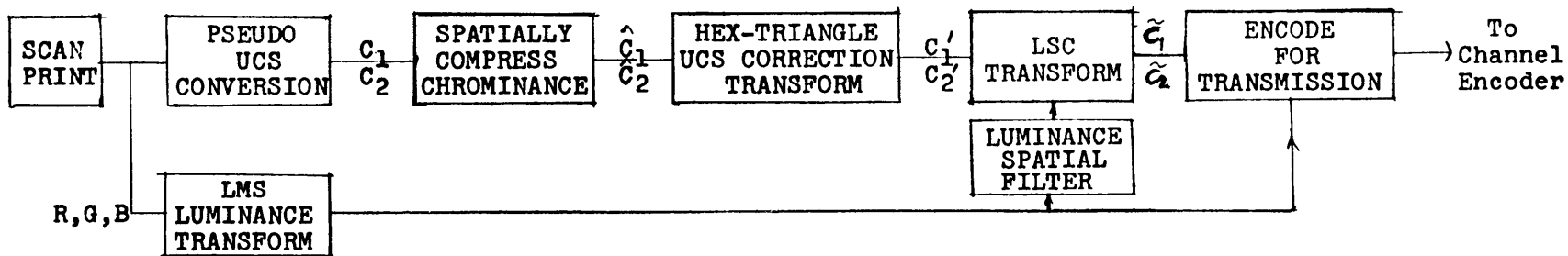


Figure 4-13 Transmitter Encoder with Color Head Correction Transforms

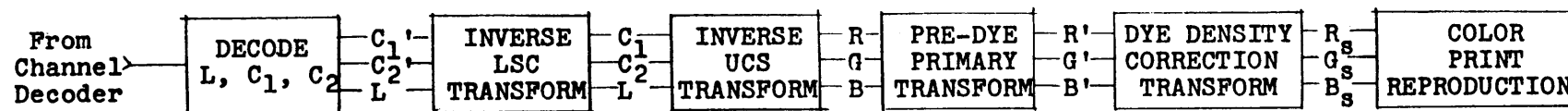


Figure 4-14 Receiver Decoder with Pre-Dye Primary and Density Transforms

negative R,G, or B values. Thus, it is necessary to transform the R,G,B coordinates to a new set R',G',B' where the new primary triangle encloses the dye gamut. A naive reproduction of the CIE R,G,B values as the separation R_s, G_s, B_s (clipping negative values to zero) would result in the grossly distorted dye gamut of figure 4-15.

Unfortunately, the block dye approximation of equation 4.1-3 does not accurately model a real dye. A simple generalization of the block model assumes constant density values of each dye in three color bands. For the cyan dye:

$$\begin{aligned} -\text{Log } R_c &= C_r \\ -\text{Log } G_c &= C_g = a_g C_r \\ -\text{Log } B_c &= C_b = a_b C_r \end{aligned} \quad (4.3-4)$$

where a_g and a_b are the fraction of unwanted cyan dye density for green and blue. The subscript c refers to the cyan component.

Assuming that the unwanted dye coefficients yield very small dye concentrations, we may approximate the net color coordinate as follows:

$$-\text{Log } R_{\text{total}} \approx C_r + M_r + Y_r \quad (4.3-5)$$

For most primary systems (e.g., CIE R,G,B primaries), this approximation is very poor. The primary values give rise to chromaticities which vary with dye concentration. A paper by MacAdam in 1938⁽⁴⁰⁾ subtly gives great insight into the problem of subtractive dye reproduction. He suggests that a particular set of primaries will result in much more stable chromaticities for a particular linear combination of dyes. In other words, R',G',B' color coordinates can be found such that:

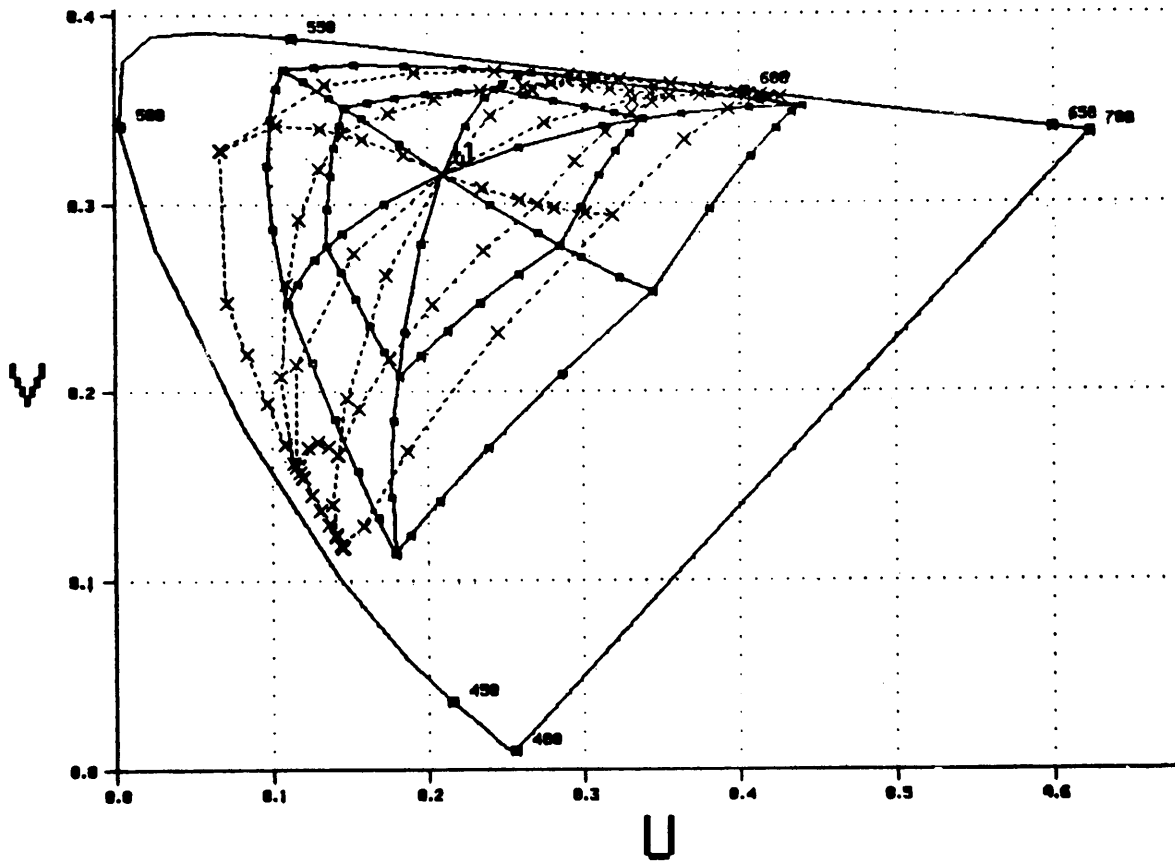


FIGURE 4-15. DYE GAMUT OF PHOTOGRAPH MADE DIRECTLY FROM CIE R, G, B SEPARATIONS

$$x_j' = \int x_j'(\lambda) 10^{-(\text{Log } \hat{x}_j') [\bar{d} \cdot \bar{D}(\lambda)]} d\lambda \quad (4.3-6)$$

approximately yields

$$-\log x_j' = -\log \hat{x}_j' \quad (4.3-7)$$

where \bar{d} is a particular linear vector combination of the dyes which stabilizes the x_j' color coordinate.

Thus, two transformations are involved. The first is a linear transformation from the CIE color coordinates to another more stable set of coordinates which are positive for all colors in the dye gamut.

$$\begin{pmatrix} R' \\ G' \\ B' \end{pmatrix} = \underline{T}_L \begin{pmatrix} R \\ G \\ B \end{pmatrix} \quad (4.3-8)$$

The major issue now is how to determine T_L . MacAdam suggests that the new primaries should be chosen in the chromaticity plane (Appendix I) by noting where straight line loci of certain fixed ratios of dyes converge. Figure 4-16 shows the chosen primaries for the dye gamut of RC paper dyes. The new primary triangle encloses the entire dye locus. With just this transform, the dye gamut locus processed by the film is greatly improved (figure 4-17).

The second transform is in the logarithmic density domain and is in fact a dye correction transform which corrects for unwanted absorptions as measured in the new color coordinates. This transform converts the R', G', B' into the separation values R_s, G_s, B_s used to activate the film as in equation 4.1-6. The exact physical process is detailed in Chapter Five,

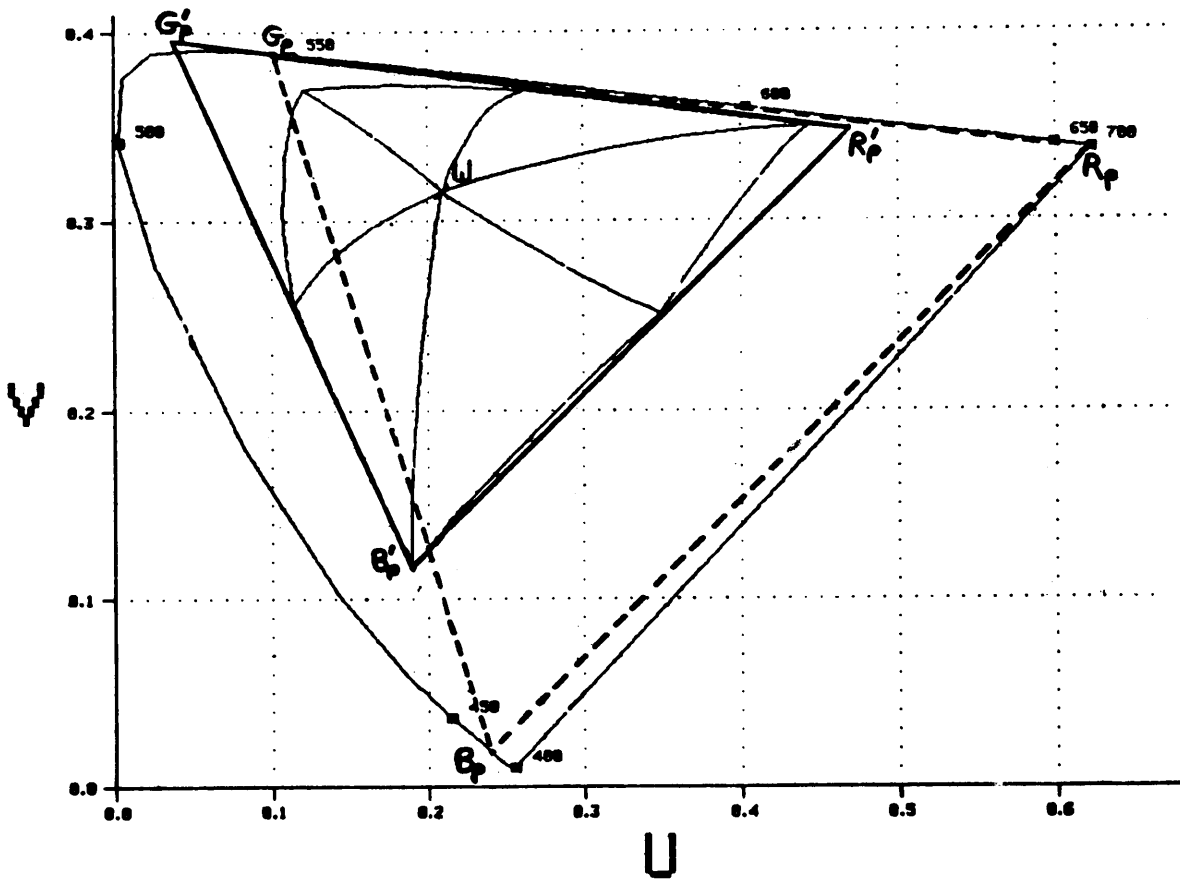


FIGURE 4-16. CIE (DASHED LINE) R,G,B AND THE NEW R',G',B' PRIMARY TRIANGLES

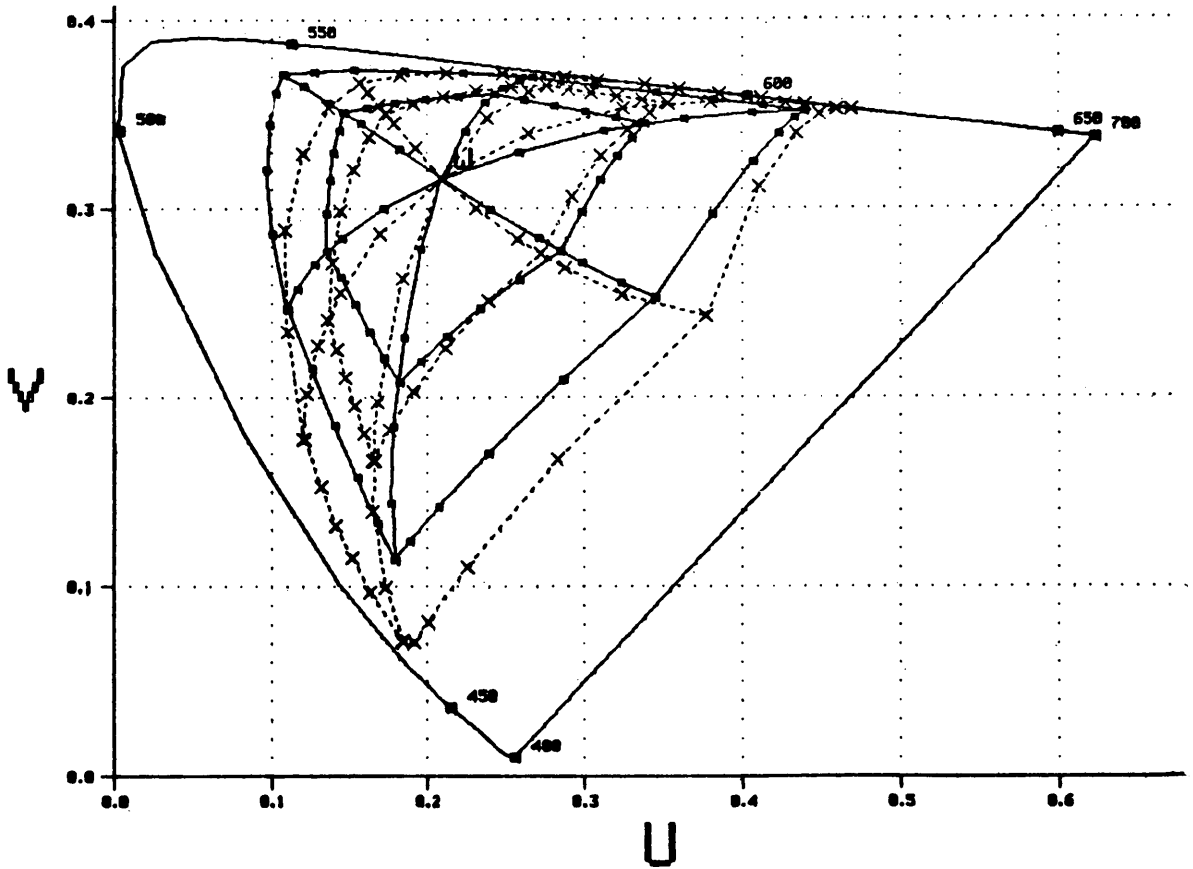


FIGURE 4-17. DYE GAMUT OF PHOTOGRAPH MADE FROM R',G',B' SEPARATIONS

where R_s, G_s, B_s are shown to be equivalent to R_a, G_a, B_a .

$$\begin{bmatrix} \log R_s \\ \log G_s \\ \log B_s \end{bmatrix} = \frac{T_D}{1} \begin{bmatrix} \log R' \\ \log G' \\ \log B' \end{bmatrix} \quad (4.3-9)$$

The T_D transform of equation 4.3-9 is the first term of a vector Taylor series approximation to the non-invertible film transform of equation 4.3-1. Thus equation 4.3-9 allows only two color coordinates to be exactly reproduced if neutrality is to be preserved, since:

$$\underline{T_D} = \begin{bmatrix} T_{11} & T_{12} & (1 - T_{11} - T_{12}) \\ T_{21} & T_{22} & (1 - T_{21} - T_{22}) \\ T_{31} & T_{32} & (1 - T_{31} - T_{32}) \end{bmatrix} \quad (4.3-10)$$

so that when $R' = G' = B'$, $R_s = G_s = B_s$

A practical solution of equation 4.3-10 is to first choose the CIE R,G,B color coordinates of the three points and convert these to R',G',B' values. Then various values for R_s, G_s, B_s are fed into equation 4.3-1 and the R',G',B' color coordinates are computed. After a few iterations, triads of R_s, G_s, B_s can be found which yield the desired R',G',B'. Thus, the T_D coefficients to exactly reproduce the two points can be calculated. Using the techniques of the HAT transform, the chromaticity of the color to be reproduced may be determined from equation 4.2-9 to lie in one of six triangular regions. Thus, six T_D transforms may be found for exactly reproducing the chromaticity of two colors and the entire achromatic axis. Figure 4-18 shows the chromatic accuracy for a set of such transforms listed in Table A-3. These transforms were chosen to exactly reproduce the color head measured R_H, G_H, B_H for the six basic colors at density 1.0 .

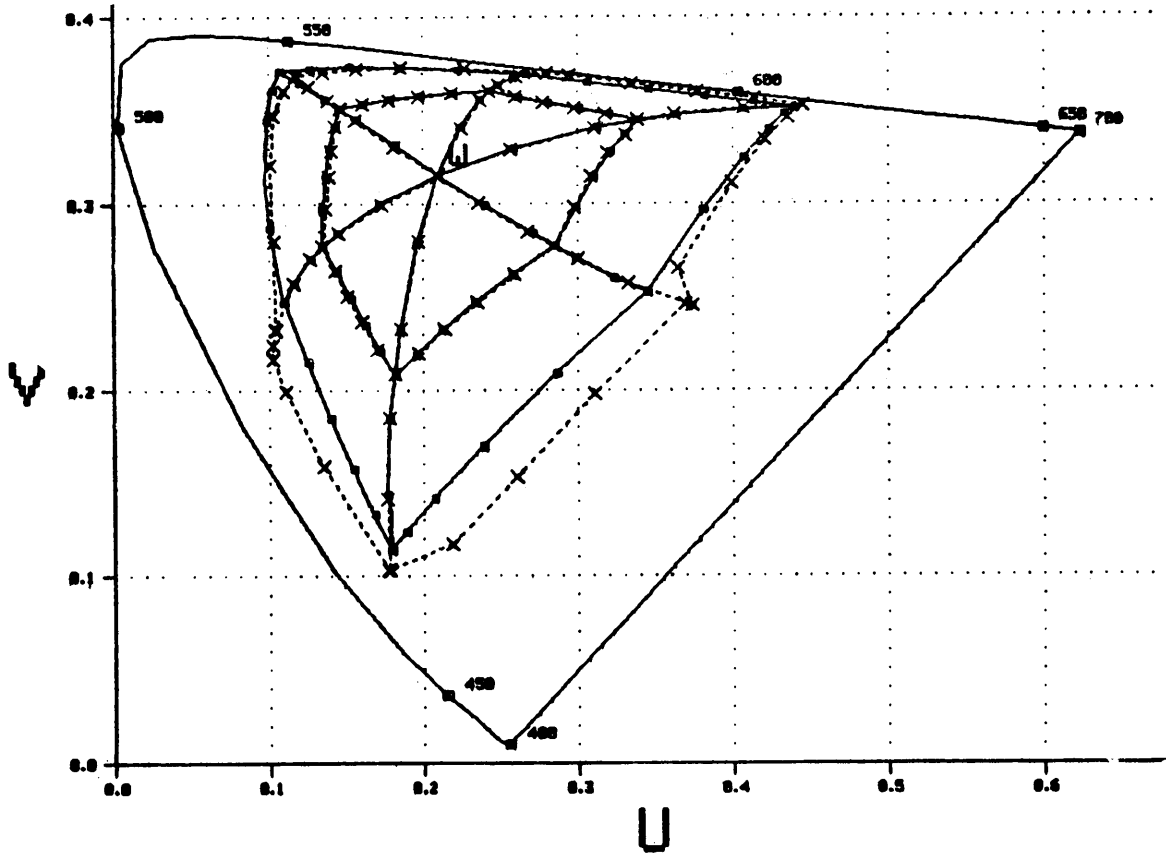


FIGURE 4-18. DYE GAMUT OF PHOTOGRAPH MADE FROM THE HEX DYE CORRECTION TRANSFORMED R',G',B'

The reproduction of very dark saturated magentas and cyan-blues is somewhat compromised so that the more frequently occurring pastels are reproduced very accurately.

The overall chromatic accuracy of the color facsimile system, from the scanned original picture to the reproduction from separations, is plotted in figure 4-19. In summary, the use of piecewise linear transforms in the chromaticity domain has yielded a system with exceptionally high color fidelity.

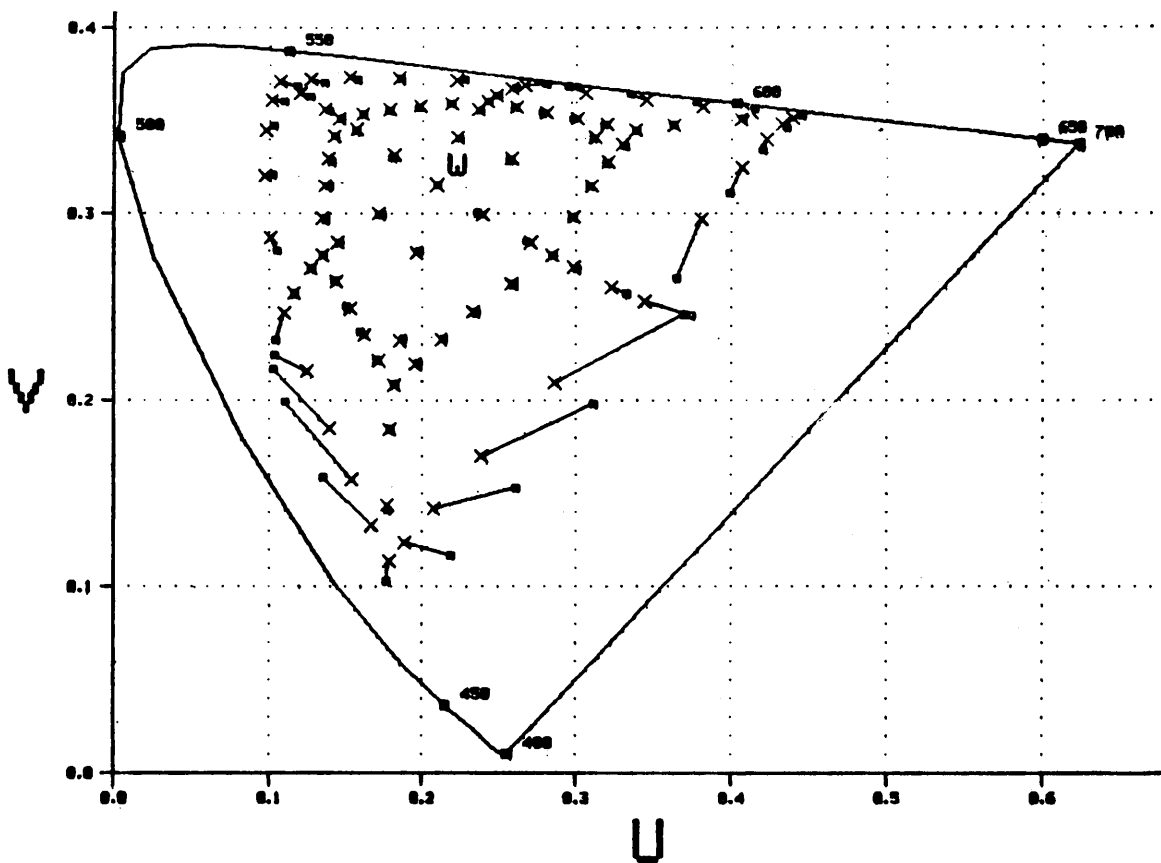


FIGURE 4-19. OVER-ALL CHROMATIC ACCURACY OF THE
COLOR HEAD & DYE CORRECTION TRANSFORMS

V. Simulation of the Color Facsimile System

5.1 Introduction

5.2 The Color Scanner

5.3 The Computer and Software System

5.4 Reconstruction of Color Pictures

5.1 Introduction

Three basic components are necessary to simulate the color facsimile system: a color scanner, a digital computer with large storage capacity, and a color output receiver. The next section describes the color scanner and the facsimile computer interface. Once a few standard pictures have been scanned it is convenient to store them on a portable nonvolatile medium such as magnetic tape so they may be easily read into the computer each time a new algorithm is to be subjectively tested. The color reproduction cannot be conveniently done in one operation. It is first necessary to make black and white separations on a monochrome receiver and then recombine the separations through color filters to reconstruct the color picture.

Figure 5-1 shows the interrelationship between the major hardware components. PIXMON is a 256 pel by 256 line by 4 bit per pel television frame freeze memory which provides fast soft copy output of separations for diagnostic purposes. Most of the filtering and quantizing algorithms were developed and debugged without having to look at many color pictures. The PIXMON and hard copy monochrome separations provide much information as to the degree of artifacts and of course, programming errors. In fact, artifacts often are more noticeable in separations since they tend to be reduced in the color print because of psychophysical factors referred to in Chapters Two and Three. In addition, the test picture provides a tough test of a processing system, since all possible colors are generated with severe discontinuities.

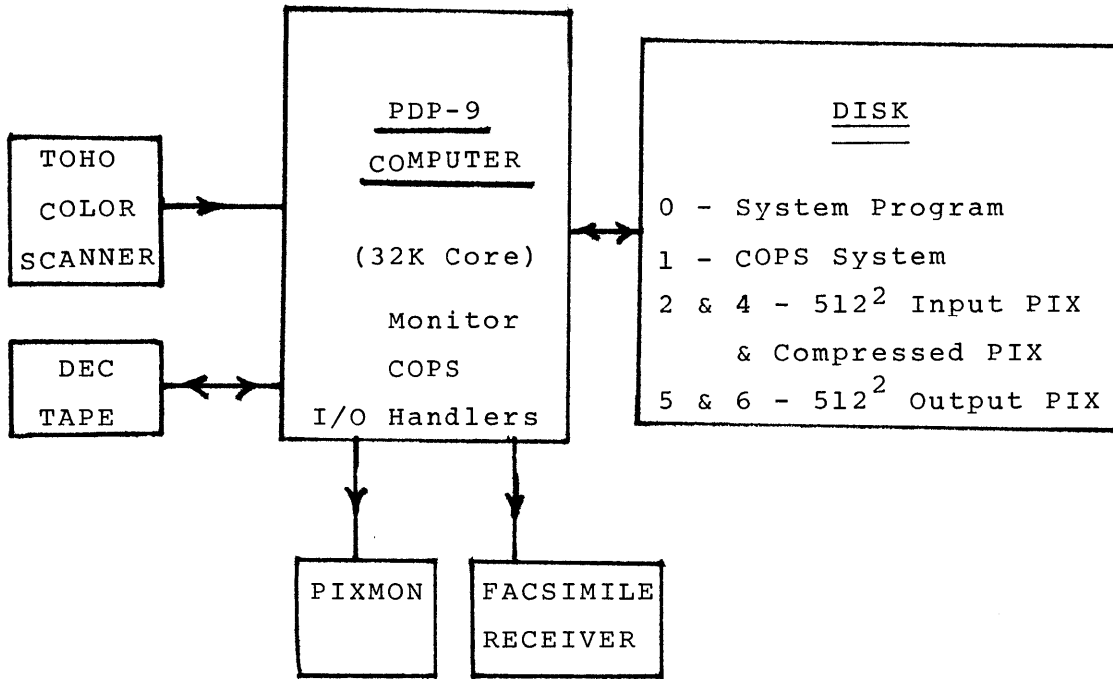


FIGURE 5-1. PDP-9 COLOR IMAGE PROCESSING COMPUTER SYSTEM

5.2 The Color Scanner

Measurement of the color coordinates at each pel of a color print is accomplished with a color scanner. A conventional rotating drum, TOHO facsimile transmitter was modified by removing the photomultiplier tube and replacing it with a color head. The head images an illuminated section of the print through dichroic mirrors and color filters onto three phototransistor detectors (figure 5-2). The light source is a conventional incandescent high current lamp operated at 50% overvoltage from a regulated source to produce a 3200°K filament color temperature. The overall spectral response of the red, green, and blue color head sensors (figure 5-2) is determined from the various optical components (figure 5-3).

The red, green, and blue signals from the photodetectors are amplified by three preamps, sampled at a 1.92KHz rate, and analog to digital converted to six-bit bytes which are packed in an 18-bit computer word (figure 5-4). A print fastened to the TOHO scanning drum is rotated at 100 RPM by a motor which is synchronized by pulses counted down from the master system clock. The color head is slowly advanced perpendicular to the scan direction by a lead screw. It moves .0107 inches each revolution yielding 93 lines per inch resolution. The sample resolution along a scan line is 98 pels per inch. Since the color head sample aperture is determined by the active area of the phototransistor detector, the imaging system is designed to image a .01 inch diameter pel onto this area. Calibration for neutral white is accomplished by setting

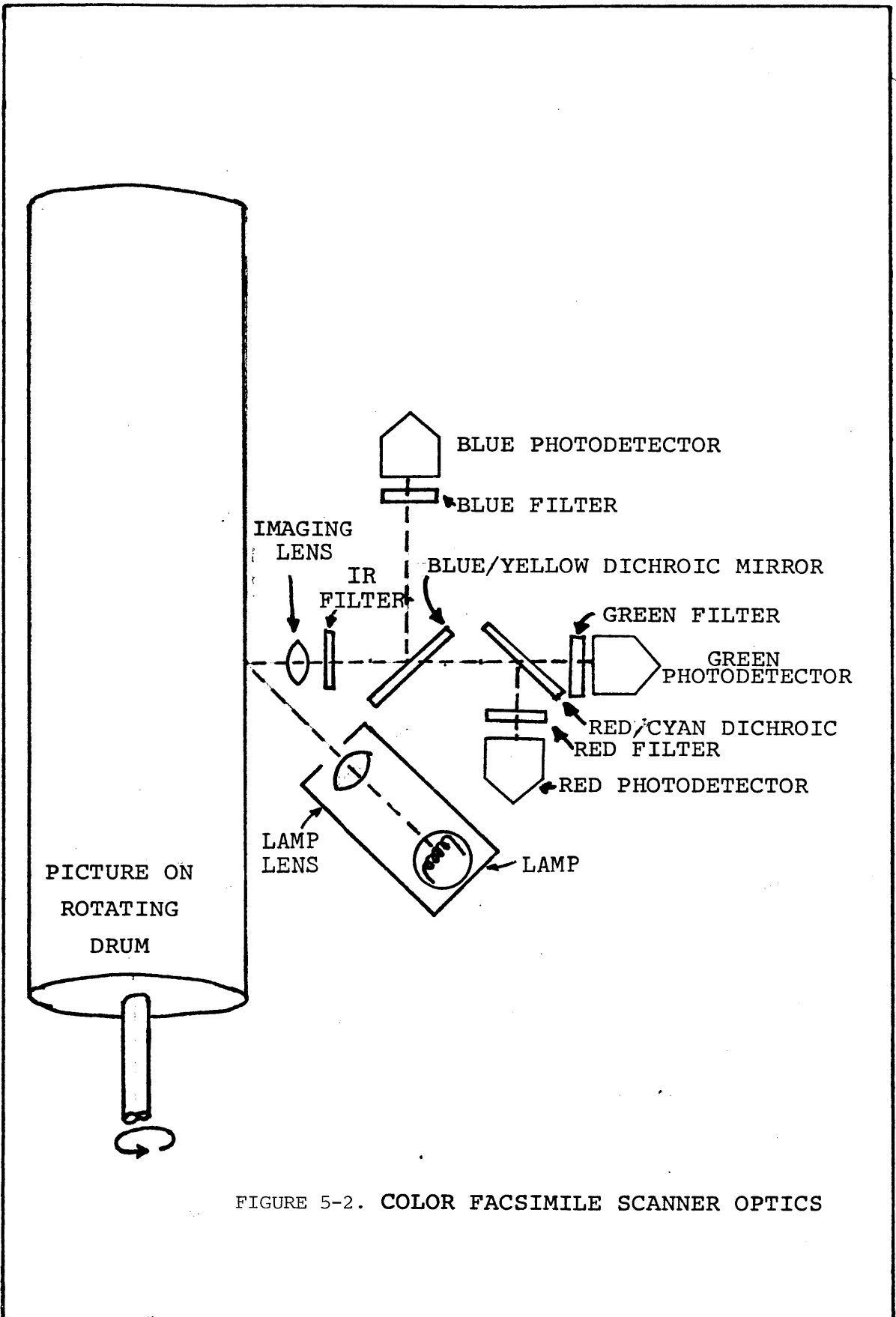


FIGURE 5-2. COLOR FACSIMILE SCANNER OPTICS

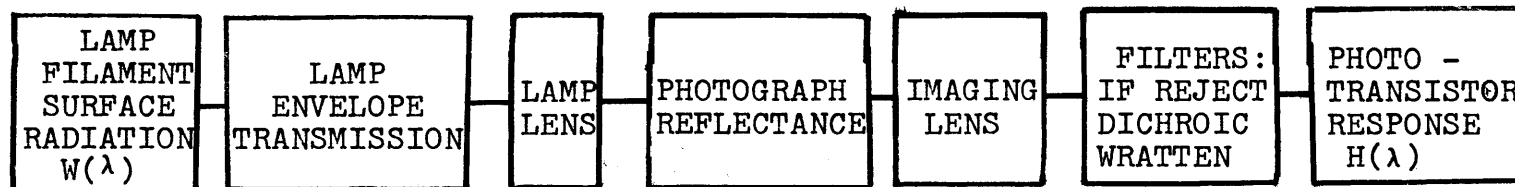


FIGURE 5.3 SCHEMATIC REPRESENTATION OF THE COLOR HEAD RESPONSE FUNCTIONS

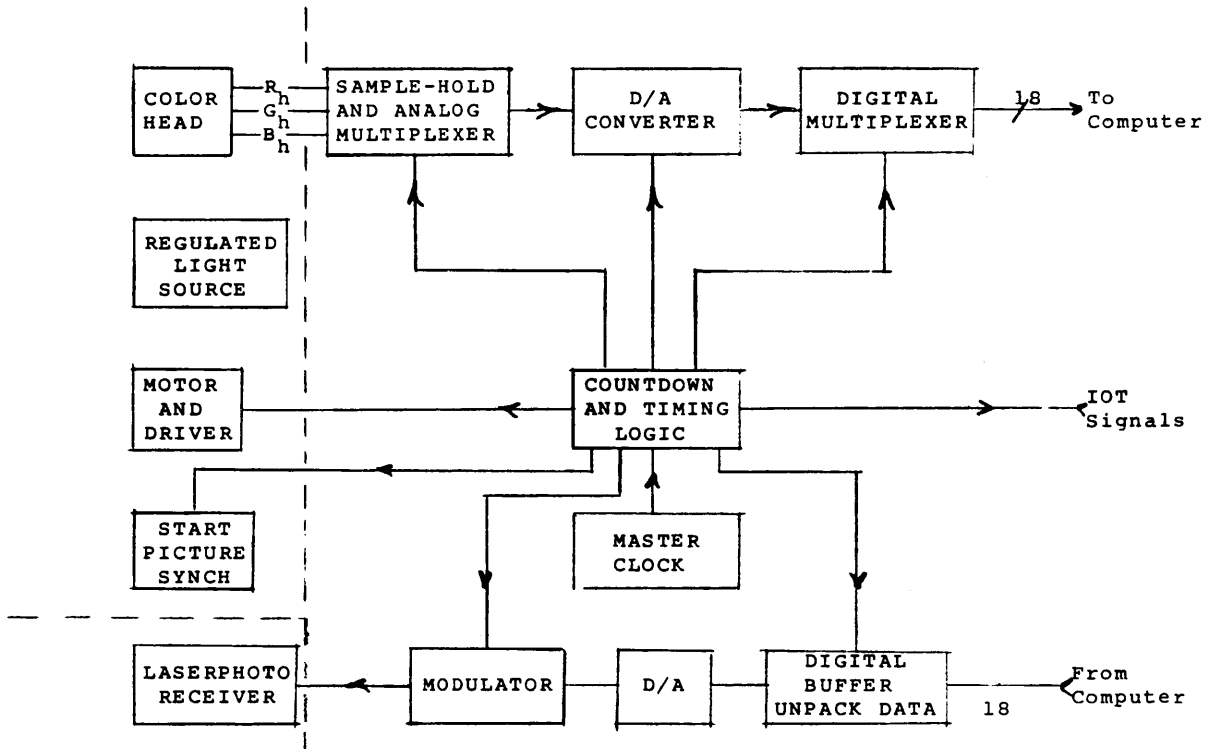


FIGURE 5-4. MONOCHROME RECEIVER AND COLOR TRANSMITTER FACSIMILE INTERFACE

the color head outputs equal to the maximum white level for the white border of the print.

The picture is initially synchronized by a single start pulse. Thereafter, 18-bit digitized packed color pels are transferred to the computer at a 1.92KHz rate along with a beginning-of-line synchronization signal.

5.3 The Computer and Software Systems

All of the color transforms, digital signal processing, and picture management are performed on a DEC PDP-9 computer (figure 5-1). In addition to 32,000 words of 18-bit computer memory, there are six disks with a capacity of over one million words. A 512-pel square picture requires two disks for storage. The compressed picture uses less than one disk, but the system programs require two disks and so a picture cannot be completely processed on a disk system. Half of the original picture must be deleted before recovery of the output picture from the compressed data. A disk may be stored on a single DEC tape.

The color processing software system (COPS) emulates the entire transmitter source encoder and receiver source decoder of the color facsimile system. In addition, the computer disks simulate the storage of the original, compressed, and recovered pictures. Original pictures as large as 512 pels square can be processed with the disk system, and any arbitrary size picture could be processed with a much slower tape system.

COPS reads a picture onto a disk from the TOHO or tapes and can output the red, green, or blue separations to PIXMON or the facsimile receivers. Once the particular parameters are specified in COPS, RGBE, the transmitter encoder simulator, performs the algorithm outlined in figure 5-5. The color facsimile system processes pictures in real time with a four-line buffer delay. As each line of luminance and chrominance is transformed, filtered and quantized, the encoded data is stored on the disk in a compressed format. A 512-pel square picture requires 2^{18} computer words, but a compressed version requires only 37% of that storage space.

It can be argued that filtering after quantization has two computational advantages. First, the quantized chromaticity values have fewer bits and therefore the necessary four lines of C_1 and C_2 storage require less memory. Secondly, the linear superposition filter effectively sums the quantized chrominance values helping to reduce the truncation noise. However, as was pointed out in Chapter Three, chrominance filter line memories are a small fraction of the line storage requirements of the luminance delay. Most important, the transmitter HAT and LSC transforms are most efficiently performed after spatial filtering and coarse sampling. There is no reason to coarse quantize the chrominance until just before packing for transmission.

The receiver decoder, RGBD, performs the algorithms shown in figure 5-5. The output picture can also be sent to PIXMON or the facsimile receiver as computer registered red, green and

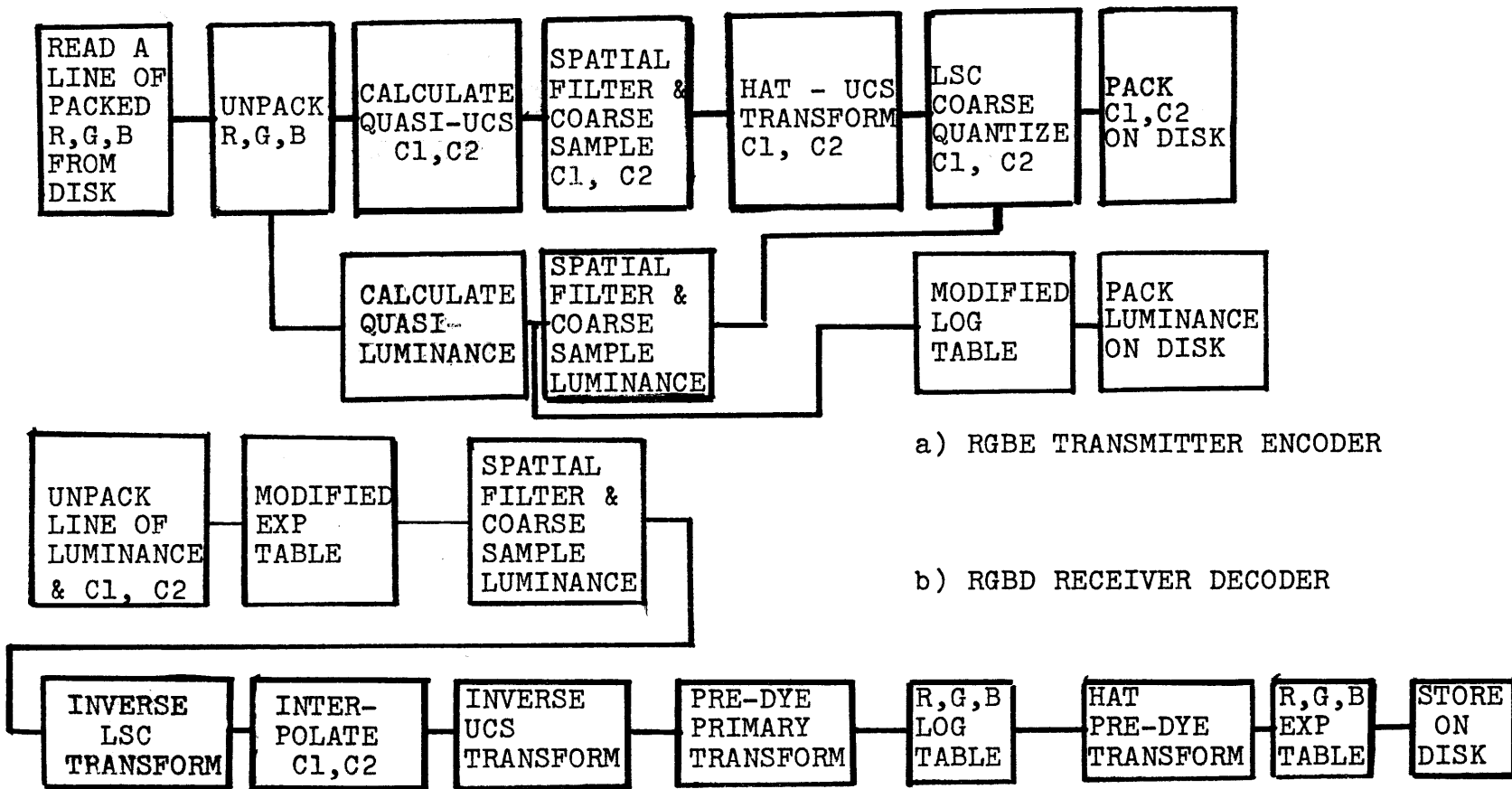


FIGURE 5-5. COPS SYSTEM BLOCK DIAGRAM

blue separations with computer generated registration points and a color scale.

The pictures are coded and decoded on a line-by-line basis and a significant percentage of the processing time is due to disk transfers. Several look-up tables are used to trade off memory space for speed, thereby minimizing the time required for long transforms performed at every pel, which require transcendental functions and multiplications. Tables of log and exponential conversion and red, green, and blue luminances are included as well as chrominance conversion tables.

The various programs in the COPS software package fall into one of four categories:

1. Executive system software written in FORTRAN
2. Bit manipulation packing, unpacking, scaling, and data transfer routines written in MACRO assembly language
3. Transforms operating on each pel written in MACRO
4. Transforms operating on the coarsely sampled, filtered pels (1/16 the total number of pels) written in FORTRAN

Practical implementation of real time stream processing necessitates a judicious choice of algorithms which share operations and combine several transformation steps into one. The COPS system is much slower than an optimum fixed system written entirely in MACRO, because there must be provisions for trying different transforms and setting various parameters.

Also, many frequently modified arithmetic routines are written in FORTRAN which compiles very inefficiently on the PDP-9. The capabilities of the PDP-9 central processing unit are quite primitive, compared to modern microprocessors fitted with a high speed arithmetic processor. The absence of multiple registers and of a stack memory results in very inefficient transferring of data in multiple argument algorithms. However, the optimum all-MACRO version of the encoder and decoder run on the PDP-9 would operate in real time (i.e., pel processing operations with filtering and packing overhead are under 500 sec.).

5.4 Reconstruction of Color Pictures

Red, green, and blue separations are reproduced on a Laserphoto facsimile receiver. The receiver uses a scanning laser beam to expose dry silver paper which is heat developed in a matter of seconds to yield a fairly high resolution print with a 0.2 to 1.8 density range. The receiver tone scale is not very stable or linear in density or reflectance and so a table of look-up values must be generated to linearize the tone scale. A computer generated stepwedge is measured on a digital reflectance densitometer. The density levels are fed into a tone scale correction program which linearly interpolates reflectances according to:

$$R = \frac{10^{-D+D_{\min}} - 10^{-D_{\max}+D_{\min}}}{1 - 10^{-D_{\max}+D_{\min}}} \quad (N) \quad (5.4-1)$$

The computer translates the red, green, or blue six-bit pel value into an eight-bit reflectance value which is sent to the facsimile interface (figure 5-4).

Computer registered separations cannot be easily viewed in an optical additive viewer because the intense light flux necessary to overcome filter and lens losses would continue to develop the unfixed dry silver paper. In other types of additive viewers, the prints must be registered each time they are viewed. The most important reason not to use an additive viewer, however, is that facsimile separations are always reproduced by a subtractive dye process. Part of the design of the facsimile system requires a good understanding of the dye reproduction system. Even if additively viewed, the pictures must eventually be photographically reproduced.

Color photographic reproduction of the separations is accomplished by multiply exposing the pin registered separations through red (W29), green (W61), and blue (W47B) filters which are chosen so that only one emulsion layer will be sensitized at a time. The illumination is provided by two 3200°K bulbs mounted in bowl reflectors, and the lamp voltage is regulated by a variac. A Nikon camera back is used with a Schneider leaf shutter copy lens to eliminate any movement of the 35mm frame during multiple exposures. By both calculation (using the illuminant spectra and the filters, and taking sensitivity spectral curves) and experiment, the exposure ratios for the three separations are calculated.

VI. Color Picture Evaluation and Conclusions

6.1: Subjective Analysis of Compressed Color Pictures

6.2: Topics for Further Research

6.3: Conclusion

6.1 Subjective Analysis of Compressed Color Pictures

In the picture processing field, the old adage that "a picture is worth a thousand words" is an understatement. In fact, it is the subjective evaluation of the processed picture, not the seemingly endless number of words in a dissertation on the topic, which determines the success of a particular coding algorithm. All of the effort expended in developing a color coding system is worthless if the compressed picture appears to be an unacceptably degraded version of the original photograph.

A human observer comparing two photographs placed side by side functions as a fault detector. His/her assessment of color picture quality will depend on many factors. For example, the observer's color memory serves to ascertain if certain common colors such as skin tone, green grass, blue sky, etc., appear natural. Another critical quality judgment factor is the detection of artifacts such as defocused edges or quantization contours which appear on the processed picture and not on the original. In general, the difficulty observers have in determining which one of two pictures has been compressed provides a good measure of the processed picture quality.

To thoroughly evaluate the color facsimile system, it is necessary to process several different types of test pictures. The first picture (figure 6-1), showing a group of men wearing brightly colored shirts, was chosen to evaluate the chromatic reproduction accuracy. An outdoors scene of a cameraman (figure 6-2) was selected as the second picture since it shows a blend of grass, sky, and flesh tones, as well as sharp foreground and defocused background objects. The final test picture is a portrait (figure 6-3) with large areas of very small brightness and hue gradations which are particularly susceptible to severe chrominance quantization contours.

All of the prints are 3R positive to positive reproductions of Ektachrome-B slides made from separations as described in Section 5.4. The top pictures (6-1a, 2a, 3a) of each set of test pictures are the unprocessed controls which were scanned. The red, green, and blue components have each been quantized to six bits and have been processed by the color head and output dye correction transform. A full implementation of the color compression algorithms results in picture 6-1c, which most observers were unable to positively identify as the processed picture, compared with 6-1a.

Pictures 6-2b and 6-3b are examples of compressed color pictures in which the chromaticity components have not been LSC transformed before quantization. The severe artifacts due to chrominance quantization contours and degradation in chromatic fidelity yield unacceptable pictures. In contrast, pictures 6-2c and 6-3c are fully processed, showing how the LSC transform drastically reduces the artifacts and provides an excellent quality color reproduction.

Color pictures processed by the chrominance compression coding algorithms were informally judged by many trained observers to be a very accurate reproduction of the unprocessed picture. In the cases of the group and cameraman subjects, the unprocessed and compressed pictures were indistinguishable, even after some close scrutiny. The processed pictures, however, contain only 1/16 the chromaticity information and 37 percent of the total information of the original.



FIGURE 6-1.

GROUP PICTURE

a) SCANNED COLOR
CORRECTED
UNPROCESSED



b) SCANNED
UNPROCESSED

WITHOUT OUTPUT
DYE CORRECTION



c) FULLY PROCESSED,
COMPRESSED WITH
LSC TRANSFORM



FIGURE 6-2.

CAMERAMAN PICTURE

- a) SCANNED COLOR
CORRECTED
UNCOMPRESSED
ORIGINAL



- b) COMPRESSED
WITHOUT LSC
TRANSFORM



- c) COMPRESSED
WITH LSC
TRANSFORM

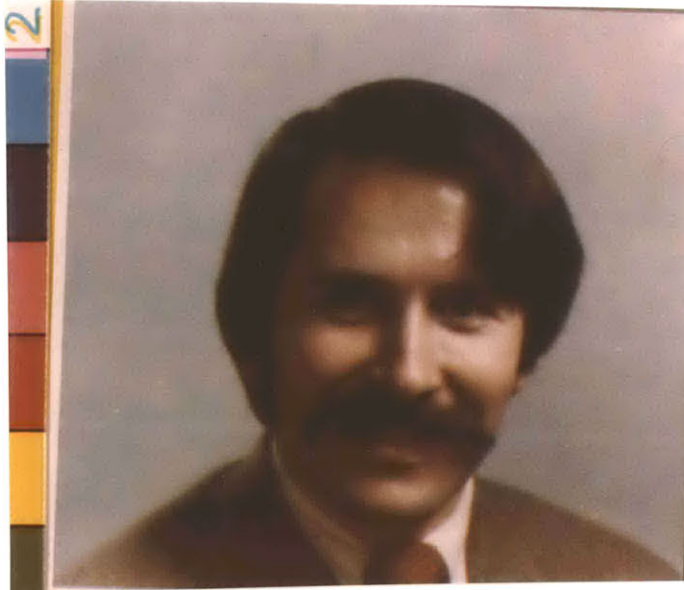
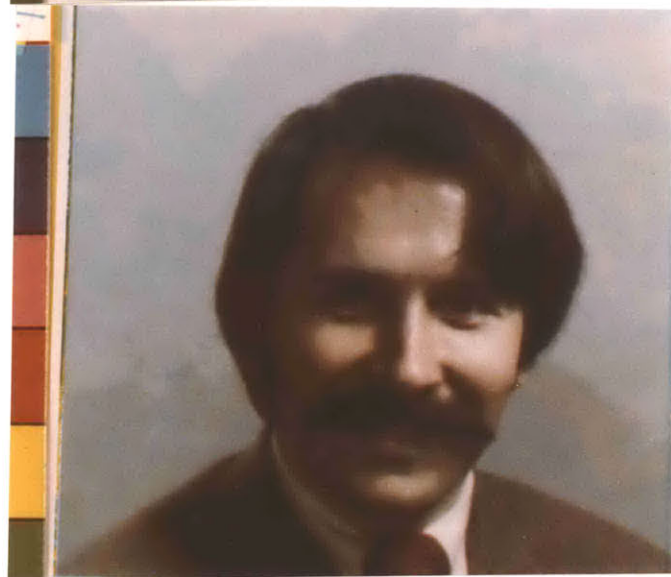
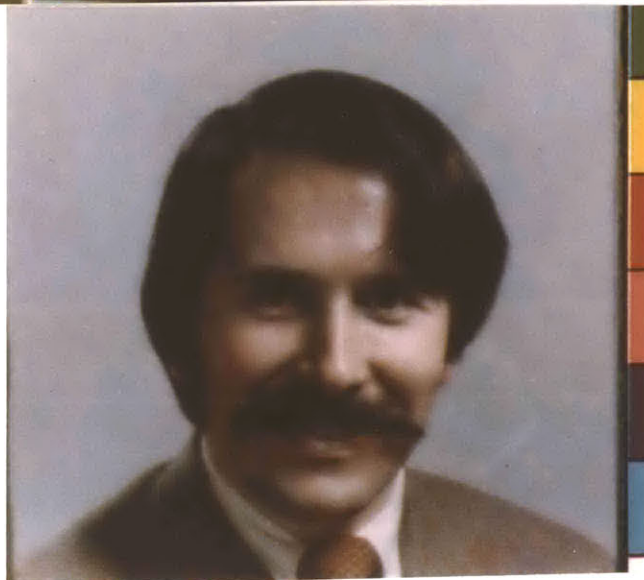


FIGURE 6-3.
PORTRAIT PICTURE

a) SCANNED COLOR
CORRECTED
UNCOMPRESSED
ORIGINAL



b) COMPRESSED
WITHOUT LSC
TRANSFORM



c) COMPRESSED
WITH LSC
TRANSFORM

6.2 Topics For Further Research

In any research project of the scope of this dissertation, many interesting theoretical and design problems must be lightly treated or not completely optimized in the interest of a reasonable time schedule. Although the color facsimile system developed in this thesis is quite complete, in that color pictures were scanned, compressed, and reproduced with excellent quality, there are a number of areas for future work. At the present time, the author, himself, is working on a number of these problems:

- 1) The LSC transform provides excellent reduction of chrominance quantization noise, but for certain critical test pictures, some contour artifacts are noted. Techniques exist for reducing these contours by adding pseudo-random noise with half of the least significant bit amplitude before the coarse quantizer, and subtracting out the noise at the output. These Robert's noise techniques will no doubt remove whatever contour artifacts presently exist in some pictures.

- 2) At the present time, if the color facsimile system were put into operation, the receiver decoder electronics would have to be connected to three monochrome facsimile receivers to produce the red, green, and blue separations. It is feasible to construct a laser receiver, using dry silver, heat developed paper, which uses a single laser and mirror galvanometer deflection system to simultaneously scan three sections of a piece of dry silver paper through a triple beam splitter. The beams would be individually modulated by three electro-optical light

modulators.

3) As was mentioned in chapter two, the chromaticity components cannot be optimally encoded due to the nonrectangular region of reproducible colors. If the components were quantized to five bits instead of four, then the resulting ten bits of chrominance information might only represent eight bits of valid codewords. The ten bits of data can be sent to an 8K bit read only memory, which would output a new set of single eight bit code words which would all be valid.

4) The HAT transform techniques for correcting the color head sensor response functions and most important, for correcting for the unwanted absorptions of the subtractive dyes, can be further optimized. In the cases of the dye correction, the trade-offs are between accurately reproduced pale colors with large errors for the magenta dye at high densities, or accurate reproduction of the darker, more saturated colors. In addition to determining the quadrant and slope of the chromaticity components, one might also determine the distance from the white point. In this way, twelve transforms can be derived, six for the pale colors and six for the darker colors.

5) In the facsimile receiver, the luminance must be again filtered to determine the LSC transformed inverse values of the coded chromaticity components. This filtering requires a twelve line luminance buffer memory in the receiver. Techniques may exist for somehow encoding the filtered luminance information in one of sixteen high resolution luminance pels as a dithered position. In this way the receiver luminance buffer memory could be reduced to four lines.

6.3 Conclusions

Starting with a few constraints based on psychophysical data, the existing facsimile system specifications, a basic model of the photographic process, and data for a particular photographic material, this dissertation has developed a practical facsimile system which produces high quality compressed color pictures. The choice of the 16:1 compression ratio was dictated by the requirement of encoding the color information into the retrace blanking region of standard monochrome facsimile signal. The possibility of such a compression was established in earlier research. The major contributions of original work in this dissertation result from examining in detail the four steps in the color processing system which appeared to most severely limit the color picture quality:

- 1) The efficiency of chrominance codeword utilization is greatly improved by the LSC transform developed in Chapter Two.
- 2) The concept of overall filter function developed in Chapter Three permits parameters to be chosen which minimize artifacts resulting from chrominance spatial filtering, coarse sampling, and interpolation.
- 3) The outputs of three colorimetrically inaccurate color head functions are transformed to values which closely approximate the tristimulus components. The transform is separately optimized by both the luminance (by least mean square technique) and the chrominance (by piecewise linear transformations).
- 4) Accurate photographic reproduction of colorimetric values is accomplished by a color primary transform and a piecewise linear density domain transform which together approximate the inverse transform of the photographic process.

APPENDIX I

LINEAR TRANSFORMATION TO A NEW SET OF COLOR PRIMARIES

As discussed in section 2-1, color space coordinates may be represented by an infinite number of primary bases. To transform to a new basis, the three primaries, $P_j(\lambda)$ must be chosen to match the unknown color. The three primary spectral distributions may be represented as a column vector:

$$P(\lambda) = \begin{pmatrix} P_1(\lambda) \\ P_2(\lambda) \\ P_3(\lambda) \end{pmatrix} \quad (\text{AI-1})$$

Fortunately, the 1931 CIE measurements were made with simple narrowband sources so AI-1 simplifies to:

$$P(\lambda) = \begin{pmatrix} P_1(\lambda_1) \\ P_2(\lambda_2) \\ P_3(\lambda_3) \end{pmatrix} \quad (\text{AI-2})$$

where $P_i(\lambda_i)$ are normalized so that equal amounts of the primary radiances match the standard equi-energy white. Since Grassmann's laws are linear, any new set of primaries, $P'(\lambda)$ is metamERICALLY equivalent to a linear sum of the simple narrowband primaries in AI-2.

$$P'(\lambda) = T P(\lambda) \quad (\text{AI-3})$$

The new color coordinates, $X'_j(\lambda)$, are related to the CIE color coordinates by:

$$\int X'_\lambda \cdot P(\lambda) d\lambda = \int X'_\lambda \cdot P(\lambda) d\lambda \quad (\text{AI-4})$$

Thus the new color coordinates can be calculated as the transpose of the inverse of the transform for the primaries, since the dot product is the matrix product of the transpose of X with $P(\lambda)$.

$$x' = (T^{-1})^t x \quad (\text{AI-5})$$

Likewise from equation 2.1-1, the new matching function vector, $x'(\lambda)$ is similarly related to the old matching functions:

$$x'(\lambda) = (T^{-1})^t x(\lambda) \quad (\text{AI-6})$$

Inversion of Bilinear Chromaticity Color Space

The transformation from the R, G, B primaries to the two chromaticity components in coding space is a UCS bilinear transformation.

In terms of the R,G,B primaries:

$$\begin{aligned} c_1 &= (c_1^r R + c_1^g G + c_1^b B) / S(R,G,B) \\ c_2 &= (c_2^r R + c_2^g G + c_2^b B) / S(R,G,B) \\ S(R,G,B) &= s^r R + s^g G + s^b B \end{aligned} \tag{A2-3}$$

The third coordinate of the coding space is the luminance.

$$L = l^r R + l^g G + l^b B \tag{A2-4}$$

The inverse transform of these coordinates cannot be found by simply inverting a matrix but must be calculated by solving a set of three homogeneous equations with an inhomogeneous input by Cramer's rule.

$$\begin{aligned} R &= Lf^r(c_1, c_2) / P(c_1, c_2) \quad G = Lf^g(c_1, c_2) / P(c_1, c_2) \\ B &= Lf^b(c_1, c_2) / P(c_1, c_2) \end{aligned} \tag{A2-5}$$

where: $P(c_1, c_2) = l^r f^r(c_1, c_2) + l^g f^g(c_1, c_2) + l^b f^b(c_1, c_2)$

$$f^r(c_1, c_2) = (c_1^g c_2^b - c_1^b c_2^g) + c_1 (c_2^g s^b - c_2^b s^g) + c_2 (c_1^b s^g - c_1^g s^b)$$

$$f^g(c_1, c_2) = (c_1^b c_2^r - c_1^r c_2^b) + c_1 (c_2^b s^r - c_2^r s^b) + c_2 (c_1^r s^b - c_1^b s^r)$$

$$f^b(c_1, c_2) = (c_1^r c_2^g - c_1^g c_2^r) + c_1 (c_2^r s^g - c_2^g s^r) + c_2 (c_1^g s^r - c_1^r s^g)$$

APPENDIX III

Derivation of the LSC Transform

The LSC transform consists of a set of luminance dependent functions which scale and shift the UCS chromaticity components which we defined in equation 2. -4:

$$U = \frac{U_r R + U_g G + U_b B}{S_r R + S_g G + S_b B} \quad (\text{AIII-1})$$

$$V = \frac{V_r R + V_g G + V_b B}{S_r R + S_g G + S_b B}$$

where we assume that R, G, B lie in the primary cube and are constrained to take on values between zero and one.

As a first step, the blue component is written as a function of the luminance and the other two components,

$$B = (L - L_r R - L_g G) / L_b \quad (\text{AIII-2})$$

The minimum and maximum values of the functions of AIII-1 are simply derived by noting that as L increases, U and V will be minimum if the primary, H_1 , with the smallest ratio of numerator to denominator coefficient is set to its maximum value:

$$H_1 = \begin{matrix} L/L_{H_1} & L < L_{H_1} \\ 1 & L > L_{H_1} \end{matrix} \quad (\text{AIII-3})$$

As L increases, it will eventually exceed L_{H_1} and at this point H_1 should be set to one, and the primary H_2 , whose ratio of numerator to denominator coefficients is the next smallest, should be set to the maximum possible value, with $H_1 = 1$:

$$H_2 = \frac{(L - L_{H1})/L_{H2}}{1} \quad \begin{matrix} L_{H1} < L < L_{H1} + L_{H2} \\ L > L_{H1} + L_{H2} \end{matrix} \quad \text{(AIII-4)}$$

Likewise, as L is further increased, the final component, H₃, which has the largest numerator to denominator coefficient ratio, will be increased according to:

$$H_3 = \frac{(L - L_{H1} - L_{H2})/L_{H3}}{1} \quad \begin{matrix} L_{H1} + L_{H2} < L < L_{H1} + L_{H2} + L_{H3} \\ L > L_{H1} + L_{H2} + L_{H3} \end{matrix} \quad \text{(AIII-5)}$$

To determine the maximum u and v functions of L, the above procedures are repeated but the three primaries are increased as L increases in order of their decreasing numerator to denominator coefficient ratios. Thus the LSC function of equation 2.4-2 may consist of as many as seven piece-wise continuous functions due to the three boundaries of each of the minimum and maximum functions for u and v. The LSC transform is specified once the coefficients of equation AIII-1 are known. As an example, assume S_g, S_r, S_b, u_b, u_g, u_r, v_g, v_b, v_r. The LSC transform for u has the form:

$$\begin{aligned} \min[u(L)] &= u_r/S_r \quad \text{for } L_b < L < L_r & \text{(AIII-6)} \\ &= [u_r + u_g(L - L_r)/L_b] / [S_r + S_g(L - L_r)/L_b] \\ &\quad \text{for } L_r < L < L_r + L_g \\ &= \frac{[u_r + u_g + u_b(L - L_r - L_g) / L_b]}{[S_r + S_g + S_b(L - L_r - L_g) / L_b]} \quad \text{for } L > L_r + L_g \end{aligned}$$

Likewise:

$$\max[u(L)] = u_b/S_b \quad \text{for } L \geq L_b \quad (\text{AIII-7})$$

$$\begin{aligned} &= [u_g(L - L_b)/L_g + u_b] / [S_g(L - L_b)/L_g + S_b] \quad \text{for} \\ &= \frac{u_r [L - L_g - L_b]/L_r + u_g + u_b}{S_r (L - L_g - L_b)/L_r + S_g + S_b} \quad \text{for } L \geq L_r + L_b \end{aligned}$$

A MATHEMATICAL ANALYSIS OF DYE CORRECTION

Nomenclature:

H - hue band defined by a specific spectral weighting function such as a Wratten filter or a taking sensitivity curve over the color bands: H=R for the red 600-700nm band, H=G for the green 500-600nm band, and H=B for the 400-500nm blue band. \bar{H} is most often used as a superscript.

d - dye layer. d=c (cyan), =m (magenta) =y (yellow) . d is always a subscript.

R_o^H - reflectance measured in color band "H" of object, "o". o is replaced by s for the original subject or p for the photographic print.

D_d^H - density of dye d measured in color band H.

D^H - total density, $D_c^H + D_m^H + D_y^H$ measured in color band H. $D^H = -\text{Log}(R_p^H)$

Y_d^H - slope of the curve of the density of dye d measured in color band H, vs the log exposure to white light of the photographic material.

A_d^H - ratio of the unwanted density of dye d in color band H, to the density of the dye as measured in the desired complementary band \bar{d} .

$$A_d^H = D_d^H / D_{\bar{d}}$$

The densities of the individual dye layers in a color print can be calculated from the reflectances, R_p^H measured in the three color bands.

$$D^H = - \text{Log} \left(\frac{R_p^H}{R_{p_{\min}}^H} \right) \quad (\text{AIV -1})$$

Where the calculated densities are the sum of the desired density D_d^H and the unwanted absorption densities which can be related to the wanted absorption density levels through the unwanted absorption coefficients A_d^H :

$$\begin{aligned} D^R &= D_C^R + A_M^R D_M^G + A_Y^R D_Y^B \\ D^G &= A_C^G D_C^R + D_M^G + A_Y^G D_Y^B \\ D^B &= A_C^B D_C^R + A_M^B D_M^G + D_Y^B \end{aligned} \quad (\text{AIV -2})$$

In matrix form, we may define a density vector calculated from the reflectances, \hat{D} and a density vector representing the true dye densities, D .

$$\hat{D} = [A]D \quad (\text{AIV-3})$$

where the $[A]$ matrix is the transformation matrix defined in A-2. The densities are independent variables and so the matrix has an inverse:

$$D = [A^{-1}] \hat{D} \quad (\text{AIV-4})$$

where:

$$[A^{-1}] = \frac{\begin{matrix} 1 - \frac{G B}{A_Y A_M} & \frac{R B}{A_Y A_M} - \frac{R}{A_M} & \frac{R G}{A_M A_Y} - \frac{R}{A_Y} \\ \frac{G B}{A_Y A_C} - \frac{G}{A_C} & 1 - \frac{R B}{A_Y A_C} & \frac{R G}{A_Y A_C} - \frac{G}{A_Y} \\ \frac{G B}{A_C A_M} - \frac{B}{A_C} & \frac{R G}{A_Y A_C} - \frac{B}{A_Y} & 1 + \frac{R G}{A_M A_C} \end{matrix}}{\begin{matrix} 1 + \frac{R G B}{A_M A_Y A_C} + \frac{R G B}{A_Y A_C A_M} - \frac{R B}{A_Y A_C} - \frac{B G}{A_M A_Y} - \frac{G R}{A_C A_M} \end{matrix}} \quad (\text{AIV-4})$$

Thus the density of each dye layer may be determined from the negative logarithm of the color head reflectance measurements. The A_d^H are determined from the spectral responses of the filters, photodetectors, etc., and the dye reflectance functions for a specific illumination. The A_d^H will therefore vary with photographic material.

The filters should be chosen to be as narrow as possible since the dye density functions are not block functions and thus the shape of the reflectance spectral characteristics changes with density level. The filters must be wide enough so that electronic signal to noise ratio does not limit the dynamic range of measurement.

The measurements of each dye density in the three color bands results in nine contrast coefficients γ_d^H which relate the D_d^H densities to the log of the exposure E , of that particular emulsion layer. As with the A_d^H , a matrix may be formed $[\gamma] = (\gamma_d^H)$:

$$D_d^H = D_{d_{\min}}^H + \gamma_d^H \text{Log } e_H E = \gamma_d^H \text{Log } k_d^H E$$

(AIV-5)

The total reflectance from the color print in color band H may be calculated from the density in that color band:

$$R^H = a^H [10^{[D_{\min}^H - D^H]}]$$

(AIV-6)

The primary requirement of any color process is that neutral tones (greys) must reproduce as neutrals. The most subjectively noticeable chromatic degradation results from not preserving neutral balance. If the original subject reflectances are normalized so that they are equal for achromatic points ($R^R = R^G = R^B$), then neutral balance requires that the total dye density measured in each color band is equal over the grey scale. This can only be achieved if the total gamma coefficient for each color band are equal.

$$\gamma^R = \gamma^G = \gamma^B \quad -7)$$

where:

$$\gamma^H \hat{=} \sum_d \gamma_d^H \quad (1-8)$$

The ratio of one γ_d^H value to another is proportional to the ratio of the dye densities for white light exposure in the particular color bands for the particular dye layers.

$$\gamma_{d1}^{H1} / \gamma_{d2}^{H2} = D_{d1}^{H1} / D_{d2}^{H2} \quad -9)$$

The neutrality condition forces the dye density gamma values in the band of desired absorption to be unequal. This results in the color of a particular dye varying with density. Thus the reproduced hue and saturation level of a reproduced color will vary with the luminance. This arises because the color is determined by a ratio of reflectances, whereas the dye densities are the negative logarithm of reflectance and the photograph reflectances are exponential functions of the densities. As an example of this non-linear effect, the purity of a blue object can be formulated as a function of its luminance. One possible

measure of blue fidelity $F(B)$ is the ratio of the blue to yellow light reflected by a print reproduction of a spectrally pure blue object.

$$D_Y^B = \frac{B}{Y} \text{Log } k_1 L_S^B \quad D_Y^G = \frac{G}{Y} \text{Log } k_2 L_S^B \quad (\text{AIV-10})$$

then: $F(B) = R_Y^B / R_Y^G = 10^{[-D_Y^B - D_Y^G]} \quad (\text{AIV-11})$

or: $F(B) = (L_S^B)^{\left[\frac{B}{Y} - \frac{G}{Y} \right]} \quad (\text{AIV-12})$

Since the H_d are non-negative, and $\frac{B}{Y} > \frac{G}{Y}$, the fidelity decreases as the original luminance decreases. Thus a light blue will reproduce more inaccurately, colorimetrically speaking, than a dark blue. The light blue will be darker and shifted toward the green. Thus to maximize the exponent of AIV-12 the overall γ of the system must be increased. The effective ratio of wanted to unwanted absorptions will therefore be increased. The overall gamma cannot be increased too much before the dynamic range of the reproduction material is exceeded for a given input range of grey levels. Also the achromatic colors are best reproduced with a gamma of unity. The commonly chosen value is about 1.2 for reflectance prints, and 1.8 for the much larger dynamic range of transparencies.

The larger gamma in transparencies necessitates a pre-dye correction transform (Chapter four) since when a slide is again reproduced, the resulting gamma of 3.24 is unacceptably high.

APPENDIX V

COLOR TRANSFORM FOR NEW PRIMARIES WITH SPECIFIED CHROMATICITIES

In appendix I, the transform of the color coordinates for a new set of primaries is derived. This appendix examines this transformation when the new primaries are specified in the chromaticity plane. Knowing the u and v coordinates for each of the three new primaries specifies six of the nine coefficients of the transform of equation AI-3. The other three coefficients are determined from the constraint of the luminosity coefficients which requires the new color coordinates R' , G' , B' to each equal one, when the CIE R , G , B coordinates each equal one.

From AIII-1, specifying u_i and v_i at each "i" new primary point determines the values of the G' and B' coordinates in terms of the red coordinate. By solving the two equations in two unknowns, G_i and B_i for each of the three new primaries can be expressed in terms of R_i .

$$R_i (u_i S_r - u_r) = G_i (u_g - u_i S_g) + B_i (u_b - u_i S_b) \quad (\text{AV-1})$$

$$R_i (v_i S_r - v_r) = G_i (v_g - v_i S_g) + B_i (v_b - v_i S_b)$$

Thus the transform to the new primaries is of the form:

$$\underline{T} = \begin{bmatrix} 1 & T_{11} & T_{21} \\ 1 & T_{12} & T_{22} \\ 1 & T_{13} & T_{23} \end{bmatrix} K \quad (\text{AV-2})$$

where the matrix is known up to a constant multiplier.

The transpose of the inverse of this matrix may now be calculated:

$$\underline{Q} = (T^{-1})^t = \begin{bmatrix} aQ_{11} & aQ_{12} & aQ_{13} \\ bQ_{21} & bQ_{22} & bQ_{23} \\ cQ_{31} & cQ_{32} & cQ_{33} \end{bmatrix} \quad (AV-3)$$

As a final step, the luminosity coefficient constraint requires that the rows of coefficients are normalized:

$$Q_{i1} + Q_{i2} + Q_{i3} = 1 \quad i = 1, 2, 3 \quad (AV-4)$$

The \underline{Q} matrix is the transform from the CIE R, G, B coordinates to the new R', G', B' coordinates.

APPENDIX VI

NUMERIC SYSTEM PARAMETERS AND TRANSFORMS

For purposes of generality, the exact numeric values of constant coefficients have been omitted in most of the equations in the body of this dissertation. This appendix now list these values in case any researcher wishes to extend the work or replicate the results.

1. UCS TRANSFORM FROM CIE R,G,B TO u and v:

$$u = [1.9600 R + 1.2400 G + .8000 B]/S(R,G,B)$$

$$v = [1.0618 R + 4.8744 G + .0638 B]/S(R,G,B)$$

where $S(R,G,B) = 3.1445 R + 12.5260 G + 3.3294 B$

2. INVERSE UCS TRANSFORM FROM u and v to CIE R,G,B:

$$R = L [15.4297 u + 5.8923 v - 3.8204]/P(u,v)$$

$$G = L [-3.3345 u + 4.0100 v + .7244]/P(u,v)$$

$$B = L [-2.0274 u - 20.6518 v + 8.2372]/P(u,v)$$

where $P(u,v) = -.0010 u + 4.0812 v$

3. LUMINANCE

$$L = .1769 R + .8124 G + .0106 B$$

4. QUASI-LUMINANCE FUNCTION IN TERMS OF R_H, G_H, B_H

$$L = .257 R_H + .670 G_H + .073 B_H$$

TABLE A-1

QUASI-LUMINANCE FUNCTION ACCURACY

<u>Equivalent Neutral Density</u>			<u>Luminance</u>	
<u>cyan</u>	<u>magenta</u>	<u>yellow</u>	<u>actual value</u>	<u>LMS Approximation</u>
.0	.0	.0	1.0	1.0
.1	.1	.1	.7536	.7535
1.0	1.0	1.0	.0592	.0591
2.0	2.0	2.0	.0035	.0035
1.0	.0	.0	.3490	.4005
.0	1.0	.0	.3470	.3883
.0	.0	1.0	.7824	.7178
.1	.1	.0	.7782	.7876
.1	.0	.1	.8535	.8525
.0	.1	.1	.8594	.8515
2.0	.0	.0	.1699	.2126
.0	2.0	.0	.1681	.2379
.0	.0	2.0	.6596	.5763
2.0	2.0	.0	.0138	.0210
2.0	.0	2.0	.0619	.0705
.0	2.0	2.0	.1348	.1832

5. Pre-Dye Correction Primary Transform:

$$\begin{array}{rcccc}
 R' & & .667 & .316 & .017 & R \\
 G' & = & -.128 & 1.262 & -.133 & G \\
 B' & & -.007 & -.032 & 1.039 & B
 \end{array}$$

6. HEXAGONAL - AFFINE - TRIANGULAR TRANSFORM REGIONS:

For an exact mapping of the D = 1.0 R,G,B,C,M,Y points.

<u>TRANSFORM</u>	<u>QUADRANTS</u>	<u>MAP POINTS</u>	<u>SLOPE LIMITS</u>
1	I & IV	R - M	----- .2302
2	III & IV	M - B	----- -.5081
3	III	B - C	----- 3.7282
4	III & II	C - G	----- .5070
5	II & I	G - Y	----- -.5557
6	I	Y - R	----- 1.3704
			----- .2302

TABLE A-2.

HEXAGONAL AFFINE TRANSFORM FOR THE COLOR HEAD SENSORS

<u>TRANS- FORM #</u>	C_{11}	C_{12}	C_{21}	C_{22}
1	.69719	.15395	.06351	.90967
2	.65651	.05003	.04507	.86255
3	1.31587	.20655	.44726	.94229
4	1.21798	.41849	.28557	1.29234
5	.97948	.05535	.93950	.05384
6	.63675	.03969	.95300	.38237

A-3. HEXAGONAL AFFINE TRANSFORM FOR THE PRE-DYE DENSITY APPROXIMATION

<u>TRANSFORM REGION</u>	T_{11}	T_{12}	T_{13}	T_{21}	T_{22}	T_{23}	T_{31}	T_{32}	T_{33}
1	1.478	-.493	.015	.423	.638	-.061	.797	-.445	.648
2	.563	-.427	.864	-.366	.693	.673	-.120	-.379	1.499
3	.687	-.580	.893	-.394	.727	.667	-.106	-.396	1.502
4	.328	.825	-.153	-.798	2.305	-.508	-.473	1.039	.435
5	.287	.836	-.123	-1.062	2.376	-.314	-.549	1.059	.490
6	1.495	-.543	.048	.398	.709	-.107	.816	-.498	.683

-127-

REFERENCES

1. Yule, J.A.C., Principles of Color Reproduction, John Wiley & Sons, Inc., New York, 1967.
2. Pugsley, P.C., Electronic Scanners in Colour Printing, *Electronics & Power*, January 10, 1974.
3. Pratt, W.K., Spatial Transform Coding of Color Images, *IEEE Trans. on Communication Technology*, December 1971, Vol. COM-19, No. 6, pp. 980-992.
4. Fink, D.G., Television Engineering, 2nd ed., McGraw-Hill, New York, 1952.
5. Wentworth, J.W., Color Television Engineering, McGraw-Hill, New York, 1955.
6. McIlwain, K., Requisite Color Bandwidth for Simultaneous Color-Television Systems, *Proc. IRE*, Vol. 40, No. 8, August 1952, pp. 909-912.
7. Loughren, A.V., Psychophysical and Electrical Foundations of Color Television, *Proc. IRE*, January 1954, pp. 9-11.
8. Schade, O.H., On the Quality of Color Television Images and the Perception of Color Detail, *J. SMPTE*, Vol. 67, 1958, p. 801.
9. Brown, G.H., The Choice of Axes and Bandwidths for the Chrominance Signals in NTSC Color Television, *Proc. IRE*, January 1954, pp. 58-59.
10. Gronemann, U.F., Coding Color Pictures, MIT RLE report 422, June 1964.
11. Wacks, K.P., Design of a Real Time Facsimile Transmission System, MIT Ph.D. Thesis, 1973.
12. Legrand, Y., Light, Colour and Vision, Chapman and Hall Ltd., London, Copy 1957.
13. Bouma, P.J., Physical Aspects of Colour, N. V. Philips Gloeilampenfabrieken, Eindhoven (Netherlands), 1947.
14. Kelly, D.H., Spatio-temporal Frequency Characteristics of Color-Vision Mechanisms, *J. Opt. Soc. Am.*, Vol. 64, July 1974, pp. 983-990.

15. Wintringham, W.T., Color Television and Colorimetry, Proc. IRE, October 1951, pp. 1135-1172.
16. Stockham, T.G., Jr., The Importance of Nonlinear Image Enhancement in Visual Prosthesis Design, Visual Prosthesis, Academic Press, 1971, pp. 173-192.
17. Tretiak, O.J., The Picture Sampling Process, MIT ScD. Thesis Elec. Eng., September 1963.
18. Judd, D.B., Estimation of Chromaticity Differences and Nearest Color Temperature on the Standard 1931 ICI Colorimetric Coordinate System, J. Res. Nat. Bur. Stds., Vol. 17, 1936, pp. 771-779.
19. Rubinstein, C.B. and Limb, J.O., Statistical Dependence Between Components of a Differentially Quantized Color Signal, IEEE Transactions on Communications, Vol. COM-20, No. 5, October 1972, pp. 890-899.
20. Committee on Colorimetry Optical Society of America, The Science of Color, Thomas Y. Crowell Company, New York, 1953.
21. Willmer, E.N., Color of Small Objects, Nature, Vol. 153, June 24, 1944, pp. 774-775.
22. Middleton, W.E. and Holmes, M.C., The Apparent Colors of Surfaces of Small Substance - A Preliminary Report," J. Opt. Soc. Am., Vol. 39, July 1949, pp. 582-592.
23. Luckiesh, M., The Dependence of Visual Acuity on the Wavelength of Light, Electronics World, Vol. 58, November 18, 1911, p. 1252.
24. Hartridge, H., The Change from Trichromatic to Dichromatic Vision in the Human Retina, Nature, Vol. 155, June 2, 1945, pp. 657-662.
25. McIlwain, K. and Dean, C.E. (eds.), Principles of Color Television, John Wiley & Sons, Inc., New York, 1956.
26. Hacking, K., The Relative Visibilities of Spatial Variations in Luminance and Chromaticity, BBC Research Report No. T-146, August 1965.
27. Ratcliff, F., Mach Bands: Quantitative Studies on Neural Networks in the Retina, Holden Day, Inc., Copy 1965.
28. Green, D.G., The Contrast Sensitivity of the Colour Mechanisms of the Human Eye, J. Physiology (Great Britain), Vol. 196, 1967, pp. 415-429.

29. Fink, D.G. (ed.), Color Television Standards: Selected Papers and Records, McGraw-Hill, New York, 1955.
30. Baldwin, M.W., Jr., Subjective Sharpness of Additive Color Pictures, Proc. IRE, October 1951, pp. 1173-1176.
31. Petersen, D.P. and Middleton, D., Sampling and Reconstruction of Wave-Number Limited Functions in N-Dimensional Euclidean Spaces, Information and Control, Vol. 5, 1962, pp. 279-323.
32. Brown, W.M., Optimum Filtering of Sampled Data, IRE Trans. Info. Theory, Vol. IT-7, October 1961, pp. 269-270.
33. Hardy, A.C. and Wurzburg, F.L., Jr., Color Correction in Color Printing, J. Opt. Soc. Am., Vol. 38, No. 4, April 1948.
34. Hardy, A.C. and Wurzburg, F.L., Jr., The Theory of Three-Color Reproduction, J. Opt. Soc. Am., Vol. 27, No. 7, July 1937, pp. 227-240.
35. Friedman, J.S., History of Color Photography, The American Photographic Publishing Co., Boston, 1944.
36. Kodak Publication E-78, Sensitometric and Image Structure Data for Kodak Color Films, CAT 178-6680.
37. Yule, J.A.C., Principles of Color Reproduction, John Wiley & Sons, Inc., New York, 1967.
38. Miller, T.H., Masking: A Technique for Improving the Quality of Color Reproductions, J. Soc. of Motion Picture & TV Engs., Vol. 52, February 1949, pp. 133-155.
39. Hanson, W.T., Jr., and Brewer, W.L., Subtractive Color Photography: The Role of Masks, J. Opt. Soc. Am., Vol. 44, February 1954, pp. 129-134.
40. MacAdam, D.L., Subtractive Color Mixture and Color Reproduction, J. Opt. Soc. Am., Vol. 28, December 1938, p. 466.

BIOGRAPHICAL NOTE

Born in Brooklyn, New York on August 9, 1945, Robert Solomon attended Brooklyn Technical High School and then Polytechnic Institute of Brooklyn where he received the B.E.E. summa cum laude. While he was an NSF fellow he received the S.M. and Engineer degrees in electrical engineering at M.I.T. in 1968 and 1970. From 1970 until 1974 he worked on a laser facsimile transmitter and receiver and various color facsimile hardware and theoretical projects. For the past seven years, he has been a senior development engineer and project leader at General Radio Company, where he developed various audio spectrum analyzer instruments and systems using analog and FFT digital processing techniques and also conducted research on interactive color display systems. In addition, he has conducted much private research in his consultant practice in the areas of video instrumentation and special effects, color reproduction, biomedical instrumentation, and microprocessor systems.

Robert Solomon is a member and past chapter president of both Tau Beta Pi and Eta Cappa Nu, and a member of Sigma Xi, the IEEE, and the Optical Society of America. He has had accepted for publication and presentation several papers in his areas of expertise.